I, 1

APPENDIX 1

I, 2

Aircraft Engine Speciated Organic Gases: Speciation of Unburned Organic Gases in Aircraft Exhaust

EPA United States Environmental Protection Agency

FEDERAL AVIATION ADMINISTRATION

I, 3

Aircraft Engine Speciated Organic Gases: Speciation of Unburned Organic Gases in Aircraft Exhaust

Assessment and Standards Division
Office of Transportation and Air Quality
U.S. Environmental Protection Agency

and

AEE-300 - Emissions Division
Office of Environment and Energy
Federal Aviation Administration

EPA-420-R-09-902
May 2009

I, 4

Aircraft Engine Speciated Organic Gases: Speciation of Unburned Organic Gases in Aircraft Exhaust

W.B. Knighton, S.C. Herndon, and R.C. Miake-Lye

Purpose and Scope: The FAA and EPA are evaluating the methodology to quantify Hazardous Air Pollutants (HAPs) emissions from commercial aircraft engines, to be used when an aircraft HAPs emissions inventory is requested. Central to the methodology is a singular HAPs speciation profile. The final HAPs speciation profile will be:

- Nationally consistent,
- Supported by state-of-the-science data,
- Representative of today's commercial aircraft fleet, and
- "Living" to continue to reflect the state-of-the-science as studies are conducted and new data becomes available.

A second outcome of this effort is to evaluate and, if necessary, update the factors needed to convert between total unburned hydrocarbons (HC), volatile organic compounds (VOC), and total organic gases (TOG).

The scope of this work is to update the current HAPs profile that exists for commercial aircraft engines, using recent HAPs measurements conducted on more modern commercial aircraft engines. The original HAPs profile has been in existence unchanged for over 2 decades, based upon a single 1984 measurement campaign by Spicer et al.[1] To support the update of the existing HAPs profile, consolidated data from Spicer and more recent measurements (EXCAVATE, APEX) will be investigated and discussed in this document. Important questions to address in this scope of work are: how to combine all of the data sets into a single profile given the various methods used to collect the samples; and how to address combustor technologies, etc. not yet tested. We still have very limited data to work with at this time, which limits the conclusions we can make, so it is necessary to be mindful of these questions as new HAPs data becomes available in the future and we endeavor to update this methodology.

Introduction: Aircraft gas turbine engines are designed to burn their hydrocarbon (HC) fuel efficiently, since any inefficiency translates into carrying more fuel, a greater take-off weight, and a steeply rising cost of operation as efficiency decreases. Because most of the fuel is consumed at higher power settings and most of the operational time is spent at cruise, for power settings of cruise and above most engines convert significantly more

---

[1] HAPs profile No. 1098 in EPA's SPECIATE database. http://www.epa.gov/ttn/chief/software/speciate/index.html Composite profile developed from data for a CFM-56 jet engine fired with JP-5 fuel at idle, 30% thrust and 80% thrust. Data collected by GC/MS and DNPH analyses were combined according to average LTO cycle times obtained from AP-42. Spicer, C. W., et al., Battelle Columbus Laboratories, Composition and Photochemical Reactivity of Turbine Engine Exhaust, Report No. ESL-TR-84-28, Prepared for Air Force Engineering and Services Center (RDVS), Tyndall AFB, FL, September 1984.

than 99% of the fuel through complete combustion to carbon dioxide (CO_2) and water (H_2O). At idle conditions, much less fuel is consumed and, in the interest of maintaining stable combustion at lower power conditions, some sacrifice in combustion efficiency occurs even though this inefficiency is still only a percent or so. Any combustion inefficiency of HC fuel will result in emissions of some combination of CO and incompletely oxidized HCs, as well as some carbonaceous particles.

From the point of view of understanding the combustion process, knowing the combustion efficiency is important since any HC emission represents an inefficiency in converting fuel to CO_2 and H_2O. In order to understand the environmental impact of the emissions, it is important to quantify the amounts of the emitted species, especially those that are deemed highly toxic or carcinogenic. The US EPA considers a number of HCs (among other pollutants) as HAPs, and quantification of levels of these species takes on a special importance. This report will discuss the emissions of HAPs from aircraft engines and how the speciation of the HC emissions relates to levels of the various HAPs present in aircraft exhaust.[2] Since the concentrations of HCs and HAPs are highest in the exhaust at low power conditions, the emphasis will be on measurements under such conditions.

Components of PM emissions from aviation engines may also be classified as Hazardous Air Pollutants, but PM emissions are measured and analyzed very differently than gaseous emissions, and are not discussed in this document. Much work is currently being directed at identifying measurement approaches and resolving sampling issues for aviation gas turbine engine PM emissions (e.g. the APEX and related campaigns), and data characterizing PM emissions from a variety of commercial aircraft gas turbine engines is being accumulated.

Background: Several studies have attempted to document the speciation of the HCs emitted from aircraft engines. Most notably, in the 1980s Spicer et al. (Spicer, Holdren et al. 1994) performed a series of studies on a set of military engines using a variety of analytical techniques to quantify a wide range of HCs. Subsequently Gerstle et al. (Gerstle, Virag et al. 1999) examined another set of military aircraft, with a similar set of analytical techniques. Most recently, a set of studies initiated by NASA called Aircraft Particle Emissions eXperiment (APEX), and supported by a wide range of sponsors (NASA, FAA, CARB, EPA, DoD …) has focused attention on commercial aircraft Particulate Matter (PM) emissions (Wey 2004; Onasch, Jayne et al. 2006; Wey, Anderson et al. 2006; Lobo, Hagen et al. 2007), using a wide range of analytical techniques. These studies also included HC gaseous emissions analysis. Some of the techniques employed in APEX1-3 overlap with the earlier tests, but also some more advanced (faster time response/higher sensitivity) techniques were used during APEX.[3]

---

[2] It should be noted that because a compound is considered hazardous it does not imply health or welfare effects at current levels, or that it is appropriate to adopt controls to limit the emissions of such a compound from turbine engine aircraft or their fuels.

[3] APEX was the collaborative research effort of NASA, EPA, DoD, and the FAA. The main objective of the APEX research was to characterize both gaseous and particulate emissions to advance the understanding of emissions from commercial aircraft engines. APEX1 was conducted in April of 2004 with a NASA-owned DC-8 aircraft equipped with CFM-56-2C1 engines. APEX2 was conducted in August 2005 for typical in-use aircraft engines (CFM56 engines on B737 aircraft), APEX3 testing was conducted

The range of experiments and the variety of techniques employed can be used to provide greater confidence in the HAPs emissions measurement data, and to allow assessment of which results can be verified by multiple techniques. In addition, one engine type, a CFM56 (a high bypass turbofan engine), was part of both the Spicer and APEX studies, so that a most direct cross comparison can be made.[4]

The comprehensive measurements of Spicer et al. (Spicer, Holdren et al. 1994) have provided valuable data for the CFM56-3 and the TF-39 (forerunner to the General Electric CF6 class of high bypass turbofan engines).[5] These measurements were conducted using a mixture of on-line instrumentation and canister sampling with off-line analysis developed from a prolific program of military engine emissions characterization. This work chose to report values as ppmC present in the exhaust. The data labeled 'idle' in this work was conducted at nominal 'ground idle' and does not reflect the ICAO definition of idle, also called 7% of rated thrust. The Spicer et al. work finds that 40% of the organic gas mass is accounted for by the compounds, ethene, formaldehyde, propene, ethyne and methane.

In a report to the US Air Force, Gerstle and co-workers (Gerstle, Virag et al. 1999) reported HC emission rates for several engines not included in the ICAO databank, as well as some emissions from auxiliary power units. Some of the military engines addressed in this study represent older engine technologies that are no longer represented in the commercial fleet and, as such, there may be issues regarding combustion efficiencies at low power conditions that may cause significant differences in emissions due to raw fuel contributions to the HCs emissions at low power (personal communication Will Dodds, GE, and KBE, February 2007 et seq.).

A more recent series of measurements have focused on commercial engines. NASA's interest in charactering the emissions from commercial engines in dedicated engine tests was demonstrated during the EXCAVATE campaign. Anderson et al. (Anderson, Chen et al. 2006) measured the speciated organic gas emissions from a Rolls-Royce RB211-535-E4 engine (another high bypass turbofan engine) for two different fuel sulfur levels. A very comprehensive program continued with the APEX-1 campaign (Wey, Anderson et al. 2006) within which HAPs characterization was conducted with high time response on-line organic gas speciation using infrared fingerprint absorption spectroscopy and chemical ionization mass spectrometry for a CFM56-2C1 (Knighton, Rogers et al. 2007;

---

in October and November of 2005 spanning a range of engines from a small business jet, through a modern regional turbofan, a single-aisle transport turbofan, to a large high bypass ratio turbo fan, representing five different engine types, some measuring more than one example. In all studies, exhaust plumes were sampled at the engine exit plane and several downstream measurement locations.

[4] CFM56 and the CFM logo are for CFM International, which is a joint company of Snecma and General Electric. Snecma is a French manufacturer of engines for commercial and military aircraft, and space vehicles.

[5] The General Electric TF-39 was the first high bypass turbofan engine, and it was developed for the Air Force back in 1965 for a new transport aircraft. Turbofan engines with a bypass ratio of 5 or greater are considered to be high bypass turbofan engines (Cumpsty, N., Jet Propulsion, Cambridge University Press, 2002, p. 46.). Bypass ratio is the ratio between the mass flow rate of the air drawn in by the fan, but bypassing the engine core, to the mass flow rate passing through the engine core (Cumpsty, loc. cit.).

Yelvington, Herndon et al. 2007). Time integrated LTO cycle data were also collected at the same time (Kinsey et al, document in preparation). An analysis of the JETS/APEX-2 (Lobo et al., 2007)[6] and APEX-3 datasets is forthcoming (Timko et al., in preparation).

In all of the APEX dedicated engine tests, measurements were made at both the engine exit plane and in the plume at a downstream location (nominally 30 m for an intermediate engine size such as a CFM56). It is important to note that the measured HC profile is relatively consistent regardless of measurement location. In the ensembles of data presented below, all of the various distances, fuels, and power conditions below 30% of rated thrust are combined in demonstrating the tight correlations among HC emissions. Further, in the airport studies discussed next, much further downwind measurements also indicated no change in the relative concentrations of species, although as the exhaust continues to dilute, the species present as very small fractions of the total profile begin to fall below detection limits as distances increase further from the emission source.

In addition to dedicated engine tests, sampling from airports during routing operation have also provided useful data for HAPs emissions. Using analysis of wind-advected plumes sampled at Boston Logan International Airport, selected speciated organic gas emissions were characterized from in-use aircraft (Herndon, Rogers et al. 2006). Schürmann et al. (Schürmann, Schäfer et al. 2007) also measured volatile organic compounds using canister sampling of diluted exhaust in an operational taxiway area. They found that refueling activity altered the profile of hydrocarbons considerably. An analysis of the wind advected data collected at the Oakland GRE and taxiway/runway sampling is forthcoming (Herndon et al., in preparation).

All of the studies indicate that a wide range of combustion-related emissions are present in aircraft exhaust. Despite the long list of species present, a ranking of the species by concentration indicates that 15-20 species represent most (95% or more) of the emissions on the basis of concentration. A greater number of species are present at a fraction of a percent or smaller of the total concentration. Of the overall speciated mixture, a number of species can be considered HAPs, while another set may be significant to the overall level of VOC emissions but data indicating toxicity are lacking.

An important point to note is that no instrument measures all of the HC emissions. The fast time response instrument (Proton Transfer Reaction Mass Spectrometer: PTR-MS) used for HC measurements in APEX was focused on measuring relevant HAPs, and as such was not capable of measuring alkanes or acetylene. Since the PTR-MS is capable of measuring a wide range of HCs other than alkanes and acetylene, the measurement focus was on a list of species that were measurable by the PTR-MS, identified EPA HAPs species, and present in aircraft exhaust. Formaldehyde and ethylene were also not measurable with the PTR-MS, but were measured separately in APEX using IR techniques (Tunable Infrared Laser Absorption Spectroscopy: TILDAS). In the Spicer

[6] Additional data reported from JETS/APEX2, taken by the UC Riverside team, was not used to develop the jet aircraft speciation profile, because the compromised sampling system for that data source prevented a complete and high-confidence organic compound data set from being assembled from the UC Riverside data.

studies, a wide range of techniques was used, but no measurement of methanol was attempted, and none of the trimethylbenzenes nor several of C9-C11 aromatic species were identified with the techniques employed therein. In many of the studies, a Flame Ionization Detector (FID) was used to quantify the total "unburned hydrocarbons" (UHCs), but this is an imperfect estimation of the total emissions due to the FID's non-uniform response to different carbon-containing compounds. All this is to note that, while these several data sets provide very useful data on many individual compounds and their relationship to one another, arriving at an estimate of a total quantity by mass or by concentration is dependent on which species are included in the total. And, the measured species are determined by what measurement techniques have been employed.

Data Comparison: The most direct intercomparison between the earlier studies and the recent APEX mission is accomplished through the overlap with the CFM56 engine. Table 1 reproduces Spicer's speciation data for this engine (Spicer, Holdren et al. 1994) ranked in order of decreasing concentration. The first column lists the species present in the highest concentration, which represent about 95% of the total speciated non methane hydrocarbon (NMHC) emissions on a concentration basis as measured by Spicer. The highlighted species indicate those species measured by Spicer that were also quantified in APEX by PTR-MS (yellow) or TILDAS (green). In the first column, only acetylene and ethane are not highlighted. In subsequent columns, the sum of which represents 5% of the Spicer emissions concentration, a number of other alkanes also are not highlighted. These species, not measured by PTR-MS or TILDAS, represent about 1.4% of Spicer's total, and are not typically considered HAPs. It is worth noting that, of the species noted in the "EPA 14" and "FAA 10" HAPs lists that were developed based on relevant HC emissions from aviation engines (URS and FAA 2003), all of those species are in the highlighted (measured in both studies) elements of Table 1.

Table 1. NMHC emission ratios for the CFM56-3 engine reported by Spicer et al. listed in decreasing magnitude. The first column represents 95% of the emissions on a molar basis. Green highlighted cells indicate compounds that are measured by TILDAS. Yellow highlighted cells indicate compounds that are quantified by the PTR-MS.

Compound	ER (mmole/mole)	Compound	ER (mmole/mole)	Compound	ER (mmole/mole)
ethylene	0.77	acetone	0.0089	1-nonene	0.0027
formaldehyde	0.572	C5-ene	0.0072	propane	0.0025
acetylene	0.211	2-methylpentane	0.0066	1-CH_3-naphthalene	0.0024
propene	0.151	benzaldehyde	0.0062	hexanal	0.0023
acetaldehyde	0.135	1-heptene	0.0061	C5-cyclohexane	0.0023
acrolein	0.061	naphthalene	0.0059	ethylbenzene	0.0023
1-butene	0.044	C5-ene	0.0055	C4-benzene	0.0023
glyoxal	0.044	cis-2-butene	0.0052	o-xylene	0.0022
1,3-butadiene	0.044	styrene	0.0041	2-CH_3-naphthalene	0.0020
benzene	0.03	n-undecane	0.0040	C5-benzene	0.0020
methylglyoxal	0.029	n-pentane	0.0038	1-decene	0.0018
ethane	0.024	n-dodecane	0.0038	C13-alkane	0.0014
butanal/crotonaldehyde	0.019	m,p-xylene	0.0037	C14-alkane	0.0013
propanal	0.017	2-methyl-2-butene	0.0037	n-heptane	0.0009
1-pentene	0.015	1-octene	0.0034	n-octane	0.0008
1-hexene	0.012	n-decane	0.0031	n-nonane	0.0007
toluene	0.0097	phenol	0.0029	C12-C18 alkanes	0.0045

The highlighted sections in Table 1 indicate that comparisons can be made for the measurements of those species measured for Spicer's CFM56 and the several CFM56 engines measured in APEX. Those comparisons are listed in Table 2 as mass ratios, expressed as ratios of Emission Indices (EIs). The EI of a species is the mass of that species emitted in grams, divided by the mass of fuel consumed in kilograms (species g/kg fuel). The unhighlighted elements in Table 1 indicate that the APEX PTR-MS/TILDAS data set is missing those elements and no direct comparison can be made and are thus not included as rows in Table 2. The unhighlighted elements in Table 1 represent approximately 12% of the concentration in Spicer's list.

Table 2. Compound EIs normalized to formaldehyde (EI_x/EI_{HCHO}) for low engine powers (4-15% rated thrust) evaluated as the slopes of plots of EI(x) vs EI(HCHO)

Compound	APEX 1 EI_x/EI_{HCHO}	APEX 2 EI_x/EI_{HCHO}	APEX 3 EI_x/EI_{HCHO}	Spicer et al. EI_x/EI_{HCHO}
Methanol	0.18	0.14	0.12	--
Propene	0.36	0.39	0.38	0.37
Acetaldehyde	0.32	0.36	0.36	0.35
Butene + Acrolein	0.30	0.45	0.48	0.36
Acetone + Propanal + Glyoxal	0.18	0.16	0.20	0.24
Benzene	0.15	0.17	0.16	0.14
Toluene	0.056	0.082	0.073	0.052
mass 107	0.088	0.138	0.103	0.089
mass 121	0.074	0.119	0.085	--
mass 135	0.035	0.074	0.051	--
mass 149	0.014	0.038	0.027	--
Naphthalene	0.018	0.034	0.020	0.044
Methylnaphthalenes	0.009	0.023	0.016	0.037
Dimethylnaphthalenes	0.0026	0.011	0.0083	--
Phenol	0.063	0.064	0.050	0.016
Styrene	0.020	0.035	0.023	0.025
Acetic acid	0.16	0.057	0.084	--

propene – quantified assuming that 68% all of the ion intensity measured at m/z43 originated originates from propene.
butene + acrolein – quantified assuming the m/z 57 signal is distributed as reported by Spicer et al. 45% butenes and 55% acrolein.
acetone + propanal + gyloxal – quantified assuming the m/z 59 signal is distributed as reported by Spicer et al. 12% acetone, 25% propanal and 63% glyoxal.
Mass 107 – quantified as p-xylene and represents the sum of o,m,p-xylene, ethyl benzene & benzaldehyde
Mass 121 – quantified as 1,2,4-trimethylbenzene and represents the sum of C_9H_{12} and C_8H_8O
Mass 135 – quantified using a single rate constant and represents the sum of $C_{10}H_{14}$ and $C_9H_{10}O$
Mass 149 – quantified using a single rate constant and represents the sum of $C_{11}H_{16}$ and $C_{10}H_{12}O$

However, as is noted by the first row of Table 2, Spicer did not measure methanol, which is approximately 5% of Spicer's total concentration, which would increase the HC total by that amount. There are also several other aromatic species listed in Table 2, which were not identified in the Spicer analysis. While these compounds would fall into the second two columns of Table 1 if they were included, and thus represent only a percent or so of the total concentration profile, they do represent a significant number of aromatic compounds. These several differences in the lists of species measured in these measurement studies highlight the uncertainty in working with any "total" emissions level: the "total" is only a sum of whatever species are included in the "total".

A longer list of species measured in the APEX campaigns but not measured by Spicer is included in the accompanying spreadsheet. In that spreadsheet, the additional species are color coded by blue (from PTR-MS) and yellow (from EPA's set of integrating measurements, Kinsey et al, manuscript in preparation).

This spreadsheet also provides a normalized emission profile. This profile was developed based on Spicer's original speciation and carbon balance. Adjustments and additions were made, based on the new data available (all APEX1-3 data discussed in this report), but the measured species continue to make use of the original carbon balance. Thus, because of the longer list of species now quantified, these refinements to the speciation profile result in a decrease of the unidentified emitted mass from about 35% in the original Spicer work (34% if methane were included, but as discussed below, Spicer has shown elsewhere that the methane measurement was due to background methane and should not be included in the sum) to about 29% due to the additionally identified species and refinements to phenol and butyraldehyde/crotonaldehyde. Separate analysis of the total HC emissions by independent measurements during the APEX1-3 campaigns (J. Kinsey, personal communication) used time-integrated sampling over a range of power conditions. Because that approach is distinguished from the single power points measured by Spicer and the data presented here, precise agreement would not be expected due to different dependence on background levels and related data analysis issues. However, despite these potential differences, similar ratios of the sum of identified to the total HC mass were calculated using the time integrated measurements in APEX1-3 as compared to those of this revised profile, giving increased confidence in the overall HC mass balance presented with these data.

While the unidentified species mass has been reduced through this process, the composition of that unidentified mass remains an uncertainty. In the original Spicer profile, which used gas chromatography and various HC capture techniques, the unidentified mass could possibly include contributions from some of the species that were specifically identified. In other words, based on the original Spicer work, one could argue that some of the identified species may have been present in larger amounts than were reported because they may have also been contributing to the unidentified mass. That would be a result of some mass "sticking" to a GC column or a HC capture medium. The new additional data reduces that uncertainty considerably, since independent real-time data were collected which largely corroborated the Spicer profile. The combination of the original and new data provide good evidence that the identified species contribute to the profile at the levels measured and have little or no contribution to the unidentified HC mass fraction.

Table 2 compares the concentration of the particular species of interest to that of formaldehyde, which is one of the most prevalent emissions and serves as a useful reference species. This is done, rather than directly compare concentrations, since the combustion efficiency is highly dependent on precise fuel flow and power settings at low engine powers, with ambient temperature also having a significant impact on emission levels (Yelvington, et al.). Since engine operating point, ambient temperature, and related details are all slightly different from test to test, the combustion efficiency is also likely to vary from data set to data set. However, the relationship of the various emissions to each other is quite constant even though their levels may go up and down together.

Figure 1 shows that this is true not only for the CFM56 measured in APEX1 and discussed by Yelvington et al. but it is also true for the several CFM56 engines measured in JETS/APEX2 and, indeed, is equally true for the wider range of different commercial engine types measured in APEX3. In fact, not only is it true that the speciation is invariant as a specific engine varies power and combustion efficiency, but for the range of commercial engines measured in APEX1-3 and the range of standard jet fuels used through those tests, the relationship between the various HC emissions, (i.e. the *speciation profile* shown here as individual species plotted versus formaldehyde, HCHO), is also invariant across these different commercial engine types: all of the curves lie essentially on top of one another. ***The invariance of the speciation profile across power settings, ambient temperature, and engine types for commercial engines is very useful for interpreting HAPs emissions from commercial engines.***

The range of fuels used in the diverse set of tests presented in Figure 1 suggests that fuel also has a minimal impact on the speciation profile. Fuel sulfur and aromatic content spanned a range of values across these tests, particularly when the APEX1 fuel sulfur additions are included. However dramatic changes in the hydrocarbon composition of the fuel, as might be encountered using alternative fuels like Fischer-Tropsch or bio-fuels, have not been explored in the set of data presented here.

The correlation of each of the individual species versus formaldehyde plotted in Figure 1 show that, for the three APEX campaigns, there are very tight correlations for the several species plotted. Species present in greater concentration (propene and acetaldehyde) have a tighter correlation than species at lower concentrations (benzene and, especially, naphthalene, which is a PAH and may begin condensing on PM emissions soon after leaving the engine, which might affect its gas phase concentration).

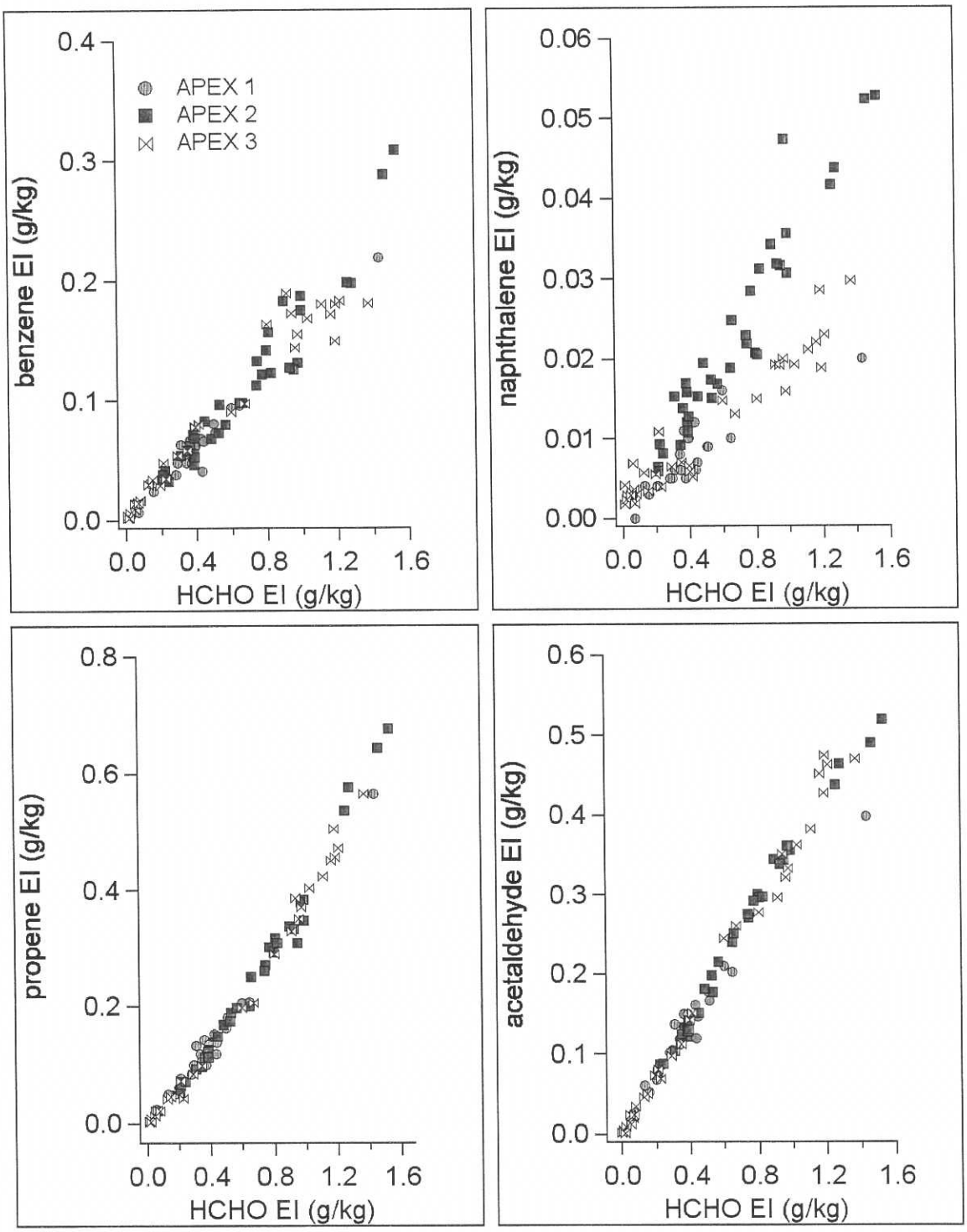

Figure 1. Correlation scatter plots of selected HC vs. HCHO emission indices measured on the 1-meter probe under low power, 4-15% rated thrust.

Table 2 provides the comparison between the speciation profile measured by Spicer and that from PTR-MS/TILDAS from APEX. The three data columns from APEX cover the CFM56-2C1 measured in APEX1, the several CFM56-3 and -7 engines measured in

APEX2, and an average over the set of engines (excluding the AE3007 for this analysis) measured in APEX3. For many species, especially those at larger concentration ratios, the variation among the various tests is no greater than the variation between APEX and Spicer. The speciation for these species appears to be very robust. Some of the more minor species show more significant variation, which may be partly due to measurement uncertainty and may be partly due to sensitivity to other variables such as minor fuel composition variations and so forth. It is worth noting that many of these smaller contributors represent less than 1% of the speciated concentration mixture.

One species of particular note is phenol. The APEX series of measurements indicate a concentration ratio three times higher than that of Spicer. That is the largest disagreement in Table 2 (excluding cases where a Spicer measurement is not available), and deserves further comment. While phenol represents only about 0.1% of the speciation concentration profile, it does represent a test of the ability to measure a minor species accurately. While further analysis might be warranted, phenol was measured by Spicer using canister capture to deliver the sample to the gas chromatographic measurement system. Given the significant differences indicated for this compound, wall losses might be suggested as a possible explanation for this unique discrepancy in the HC speciation.

The overall agreement between the Spicer and the APEX speciation profiles is shown in Figure 2. This is a direct comparison of the overall APEX speciation profile to that of Spicer for those species where the measurements are available in both studies. Except for phenol and the combination of acetone, propanal, and glyoxal (which, unlike phenol, is still within 2 sigma), all of the data are within the standard deviation of the measurements themselves to the unit line (the unity line represents perfect agreement).

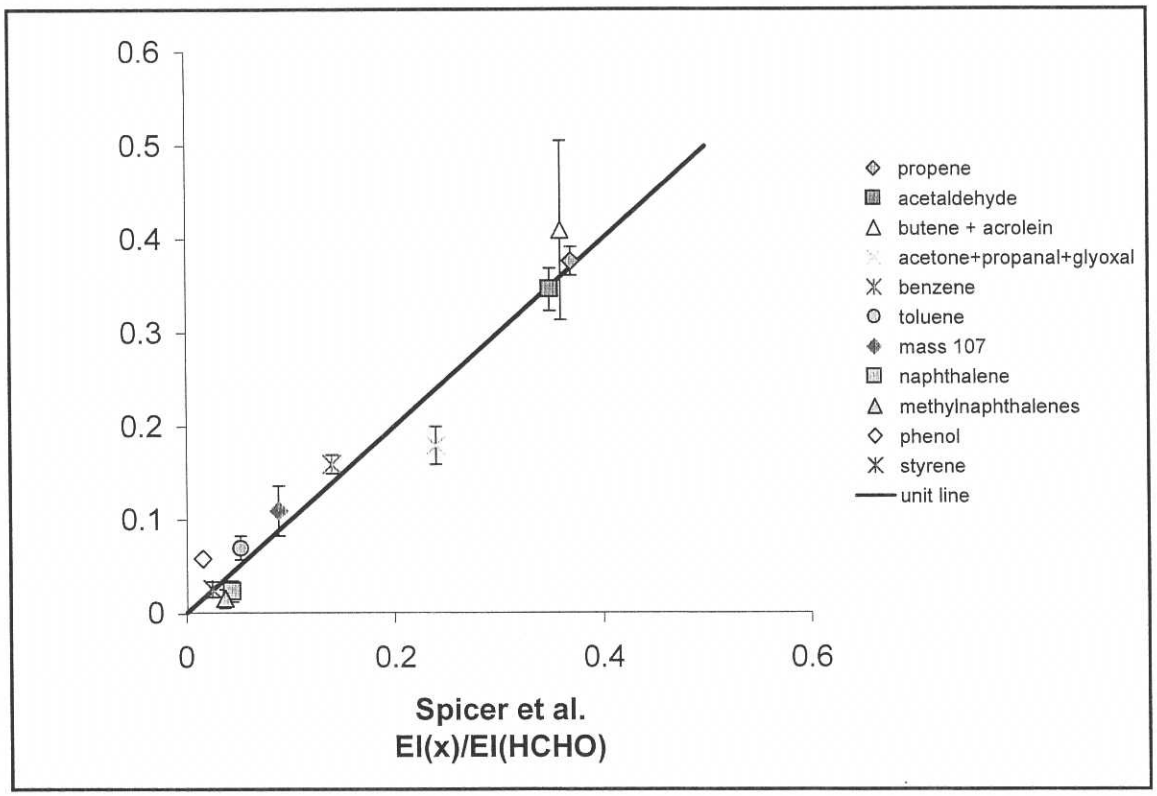

Figure 2. Correlation plot of normalized compound EIs derived from the APEX experiments versus that reported by Spicer et al. APEX data is derived from the slopes of the plots of EI(x) versus EI(HCHO) for data obtained at low power 4% - 15% rated thrust on the 1-meter probe. Error bars reflect the standard deviation of the three measurements.

The comparison of the various PTR-MS/TILDAS measurements across different engines in APEX3 provides strong support that the speciation profile is invariant across engine technologies for commercial engines. A similar question could be posed for the various military engines measured by Spicer and Gerstle. Initial analysis (data not shown here: KBE) indicates that there is much agreement between some of the relative amounts of relevant HAPs. Detailed analysis of the TF39 (a forerunner to the GE CF-6 engine) measured by Spicer is shown in Figure 3 comparing the speciation profiles for the TF39 with that of the CFM56 measured by Spicer, in analogy to what was shown in Figure 2 between the many engines of APEX1-3 and the Spicer CFM56-3. The speciation profiles for these two engines measured by Spicer, which received the careful analysis required for archival publication (Spicer et al. 1994), also support the contention that the speciation profile from aviation gas turbine engines is invariant across engine types.

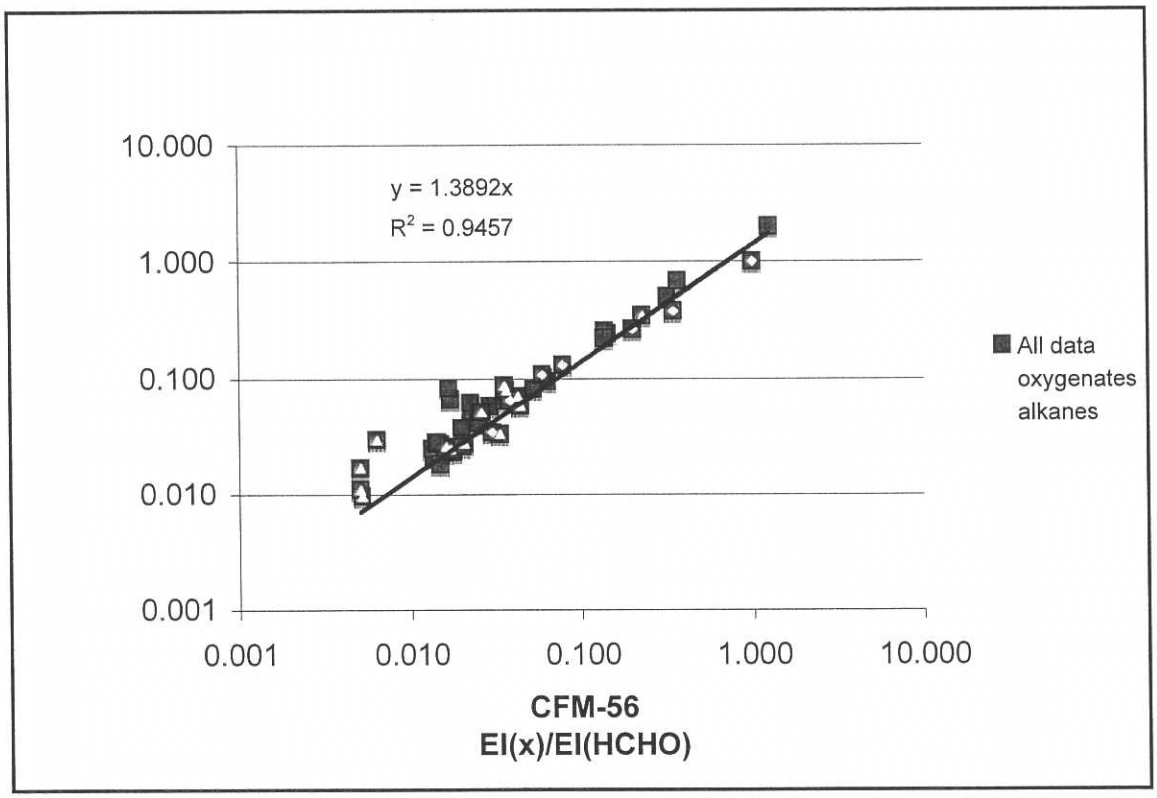

Figure 3. Correlation plot of normalized compound EIs for the TF39 vs. CFM56 engines at ground idle derived from the measurements reported by Spicer et al.

Discussion: The emissions of organic gases are controlled by combustion efficiency. The ICAO datasheets show a very clear trend of decreasing UHC emission indices from idle and approach to climb-out and take-off. There are strong dependences of the magnitude of UHC emissions between different engine models in the ICAO databank. The Yelvington et al. result from APEX-1 (Yelvington, Herndon et al. 2007) shows there is a strong dependence of the emissions of HCHO on temperature; that emissions increase at colder ambient temperatures, particularly for ground idle. This dependence is greater than estimated in the Boeing Fuel Flow Method-2[7] correction (DuBois and Paynter 2006).

Despite these strong dependences of the magnitude of UHC emissions on various factors, a remarkable and simplifying result is that the relative profile of organic gas emissions *near idle* does not have any such significant dependence, as presented in Figure 1. This has been demonstrated for various engines to be valid for conditions from ground idle up to ~15% of rated thrust. This invariant speciation profile demonstrates that despite large variations in the total amount of emissions, the ratio of benzene to ethylene, for example, is a relatively constant value among different conditions and engines.

[7] The Boeing Fuel Flow Method is a theory-based means of obtaining estimated emissions data at power conditions other than the ICAO specified power points by interpolating ICAO certification data.

One HC emission of particular note is methane (CH_4). This compound was measured by Spicer, but not in more recent studies. While methane is present in the exhaust of aircraft engines, it is present at levels below ambient levels for most power conditions (Spicer, Holdren et al. 1992, Wiesen et al, 1994, Vay et al., 1998). Indeed, in that reference Spicer notes "At power levels above idle, the exhaust is depleted in methane compared with the incoming air used for combustion. The methane concentrations observed in the engine exhaust are consistent with partial combustion of the atmospheric methane present in the inlet air, although some methane production during combustion cannot be ruled out." At idle the methane values in the exhaust during the Spicer were consistent with ambient levels, so any methane production must have been small enough to be within the experimental uncertainty or was balanced by methane consumption. Methane is not considered to be a significant emission from aircraft gas turbine engines burning Jet A, and is not included in the profile information provided here.[8]

At engine power conditions significantly higher that ~15% rated thrust, the engine combustion efficiency is so close to 100% that measurement of many HCs becomes difficult or impossible due to instrument detection levels for diluted exhaust gases (either with 1 m dilution probes or downwind sampling): the HC concentrations are too small to measure. Thus, when considering the total emissions contribution from a given aircraft operation, the amount of HCs is dominated by the low power conditions. Since the total emissions burden is the product of an emission index (g pollutant/kg fuel) times the fuel flow rate (kg fuel/sec) times the time in mode for that power condition, even the high fuel flow rates of take-off and climb-out cannot compensate for the very small emission indices for HCs and the short times in the take-off and climb-out power conditions.

The dominance of the low power conditions in determining the overall HC emission loading suggests that any changes to the HAPs profile above 15% power will have limited impact on the net HAPs loading. Since the emissions levels become too small to measure for many of the smallest percentage HAPs in the profile, a bound can be placed on how much their fractional contribution to the HAPs profile might be increasing as power increases. In lieu of specific data for these very small levels, a default of retaining the same profile as power increases beyond 15% could be suggested, which would be used for those powers above which the smallest contributors can be measured. An analysis of the potential errors introduced in using this default could be performed, however Figure 4 suggests that the limits of detection of the instruments, in combination with the rapidly decreasing overall HC emissions, will limit the overall uncertainties in the overall HC loading when using a low power HAPs profile.

Figure 4 demonstrates the relative importance of the elements of an LTO cycle by accounting for times in mode and emission indices for UHCs from the ICAO databank for a CFM56-3C1 engine (two engines for a 737-300). The LTO cycle in the figure reflects times in mode reported in the Boston Logan Airport 2005 Environmental Data

[8] When using this speciation profile in concert with reported certification HC emission indices, it is worth noting that ICAO CAEP Annex 16 Vol II makes no account for corrections to measured HCs due to ambient methane concentrations when reporting FID measurements for certification. Presumably ambient methane levels may be included in the certification FID measurements of EI HC unless otherwise noted.

Report (Wilkins 2007). Essentially, it is a modestly adjusted set of times but the same power conditions as a standard ICAO LTO cycle. Whatever the variation in the speciation profile at the higher powers, the lower EIs at the high powers preclude a significant impact on the total emissions burden from the complete LTO cycle, at least in this first attempt to assess the speciated emissions. Variation in the HC speciation profile at higher powers are unlikely to have a significant impact on airport air-quality modeling or to risk assessment from the compounds that are HAPs.

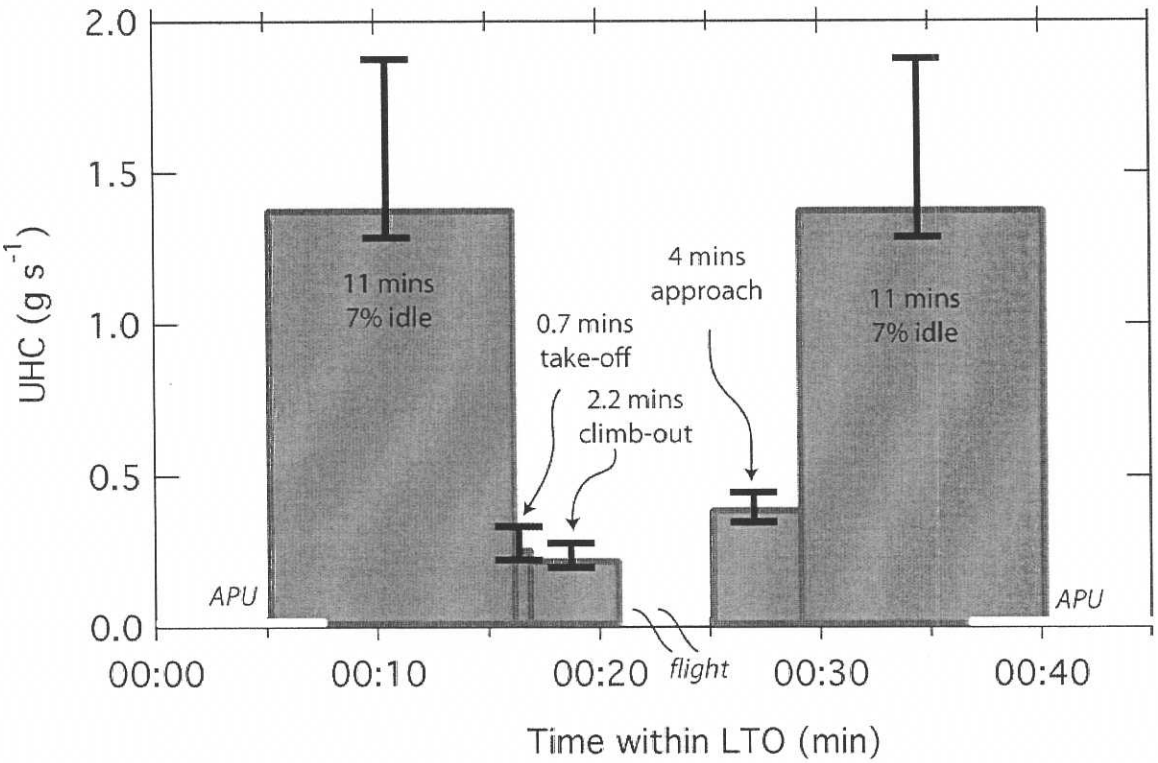

Figure 4. Emission Rate vs. Time in Mode. The estimated emission rate, coupling fuel flow and emission index for UHC for a CFM56-3C1. The LTO profile begins and ends with a 7.5 minute APU interval. In this figure the apparent area of the 'boxes' reflect the total emissions magnitude for the defined modes.

Relationship of Dedicated Engine Tests to Airport Measurements: Dedicated engine tests allow control of the engine operation. However emissions at airports are due to airplanes being operated as required to satisfy airline requirements. Table 3 compares normalized emission ratios (Species concentration/Formaldehyde concentration) for several APEX measurements and for advected plumes measured at Boston Logan, Zurich, and Oakland airports. While greater uncertainties might be expected in the advected plumes measured in a non-interference basis at airports, there is very good agreement between the emissions ratios measured in these disparate studies. In the advected plumes (last column) the error bars represent the width of the distribution of results. This uncertainty can be taken as an upper limit on the real variability in these ratios. When the detailed analysis of the instrumental contribution to this noise is complete, it will likely narrow the range of species variability, as opposed to instrument

noise. This is possible because the observed distribution in this sample is nearly Gaussian.

*Table 3. Speciated VOC Index Ratio (*HCHO relative*)*

Compound	Spicer et al.	APEX-1	Logan	EXC	Zurich	APEX-2	OAK
						Staged	Advected
HCHO	1	1	1			*1	1
Acetaldehyde	0.35	0.24	0.26			0.37	0.31±0.09
C_2H_4	1.26	0.78		1*	1*	0.76	0.85±0.3
Propene	0.36	0.31		0.32	0.32	0.45	0.42±0.2
Butenes+Acrolein	0.36	0.45	0.25	0.45	0.26[&]	0.49	
Pentenes	0.11	0.31			0.11		
Benzene	0.14	0.14	0.11	0.08	0.11	0.18	0.15±0.08
Toluene	0.05	0.06	0.06	0.01	0.13	0.09	
1-ring Aromatics	0.28	0.48	0.3	-	0.39	0.73	
Styrene	0.03	0.03			0.04	0.04	
Naphthalene	0.04	0.01				0.04	

Table Notes:

All values are in units of grams of VOC per gram of HCHO, except for the EXCAVATE column, which is grams of VOC per gram of C_2H_4.

*The EXCAVATE and Zurich datasets have been normalized by the emission index for ethene in lieu of formaldehyde.

[&]The Zurich tabulation for Butenes+Acrolein assumes the ratio of Acrolein to the sum of the butene isomers is that found in Spicer et al.

The APEX-2, Staged aircraft column represents the average result for 'ground-idle' including the following engines; 3 CFM56-7B22, 1 CFM56-3B1, 2 CFM56-3B2.

Tabulated values in the OAK Advected column represent Gaussian fits to the distribution of measured compound to HCHO ratios. The error bar is one Gaussian width.

Next Step Recommendations: First, recent work has reinforced the overall speciation for commercial engine as measured by Spicer for the CFM56-3 engine. Both in comparison to the TF39 measured by Spicer and the wider range of commercial engines in APEX1-3, this speciation profile is insensitive to engine type, engine power condition, and ambient conditions, even though those parameters significantly impact the ***total*** amount of UHCs (or VOCs or total HCs, however one wants to add up a total). Other measurements (Gerstle and airport advected plume studies) are also consistent with the general invariance, ***near idle***, of this speciation.

Several modest uncertainties are present, particularly for species that are present in small quantities. These may be due to measurement uncertainties, or due to actual variations in emissions numbers themselves. Modest dependences on fuel composition or other unknown parameters may cause some of this variation. Most of these variations are within the uncertainties between studies or engines. One notable exception is the significant variation associated with phenol. The APEX studies all agree with one another for phenol, while Spicer is significantly lower. Wall losses in the canister

sampling done by Spicer are a possible explanation for such a loss, but additional studies may be warranted to resolve this discrepancy.

For future work, two remaining questions should be kept in mind.

1. On which set of species do we need to focus to further refine the HAPs profile? (E.g.: [1] phenol discrepancy, [2] methanol and the several aromatics and long list of species present at a fraction of a percent of total mass not measured by Spicer et al., [3] questions regarding acrolein/butene etc.)
2. What is our approach to evaluating (and possibly revising) the UHC-to-VOC-to-TOG conversions?

With the completion of this analysis of Spicer and APEX data, we can offer the speciation profile provided in the accompanying spreadsheet for inclusion into the EPA's SPECIATE database.

Cited References:

Anderson, B. E., G. Chen and D. R. Blake (2006). "Hydrocarbon emissions from a modern commercial airliner." Atmospheric Environ. **40**(19): 3601-3612.

DuBois, D. and G. C. Paynter (2006). ""Fuel Flow Method2" for Estimating Aircraft Emissions." SAE Technical Paper Series **2006-01-1987**.

Gerstle, T., P. Virag and M. Wade (1999). "Aircraft Engine and Auxiliary Power Unit Emission Testing: Vol. 1." United States Air Force: IERA **RS-BR-TR-1999-0006**.

Herndon, S. C., T. Rogers, E. J. Dunlea, R. C. Miake-Lye and B. Knighton (2006). "Hydrocarbon emissions from in-use commercial aircraft during airport operations." Environmental Science and Technology **40**(14): 4406 - 4413.

Kinsey, J. S., Y. Dong, and D. C. Williams (in preparation 2008). "Characterization of Emissions from Commercial Aircraft Engines during the Aircraft Particle Emissions eXperiment (APEX)", U. S. Environmental Protection Agency, Office of Research and Development, National Risk Management Research Laboratory, Research Triangle Park, NC.

Knighton, W. B., T. Rogers, C. C. Wey, B. E. Anderson, S. C. Herndon, P. E. Yelvington and R. C. Miake-Lye (2007). "Application of Proton Transfer Reaction Mass Spectrometry (PTR-MS) for Measurement of Volatile Organic Trace Gas Emissions From Aircraft." Journal of Propulsion and Power **23**: 949-958.

Lobo, P., P. D. Whitefield, D. E. Hagen, S. C. Herndon, J. T. Jayne, E. C. Wood, W. B. Knighton, M. J. Northway, R. C. Miake-Lye, D. Cocker, A. Sawant, H. Agrawal and J. Wayne Miller (2007). "The development of exhaust speciation profiles for commercial jet engines." Final Report, Contract No. 04-344, California Air Resources Board, Sacramento, CA, October 31, 2007.

Lobo, P., D. E. Hagen, P. D. Whitefield and D. J. Alofs (2007). "Physical characterization of aerosol emissions from a Commercial Gas Turbine Engine." Journal of Propulsion and Power **23**: 919-929.

Onasch, T. B., J. T. Jayne, S. C. Herndon, P. Mortimer, D. R. Worsnop and R. C. Miake-Lye (2006). "Chemical Properties of Aircraft Engine Exhaust Aerosols Sampled During APEX." NASA/TM-2006-214382 **ARL_TR_3903**: Appendix J.

Schürmann, G., K. Schäfer, C. Jahn, H. Hoffmann, M. Bauerfeind, E. Fleuti and B. Rappenglück (2007). "The impact of NOx, CO and VOC emissions in the air quality of Zurich Airport." Atmospheric Environ. **41**: 103-118.

Spicer, C. W., M. W. Holdren, R. M. Riggin and T. F. Lyon (1994). "Chemical composition and photochemical reactivity of exhaust from aircraft turbine engines." Ann. Geophysicae **12**: 944-955.

Spicer, C. W., M. W. Holdren, D. L. Smith, D. P. Hughes and M. D. Smith (1992). "Chemical composition of exhaust from aircraft turbine engines." Journal of Engineering for Gas Turbines and Power **114**(1): 111-117.

Timko, M. T., S. C. Herndon, E. Wood, T. B. Onasch, M. J. Northway, J. T. Jayne, M. R. Canagaratna, R. C. Miake-Lye and W. Berk Knighton (manuscript in prepartion, 2008). "Gas Turbine Engine Emissions Part 1. Hydrocarbons and Nitrogen Oxides" Aerodyne Research, Inc., Billerica, MA.

Timko, M. T., T. B. Onasch, M. J. Northway, J. T. Jayne, M. R. Canagaratna, S. C. Herndon, E. Wood and R. C. Miake-Lye (manuscript in prepartion, 2008). "Gas Turbine Engine Emissions Part 2. Chemical Properties of Particulate Matter" Aerodyne Research, Inc., Billerica, MA.

URS and FAA (2003). Select resource materials and annotated bibliography on the topic of hazardous air pollutants (HAPs) associated with aircraft, airports and aviation. Technical Directive Memorandum: D01-010, CSSI Contract: DTFA 01-99-Y-01002.

Wey, C. C. (2004). Overview of the Aircraft Particle Emissions eXperiment (APEX) Program. Aircraft Particle Emissions Workshop, Cleveland, OH.

Vay, S.A., B.E. Anderson, G. W. Sachse, J. E. Collins, Jr., J. R. Podolske, C. H. Twohy, B. Gandrud, K. R. Chan, S. L. Baughcum, H. A. Wallio. (1998) DC-8-based observations of aircraft CO, CH_4, N_2O, and $H_2O_{(g)}$ emission indices during SUCCESS. Geophysical Research Letters 25 1717-1720.

Wey, C. C., B. E. Anderson, et al. (2006). "Aircraft Particle Emissions eXperiment (APEX)." NASA/TM-2006-214382 **ARL-TR-3903**.

Wiesen, P. J., J. Kleffmann, R. Kurtenbach, K.H. Becker. (1994) Nitrous Oxide and Methane Emissions form Aero Engines. Geophysical Research Letters 21 2027-2030.

Wilkins, J. (2007). Description of the 2005 Boston Logan Airport Environmental Data Report. S. Herndon. Boston: LTO times compiled from actual data collected at the airport during 2005.

Yelvington, P. E., S. C. Herndon, J. C. Wormhoudt, J. T. Jayne, R. C. Miake-Lye, W. B. Knighton and C. C. Wey (2007). "Chemical Speciation of Hydrocarbon Emissions from a Commercial Aircraft Engine." Journal of Propulsion and Power **23**: 912-918.

Aircraft Engine Speciated Organic Gases: Speciation Profile Spreadsheet

R.C. Miake-Lye

Introduction: A numerical spreadsheet[9] was developed that used both the Spicer data and APEX data to formulate a speciated profile of HC emissions, as discussed in the main body of this report. These several pages that follow are a description of the process used to develop that spreadsheet and an explanation of how the equations are used to provide the resulting calculated quantities. The spreadsheet (in Microsoft Excel format) is intended to accompany this documentation, with its data and imbedded equations.

The initial formulation of the spreadsheet was based on the several data sources (Spicer, and APEX, including both ARI/MSU and EPA contributions). These data sources are listed in columns, with the rows representing the numerous species measured by the several investigators. These data are combined to provide a single profile, as described more fully in the main body of the report. Below, the approach for that combination will be described.

After the profile was finalized, with many new species added and a few adjustments of specific species values from the original Spicer speciation, several additional quantities were calculated. The calculations are all imbedded in the spreadsheet, via the equations used to generate the quantities in the labeled cells, and the rationale behind the calculations will be presented below. The types of calculations are primarily directed at understanding how the speciated profile relates to the total amount of HCs emitted, which requires some assumptions since no measurement can quantify with complete certainty all of the HC emissions. As part of developing that understanding, calculations were also made to address questions of 1) how the limited measurements (such as that from a Flame Ionization Detector or FID, as used in certification testing) can be corrected to approximate the full HC complement and 2) how to convert HC emissions expressed in terms of methane mass equivalents, the reporting convention for HC EIs measured with a FID, into an estimate of the actual total mass of the full speciation profile, including unmeasured species. These calculations are all described below, as well.

An abbreviated version of the speciation spreadsheet is reproduced in Table 4 below. Species that have no mass fraction that are included in the spreadsheet for completeness are not included in Table 4. Also, the only columns from the spreadsheet that are shown in Table 4 are the profile species with non-zero mass fractions, their molecular mass and formula numbers, and the profile mass fraction. In the last two rows of Table 4, the fractions of the total profile mass represented by the identified species (71%) and that represented by the unidentified mass (29%) are listed, based on the total mass estimates given by Spicer and refined with the new measurements, and supported by the EPA

[9] The accompanying Microsoft Excel filename is **FAA-EPA_TSD_Speciated_HC_Aircraft_04AUG08.xls** and all references to columns, rows, or cells can be found in the worksheet titled "**Data Summary**".

APEX data as discussed in the main report. The approach for calculating these quantities is discussed below.

Table 4. Aircraft Profile Speciation

Species	Molecular Weight	Formula			Mass Fraction
		C	H	O	
Ethylene	28	2	4		0.15459
Acetylene	26	2	2		0.03939
Ethane	30	2	6		0.00521
Propylene	42	3	6		0.04534
Propane	44	3	8		0.00078
Isobutene/1-Butene	56	4	8		0.01754
1,3-Butadiene	54	4	6		0.01687
cis-2-Butene	56	4	8		0.00210
3-Methyl-1-butene	70	5	10		0.00112
1-Pentene	70	5	10		0.00776
2-Methyl-1-butene	70	5	10		0.00140
n-Pentane	72	5	12		0.00198
trans-2-Pentene	70	5	10		0.00359
cis-2-Pentene	70	5	10		0.00276
2-Methyl-2-butene	70	5	10		0.00185
4-Methyl-1-pentene	84	6	12		0.00069
2-Methylpentane	86	6	14		0.00408
2-Methyl-1-pentene	84	6	12		0.00034
1-Hexene	84	6	12		0.00736
trans-2-Hexene	84	6	12		0.00030
Benzene	78	6	6		0.01681
1-Heptene	98	7	14		0.00438
n-Heptane	100	7	16		0.00064
Toluene	92	7	8		0.00642
1-Octene	112	8	16		0.00276
n-Octane	114	8	18		0.00062
Ethylbenzene	106	8	10		0.00174
m-Xylene/p-Xylene	106	8	10		0.00282
Styrene	104	8	8		0.00309
o-Xylene	106	8	10		0.00166
1-Nonene	126	9	18		0.00246
n-Nonane	128	9	20		0.00062
Isopropylbenzene	120	9	12		0.00003
n-Propylbenzene	120	9	12		0.00053
m-Ethyltoluene	120	9	12		0.00154
p-Ethyltoluene	120	9	12		0.00064
1,3,5-Trimethylbenzene	120	9	12		0.00054
o-Ethyltoluene	120	9	12		0.00065
1,2,4-Trimethylbenzene	120	9	12		0.00350
1-Decene	140	10	20		0.00185
n-Decane	142	10	22		0.00320
1,2,3-Trimethylbenzene	120	9	12		0.00106
n-Undecane	156	11	24		0.00444
n-Dodecane	170	12	26		0.00462
n-Tridecane	184	13	28		0.00535

C14-alkane	198	14	30		0.00186
C15-alkane	212	15	32		0.00177
n-tetradecane	198	14	30		0.00416
C16-alkane	226	16	34		0.00146
n-pentadecane	212	15	32		0.00173
n-hexadecane	226	16	34		0.00049
C18-alkane	254	18	38		0.00002
n-heptadecane	240	17	36		0.00009
phenol	94	6	6	1	0.00726
naphthalene	128	10	8		0.00541
2-methyl naphthalene	142	11	10		0.00206
1-methyl naphthalene	142	11	10		0.00247
dimethylnapthalenes	156	12	12		0.00090
C4-Benzene + C3-aroald	134	10	14		0.00656
C5-Benzene+C4-aroald	148	11	16		0.00324
Methanol	32	1	4	1	0.01805
Formaldehyde (FAD)	30	1	2	1	0.12308
Acetaldehyde (AAD)	44	2	4	1	0.04272
Acetone	58	3	6	1	0.00369
Propionaldehyde	58	3	6	1	0.00727
Crotonaldehyde	70	4	6	1	0.01033
Butyraldehyde	72	4	8	1	0.00119
Benzaldehyde	106	7	6	1	0.00470
Isovaleraldehyde	86	5	10	1	0.00032
Valeraldehyde	86	5	10	1	0.00245
o-Tolualdehyde	120	8	8	1	0.00230
m-Tolualdehyde	120	8	8	1	0.00278
p-Tolualdehyde	120	8	8	1	0.00048
Methacrolein	70	4	6	1	0.00429
Glyoxal	58	2	2	2	0.01816
Methylglyoxal	72	3	4	2	0.01503
acrolein	56	3	4	1	0.02449
Sum of all identified species					**0.70787**
Unidentified mass					**0.29213**

Development of the Profile: As described in the main report, most of the species contributions measured by Spicer were supported by the APEX measurements. So, the data columns in the spreadsheet (not included in Table 4 above) show values for each measured species, in separate columns for each data source. If the data from APEX were not significantly different from Spicer's, the value from Spicer's column was used. This was true for almost all of the species measured by Spicer. The two exceptions were phenol and butyraldehyde (also called butanal). In these two cases, the more recent APEX data were used to update the values for those species. Then, additional species from either the ARI/MSU team (color coded blue in the spreadsheet) or from EPA (yellow) were also added to the species list and their contributions quantified. All of these quantifications are first entered into the spreadsheet as column L as ratios of emission indices of the species in question to the emission index of formaldehyde. Column L is titled "Revised Ratios" since these are the EI ratios of the individual species to formaldehyde accounting for both Spicer and the more recent APEX data.

Mass Fractions of Identified and Unidentified Species: Since the ratios of EIs are really mass ratios (EIs are mass ratios of the species to mass fuel burn, so ratioing EIs divides one EI by another and the fuel burn divides out), this column is a set of species:formaldehyde mass ratios. This is not useful for general application, since formaldehyde emissions are not generally measured or known. To be most generally useful, a profile for the full complement of species was desired. This could be done for the identified species, but there may be some HC species which contribute to the mass but which could not be identified.

In order to attempt to account for all of the HC species, including those not identified, Spicer's data was reviewed. Spicer attempted to do a complete carbon balance, based on the suite of instruments employed and accounting for corrections for sensitivities. With the set of species measured by Spicer, an estimate was made for the mass of the identified species and for those that were not identified. For the present purposes, we have taken Spicer's values to be correct for the unidentified species based on his measurements. We have also compared to the time-integrated LTO cycle HC data taken by EPA, which were taken under a different set of measurement protocols (integrating over power settings, including engine start, and the corresponding different effects of backgrounds) and have determined that the APEX EPA data is largely consistent with the Spicer data set (see main report).

So Spicer's unidentified mass fraction was taken as a starting point. However, the additional species included in APEX actually reduced this unidentified list and unidentified mass. And the adjustments of phenol and butyraldehyde must also be accounted for. So, in calculating column K of the spreadsheet (reproduced for non-zero mass fraction species in Table 4 above), the original species in Spicer's profile were summed (see cell K7 in the spreadsheet). In the equation in cell K7, the phenol and butyraldehyde values were individually reset to Spicer's original values rather than use the new "Revised Ratio" values in column L, and the sum was set to Spicer's original identified mass fraction so that Spicer's carbon balance could be used, albeit with the unidentified mass reduced due to the newly added species. (Note that Spicer quotes his numbers in terms of parts per million carbon (ppmC) concentrations. However, within the limits of accuracy of these calculations, the fractions of ppmC reported for identified and unidentified are equivalent to the masses identified and unidentified in that the mass/carbon for the two fractions, identified and unidentified, is not significantly different for these two fractions.)

With the sum calculated and set equal to the Spicer's identified mass fraction, the individual mass ratios in column L can be scaled such that they can be referenced to a total given by Spicer's carbon balance. Cell K7 of the spreadsheet takes the sum and uses Spicer's identified mass fraction, to give a scaling factor for each identified species in the "Revised Ratios" column (L) to give the resulting profile in column K. Because more species are now identified, the sum of the identified profile now comes to 70.8% of the total HC mass (cell K119). The new additions to the list represent 6.4 of the total HC mass (cell K120), while phenol and butyraldehyde adjust things a little as well from

Spicer's original identified mass. The unidentified mass represents 29.2% of the total mass in this new profile (K126).

Determining Effective Mass of Total Profile and Corrections for FID response: Since certification data from commercial engines are available, such data are often used for estimating HC emissions. Unfortunately, there are two problems with that certification data. The measurement device prescribed for this measurement uses a FID, which essentially "counts carbon atoms". This raises two problems. One is that the FID does not count carbon atoms that have an oxygen atom attached, and so is not equally sensitive to all HC species. Second, since the measurement is "counting carbons", it keeps track of a concentration and there is no direct indication of the mass of the species in question. (Mass is determined by the amount of hydrogen and oxygen in the molecule in addition to the number of carbons.) For the certification numbers, a mass/carbon based on the methane molecule (molecular mass 16.04) is used by convention. This is purely an assumption and has not been based on measurements to date, as far as the authors know.

These two problems can be addressed with the detailed profile provided in column K. For the known species, the mass/carbon can be calculated, since both the number of carbons and the molecular mass are known (given in Table 4 above and in spreadsheet columns D and H, as well as hydrogen and oxygen numbers provided in columns I and J). From the individual mass/carbon numbers and the mass fractions in column K, the mass-weighted mass/carbon can be calculated for the identified profile. In order to correct the mass for the total profile, one would need to have the mass-weighted mass/carbon for the complete profile. Since we do not have the molecular masses and formulas for the unidentified species (because they are unidentified), that calculation cannot be done rigorously. Thus, an estimate of the mass/carbon for the full profile is required.

In order to estimate the mass/carbon for the full profile, the mass/carbon was examined for two classes of species in the identified species. The first class represents those species present at greater than 1% of the total HC mass in column K. This includes many light oxygenated HCs, which have a large oxygen contribution to their total mass. The mass/carbon for these light species is not likely to be similar to those larger HC in the unidentified mass contributions. These light species have a mass/carbon of 17.6 (cell C130). The remaining species in the identified list have a mass/carbon of 14.4 (cell C132), which is likely closer to what might be expected for the larger, partially oxidized species in the unidentified component. Any deviation from 14.4 for the unidentified, while not expected to be large, is also devalued by the modest (29%) contribution of the unidentified to the total. This argument indicates that a good estimate for the mass/carbon for the full profile can be calculated using this approach. Thus, assigning 14.4 to the unidentified and combining with the identified, gives a total mass/carbon for the full profile of 15.97 (cell C137). (This is surprisingly close to the original convention of using methane's molecular mass of 16.04.)

The problem of the FID's lack of sensitivity to carbons bound to oxygen can also be rectified by the profile information. By a similar approach to calculating the mass-weighted mass/carbon, the mass-weighted C/H/O ratios for the various profile

components discussed above can be calculated. These are included in cells EFG130, EFG132, and EFG137. By ratioing to carbon, in cells EFG131, EFG133, and EFG138, the number of oxygens/carbon can be determined. Since each carbon effectively cancels out the measurement of one carbon by the FID, the FID response for the full profile can be estimated by subtracting cell G138 from cell E138 (or 1.00 – 0.1365). The FID response is then 0.8635 of the total carbon number, or the correction for the FID's lack of sensitivity due to oxygen containing molecules is 1.16 times the FID output.

To summarize:

To correct for the FID response to account for the oxygen content, multiply the FID measurement by 1.16.

To make use of the best estimate of the actual molecular masses of the HC species instead of using the equivalent methane convention, multiply the FID measurement by 15.97/16.04 = 0.996.

The net total correction is 1.16 times 0.996 = 1.16.

II, 1

APPENDIX 2

II, 2

6th International Conference
on Stability and Handling of Liquid Fuels
Vancouver, B. C., Canada
October 13-17, 1997

ELECTRICAL CONDUCTIVITY OF HITTS ADDITIVE PACKAGES FOR THE JP8+100 PROGRAMME

Brian Dacre* and Janice I. Hetherington

Rutherford Laboratory, Royal Military College of Science, Shrivenham, Swindon, Wilts SN6 8LA, UK.

ABSTRACT

The behaviour of two HITTS high temperature additive packages has been studied to examine possible interference with existing conductivity improver and also to assess their potential as conductivity improvers. The HITTS additives are shown to impart sufficient conductivity to fuels to meet certain fuel conductivity specifications without the addition of Stadis. Use of the HITTS additives with Stadis is shown to produce values of conductivity above the fuel specification. The conductivity performance of the HITTS additives is unaffected by the presence of phenolic or sodium salt impurities in the fuel which have been shown to have a detrimental effect on the performance of Stadis. The conductivity behaviour of the individual components of the HITTS additives is discussed. The dispersant is the main conducting component in the additive packages, but there are variations in the magnitude of the conductivity observed.

1. INTRODUCTION AND AIMS

The major objective of the JP8+100 programme is to improve the thermal stability of jet fuel using carefully selected additives. However, in this paper we examine the effects of such additives on properties which are unrelated to thermal stability characteristics, but which can have important consequences for the handling characteristics of the fuel.

In earlier papers[1,2,3] we examined the effects of a wide range of compounds, representative of naturally-occurring fuel components, on the performance of static dissipators (conductivity improvers). The work identified highly polar species capable of substantially reducing their effectiveness.

Certain HITTS packages are known to impart some conductivity to fuel. This work investigates the magnitude of this conductivity effect, on a model fuel and on three real fuels, for two Betz JP8+100 additives based on SPEC-AID 8Q405. SPEC-AID 8Q405, alone, at a concentration of

100mgl^{-1}, has been reported to produce an average conductivity increase of ~140pSm^{-1} in three reference fuels[4]. The spread of values in these fuels was not stated. The two fully formulated HITTS packages NB 345 S286 and SPEC-AID 8Q460 have been examined and components of the packages have been studied separately to identify components contributing to the conductivity.

The sensitivity of these HITTS packages to model impurities, phenols and sodium salts,has been determined and is compared with that of Stadis450. The effects of the HITTS additives on Stadis450 have also been measured.

Brief comments are made on the potential for the use of such additives as conductivity improvers.

2. EXPERIMENTAL

2.1 Materials: The composition of the HITTS additive packages NB 345 S286 and SPEC-AID 8Q460 are given in Table 1. The fully-formulated additives , SPEC-AID 8Q460 and NB234 S286A, the partially formulated package SPEC-AID8Q406 and the components SPEC-AID 8Q405(dispersant batch-1) and SPEC-AID8Q400(Betz metal deactivator) were supplied directly via Wright Patterson AFB by Betz Process Chemicals Inc. A second sample of SPEC-AID 8Q405 (batch-2), was supplied via British Petroleum. The additive BHT (2,6-diter-butyl-4-methyl phenol) was obtained from Aldrich Chemical Co Ltd., "conventional" metal deactivator (NN disalicylidene 1,2-propane diamine - abbreviated to c-MDA) from Pfalz and Bauer Inc., m-cresol from British Drug Houses and octylamine from Fluka Chemica.

Stocks of the HITTs fuels were held by and supplied to us by Shell. These were, an additive-free Merox base fuel (Merox-AF), having a kinematic viscosity of 3.698 mm^{2}s^{-1} at -20C , and two fuels produced from this to JetA1 and JP8 specification. These are designated Jet A1-MA1, which contains 1.87mgl^{-1} reformulated Stadis450 and JP8-MA2 which contains 1.87mgl^{-1} reformulated Stadis450 plus AL-48 to give a concentration of 1300mgl^{-1} of FSII and 27mgl^{-1}of Nalco 5403.

The sources and purification procedures employed for materials used previously, have been described[1,2,3].

2.2 Equipment and measurements: All measurements were made with the apparatus described previously[2,3] and made at 25C. The series of measurement was as follows:

i) time dependence of conductivity for NB 345 S286 and SPEC-AID8Q460 in dodecane.

ii) the conductivity of NB 345 S286 and SPEC-AID 8Q460 in dodecane and HITTS Fuels over

a concentration range of 10 mgl^{-1} to 800 mgl^{-1}.

iii) the conductivity of NB 345 S286 and SPEC-AID 8Q460, over a range 10mgl^{-1} to 800mgl^{-1}, in dodecane containing 3mgl^{-1} Stadis450

iv) *m*-cresol and 2,6-di-*tert*-butyl-4-methylphenol were added separately over the concentration range 50-1000 mgl^{-1} to solutions of 135mgl^{-1} NB 345 5286 in dodecane and HITTS Fuels and 127mgl^{-1} SPEC-AID 8Q460 in dodecane and HITTS Fuels. The conductivity was measured after each addition of the phenol.

v) sodium naphthenate was added, over the concentration range 0.3 to 18 mgl^{-1}, to solutions of 135mgl^{-1} NB 345 S286 in dodecane and 127mgl^{-1} SPEC-AID 8Q460 in dodecane. Conductivity measurements were made after each addition of sodium naphthenate.

vi) components of the additive packages namely SPEC-AID8Q405, SPEC-AID8Q400 and c-MDA were added separately to HITTS Fuels and the conductivity measured.

vii) test of the variability of samples of SPEC-AID8Q405 dispersant between batches (where impurity levels could be different) by measurement of the conductivity of batch 2 SPEC-AID,8Q405 in the three HITTS fuels to compare with similar results from batch 1.

viii) neutralisation of possible acidic impurities using SPEC-AID 8Q406 (SPEC-AID8Q405 + BHT antioxidant) was shaken for five minutes with finely divided $CaCO_3$ diluted with hexane, then separated and the solvent removed by evaporation. A control sample was treated in a similar way but without the $CaCO_3$.

Acid and Base Additions: In a preliminary attempt to investigate ion production mechanisms we have examined the effects of an amine and an acid on the conducting species. Octylamine, diluted in toluene, was added to a solution of 100mgl^{-1}dispersant SPEC-AID 8Q405 in the Merox-AF and the conductivity was measured after each addition. Similar measurements were made using dodecylbenzenesulphonic acid.

3. RESULTS AND DISCUSSION

3.1 The Time dependence of the Conductivity of Fully-Formulated Additives, NB345 S286 and SPEC-AID8Q460 in Dodecane Solutions

The time dependence of conductivity has been examined in a limited series of measurements over a three-hour period. These measurements were required in order to see if any large drifts in conductivity occurred during the time-scale of the experiments. The conductivity of the NB345 S286 solution(135mgl^{-1}) increases slowly with time whereas that for SPEC-AID8Q460 (127mgl^{-1})

shows a slow decrease. However in neither case were the changes sufficient to warrant detailed corrections to data obtained during the period of the experiments-normally about an hour.

3.2 Effect of Concentration of Fully-Formulated Additives on the Conductivity of Dodecane Solutions

Data in dodecane were required to provide a baseline for comparison with behaviour in real fuels. In these experiments only the the fully-formulated HITTS additive packages SPEC-AID 8Q460 and NB345 S286 were examined.

Figure 1 shows the effect of these packages on dodecane and demonstrates their ability to impart conductivity. We note also that the conductivity varies approximately linearly with concentration of the additive package, with the NB345 S286 giving a larger gradient than SPEC-AID8Q460. The recommended in-fuel concentrations of these additives are 135mgl^{-1} for the former and 127mgl^{-1} for the latter .

The behaviour of these packages in dodecane containing 3mgl^{-1} of original Stadis450 is shown in figure 2. The results of repeat runs, undertaken after an interval of nineteen months show a measurable change in behaviour. The fact that the stadis450/dodecane solution had a conductivity close to that in the original experiments suggests that the observed changes are due to ageing effects in the Hitts additives. The cause of the low concentration behaviour is not yet clear, however at concentrations >200mgl^{-1} the variation of conductivity with concentration for each package is similar to that observed in the absence of Stadis450. These low concentration effects are reminiscient of the effects of salts on Stadis450.

3.3 Effects of Polar Fuel Components on the Conductivity of Hitts Additives in Dodecane

Figure 3 shows the influence of m-cresol concentration on the conductivity of solutions containing given concentrations of (i) original-Stadis450, (ii) NB345 S286 and (iii) SPEC-AID8Q460. The concentrations chosen are recorded on the figures and correspond approximately to those used in jet fuels.

We previously reported on the influence of m-cresol on original-Stadis450[3] and this is also further discussed in an accompanying paper[5]. For SPEC-AID8Q460 we observe a small decrease in conductivity with concentration which is probably insignificant from a user viewpoint. For NB345 S286 conductivity appears to increase gradually with m-cresol concentration and the increase, after allowance for a small time correction, would be ~ 30pSm^{-1} at 1000mgl^{-1} m-cresol. For comparison figure 4 shows the effects of a highly hindered phenol of the type employed as

antioxidants. This is a good example of an almost complete lack of any antagonistic interaction with any of the three additives.

Earlier results on the effects sodium salts of a naphthenic acid, a phenol and dodecylbenzenesulphonic acid, on the behaviour of original-Stadis450, showed strong antagonistic effects on conductivity response[3] and these were qualitatively similar for all three types of salt. Sodium naphthenate was chosen as representative of these and its influence on the additive packages is shown in figure 5. For each HITTS package the concentration dependence of conductivity is quite different from that of Stadis solutions. There is no minimum, the conductivity remains approximately constant up to a concentration of ~ 2mgl^{-1} and then increases with concentration. We note that sodium naphthenate alone imparts some conductivity[3] , but this cannot account for the total observed increase. However, in this case, because the concentration of such compounds in fuels is likely to be low-probably <1mgl^{-1}, the practical effect of this will be very small.

3.4 Effects of Fully-Formulated Additives on the Conductivity of Hitts Fuels

We note that the conductivities of Jet A1-M1A and JP8-M2A, measured at the start of the study, are very similar, having values of ~ 500 pSm^{-1}. However , during the period of the work conductivity is seen to decrease for each fuel, with that for JP8 showing a fall of ~34% and for JetA1 a fall of ~20% over 250 days. This is taken into account in our comparisons of behaviour. The only difference between these fuel solutions is the presence of AL-48 in JP8-M2A. We know that in short-duration experiments AL-48 has no measurable effect on the performance of Stadis450[6]. No long-duration experiments ie up to ~250 days have yet been done.

Figure 6 shows the response of HITTs fuels to NB345 S286. This is represented by the increase in conductivity over the initial conductivity of the fuel. Dodecane data are shown for comparison. Clearly there are differences in response which follow the order : JP8 > Jet A1 > Merox-AF > Dodecane. Likewise figure 7 shows the response of HITTs fuels to SPEC-AID8Q460. In this case the differences in response are much less clear cut, though JP8 and Jet A1 again show greater resonse than Merox-AF and Dodecane. ie JetA1 ~ JP8 > Dodecane ~ Merox-AF. The lower viscosity for Merox-AF(1.45mm^{2}s^{-1}) compared with dodecane(1.86mm^{2}s^{-1}) at 25C would lead us to expect a higher conductivity in Merox-AF. Mixtures of aromatic and alkane liquids of a given viscosity are expected to promote a higher conductivity than an isoviscous pure alkane at the same temperature. Therefore the presence of aromatic components in Merox-AF(19%) will

raise the conductivity[6]. To these effects must also be added those due to interactions between additives. The net result on ion production is seen in the measured conductivity. Paradoxically the low concentration behaviour observed with these additivesin Stadis/dodecane mixtures is not observed in the more complex real fuel systems. In these cases however, the ageing effect has not yet been examined.

A practical point is that, at the recommended dosing concentration for HITTs additives in JP8 and JetA1, the total conductivities, as shown in table 2, are above the upper limit specification values of 600pSm^{-1} and 450 pSm^{-1} respectively. We also note that the conductivity of Merox-AF, containing the recommended concentrations *is* within the specification conductivity range for JetA1 without the addition of Stadis 450, but 8Q460 falls slightly short of the minimum value for JP8. However we feel that more data is required on batch-to-batch variations and on fuel composition effects.

3.5 Effect of Model Phenolic Impurities on the Conductivity of HITTS Additives in HITTS Fuels

Figure 8 shows that the total measured conductivities of SPEC-AID 8Q460 in Merox-AF are *insensitive* to the presence of *m*-cresol "impurities". Results for NB345 S286 are similar. The apparent sensitivity to *m*-cresol in the JP8 and JETA1 fuels can therefore be attributed to the interaction of the *m*-cresol with the Stadis450 in these fuels and not to any interaction of the *m*-cresol with NB 345 S286 or SPEC-AID8Q460.

3.6 Effects of Additive Components on the Conductivity of HITTS Fuels

Work on a range of phenol types[5] in dodecane has shown that highly hindered phenols have little or no effect on the conductivity of hydrocarbons nor do they adversely affect the performance of Stadis450. We have confirmed that BHT does not contribute to the conductivity of the additive package in any of the HITTS fuels.

Earlier measurements on conventional-MDA in dodecane showed it had no effect on conductivity[1]

Figure 9 shows that this is also true for solutions in Merox-AF and JP8. For Jet A1 a small decrease of ~10% is observed in the concentration range 0 to 100 mgl^{-1}.

In marked contrast, the Betz MDA, see figure 10, although it contributes only a small amount to the conductivity of Merox-AF, nevertheless has a considerable enhancing effect on the conductivity of Jet A1 and causes a modest reduction in the conductivity of JP8. These effects are clearly indicative of interaction between this MDA and components present in these fuels.

Repeat runs with this additive, after an ageing period of eighteen months, demonstrated an increased response. However, during this period the USAF decided not to consider a new MDA but to continue with conventional MDA. For this reason work on Betz MDA was discontinued. Figure 11 shows that the dispersant SPEC-AID8Q405 imparts significant conductivity to each of the fuels and conductivity varies linearly with concentration above ~50mgl^{-1}. We note the response follows the order JP8 > Jet A1 > Merox-AF as observed for the fully-formulated additive packages. In view of the results for BHT and c-MDA discussed above, it is clear that SPEC-AID8Q405 is the only conducting component in SPEC-AID8Q460 and is the main, but not the sole conducting component in NB345 S286.

3.7 Effect of Batch Variation on the Behaviour of SPEC-AID 8Q405

Figure 11, also demonstates batch to batch variation on the conductivity-improving ability of SPEC-AID 8Q405 with Batch 2 giving generally lower conductivity values. At a concentration of 100mgl^{-1}, batch-1 in Merox-AF meets the Jet-A1 and JP8 conductivity specifications, without Stadis, whereas batch-2 meets that for Jet-A1 only. Either batch added to Jet-A1 fuel causes the conductivity to be out of specification. This is also the case for addition of batch-1 to JP8 fuel. The magnitudes of some of the observed effects seems also to be influenced by ageing of the fuels and we hope to examine this further.

3.8 Preliminary Investigation of the Conducting Species

The conductivities of both carbonate-treated and untreated SPEC-AID8Q406 samples (see para 2.2) are identical. This suggests that participation of acidic species in the conduction process is unlikely.

Figure 12 shows that both dodecylbenzenesulphonic acid n-octylamine interact to increase the conductivity. Repeat experiments after an interval of sixteen months show, that apart from some small apparent differences at very low concentrations, the behaviour is generally unchanged within the experimental uncertainty. In the case of the sulphonic acid the effect is partly due to the acid itself[1,3]. However, this cannot be the explanation for the effect of the amine which alone has no effect on the conductivity[6]. More information is required before much speculation can be justified.

4. SUMMARY AND CONCLUSIONS

4.1 CONDUCTIVITY BEHAVIOUR OF HITTS PACKAGES

4.1.1 In Model Fuel (Dodecane) with Model Impurities

1 Both the HITTS packages impart conductivity which shows a small time dependence.

2 Both the HITTS packages can impart conductivity to fuel, without the use of Stadis450.

3 The conductivity response of both the HITTS packages is insensitive to phenolic impurities.

4 The conductivity response of both the HITTS packages is insensitive to sodium salts.

5 The HITTS packages have the advantage of imparting the required conductivity to fuels without the sensitivity to fuel impurities, such as phenols and sodium salts, which is detrimental to Stadis450.

4.1.2 In HITTS Fuels

1 Both the HITTS additive packages used at the recommended concentration in the HITTS fuels JP8 MA2 and JETA1 M1A, gave conductivities *above* the fuel specification.

2 The conductivity of the MeroxA-F containing the recommended levels of both HITTS packages was within the fuel conductivity specification for Jet-A1 *without* the use of Stadis450. For JP8 with the additive 8Q460, conductivity falls slightly short of the minimum conductivity specification

3 There is a simple linear relationship between conductivity and the concentration of the HITTS additives.

4 Both the HITTS additive packages appear to be unaffected by the presence of phenolic impurities in fuel.

5 Reduction in conductivity in the HITTS JP8 and JET A1 with the HITTS additives in the presence of phenolic impurities is attributed to interaction of the phenol with the Stadis 450 in these fuels.

6 The HITTS additives show potential as conductivity improvers. Additional work is required on batch-to batch variation, ageing effects and on the temperature dependence of conductivity before these additives can be given serious consideration as sole conductivity improvers.

II, 10

4.2 CONDUCTIVITY BEHAVIOUR OF *INDIVIDUAL COMPONENTS* OF HITTS ADDITIVES

1 The c-MDA contributes little to the conductivity of the HITTS additive.

2 The contribution of the Betz MDA to conductivity is complex. In the Merox-AF the Betz MDA contributes a small increment to the conductivity. In the JP8 it produced a reduction in conductivity and in the JETA1 it produced an increase in conductivity. The reasons for the variations could be due to interaction with Stadis450 and/or water in the fuels. Recently the Betz MDA has ceased to be of interest to USAF.

3 The BHT antioxidant does not contribute to the conductivity of the HITTS additives.

4 The dispersant SPEC-AID8Q405 is the main conducting component in the HITTS additives. At 100mgl^{-1} in the presence of Stadis, conductivity will generally exceed the specification upper limit. In the absence of Stadis it is likely that the Jet-A1 specification will be met but there is uncertainty with respect to JP8.

5. ACKNOWLEDGEMENTS

The authors wish to thank additive manufacturers and oil companies, in particular BP, for their constructive cooperation and for supplies of additives and fuels. Especially they would like to thank BP and DRA for many helpful and enjoyable discussions during the course of this work. They also wish to express their thanks to the DRA for its funding support provided under DRA Contract LSF/E 20093.

6. REFERENCES

1.Dacre,B.; Abi Aoun, W.G. The Effects of Fuel Components on the Behaviour of Conductivity Improvers in Jet Fuel, 4th International Conference on Stability and Handling of Liquid Fuels, Orlando, Florida,USA, November 1991.

2.Dacre,B.; Abi Aoun, W.G. Effects of Fuel Components on the Performance of Conductivity Improvers in Hydrocarbons, Journal of Electrostatics,39(1997)89-110.

3.Dacre,B.; Hetherington, J.I. Behaviour of Conductivity Improvers in Jet Fuel, 5th International

Conference on Stability and Handling of Liquid Fuels, Rotterdam, The Netherlands, October 1994.

4.Anderson, S.D.; Harrison,W.E.; Edwards,T.; Morris,R.W.; Shouse,D.T. Development of Thermal Stability Additive Packages for JP-8, 5th International Conference on Stability and Handling of Liquid Fuels, Rotterdam, The Netherlands, October 1994.

5.Dacre,B.; Hetherington, J.I. The Effect of Phenolic Impurities in Jet Fuel on the Behaviour of Conductivity Improvers, 6th International Conference on Stability and Handling of Liquid Fuels Vancouver, B. C., Canada, October 13-17, 1997 .

6.Dacre,B.; Hetherington, J.I. Preliminary unpublished work.

II, 12

Commercial Additive	Description	Concentration Added to Fuel	Comments
BHT	Antioxidant 2,6-di-*tert*-butyl-4-methylphenol	25mgl^{-1}	
MDA (conventional)	Metal Deactivator NN'disalicylidene-1,2-propanediamine	10mgl^{-1}	
8Q405	Dispersant BETZ (proprietory)	100mgl^{-1}	
Spec Aid 8Q400	Betz Metal Deactivator	10mgl^{-1}	Different chemistry from conventional DuPont MDA
Spec Aid 8Q406	8Q405 / BHT dispersant / antioxidant	125mgl^{-1}	
NB 345 S286A	Experimental 8Q405/BHT/8Q400 Dispersant / Antioxidant / Betz MDA	135mgl^{-1}	Assumed composition: 8Q405 100mgl^{-1} BHT 25mgl^{-1} MDA 10mgl^{-1} (Betz)
Spec Aid 8Q460	8Q405 / BHT /MDA Dispersant / Antioxidant / MDA (conventional chemistry)	127mgl^{-1}	Assumed composition: 8Q405 100mgl^{-1} BHT 25mgl^{-1} MDA 2mgl^{-1} (conventional)

Table 1 **Composition of HITTS High Temperature Additive Packages**

II, 13

FUELS	SPEC AID8Q460 $127mgl^{-1}$	NB 345 S286 $135mgl^{-1}$
Merox-AF	123	221
Jet-A1	666	817
JP8	668	864
Dodecane	132	200

Values taken from data in figures 7 and 8.

Specification Conductivity ranges: Jet-A1 50--450pSm^{-1}
JP8 150--600pSm^{-1}

Table 2 Measured Conductivities (pSm^{-1}) in HITTS Fuels

Fuel	Batch-1 $100mgl^{-1}$	Batch-2 $100mgl^{-1}$
Merox-AF	158	115
Jet-A1	689	584
JP8	671	557

Values taken from data in figure 11.

Table 3 Measured Conductivities (pSm^{-1}) of 8Q405 in HITTS Fuels

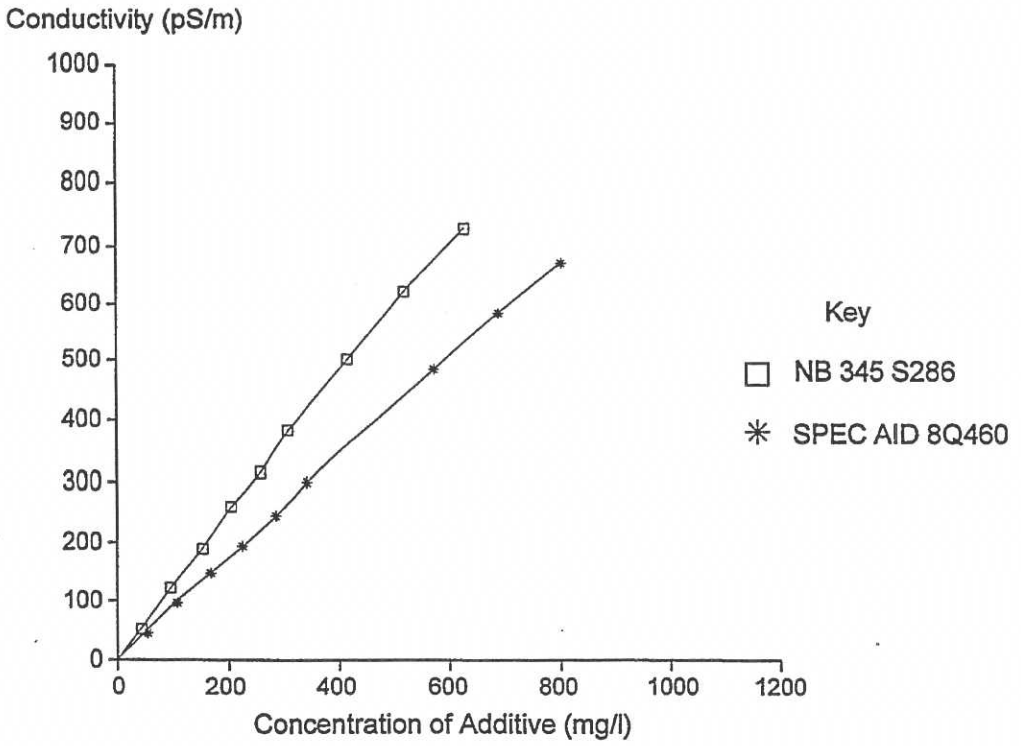

Fig. 1 Conductivity vs. Concentration for High Temperature Additive Packages in Dodecane

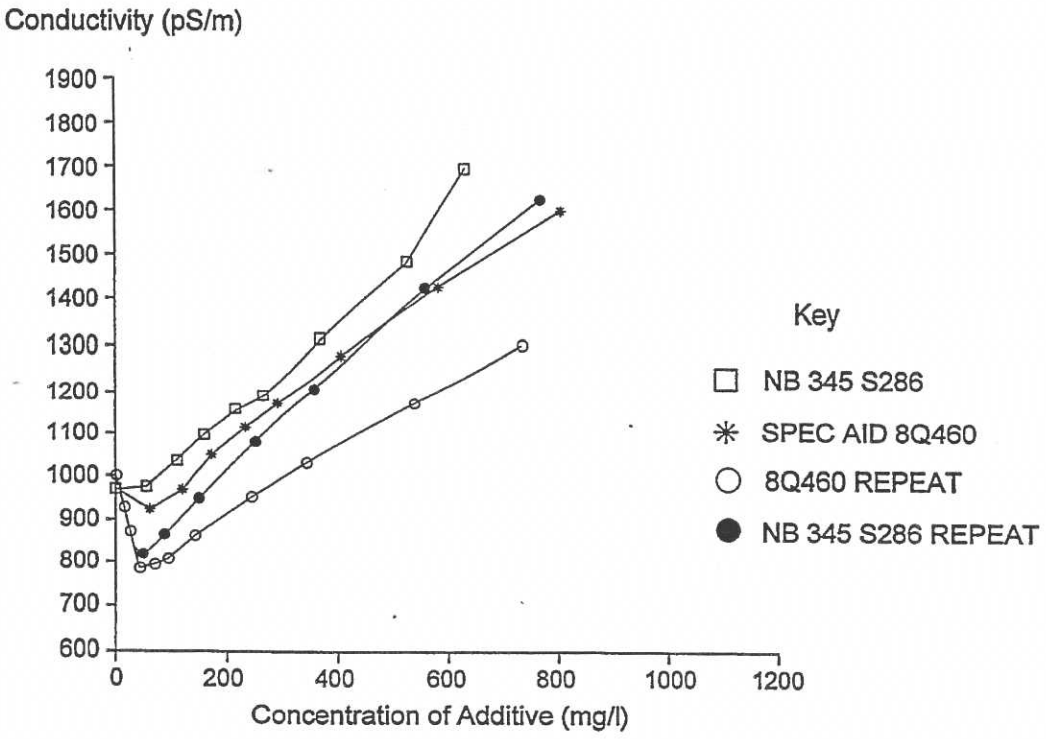

Fig. 2 Effect of High Temperature Additive Packages on Conductivity of 3mg/l STADIS 450 in Dodecane

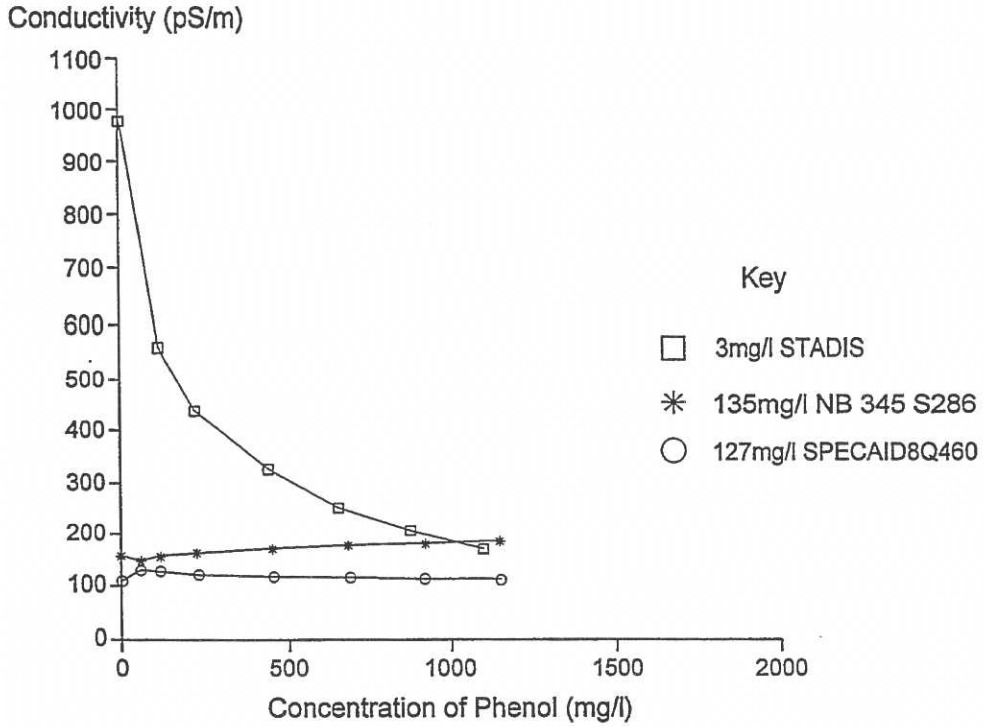

Fig. 3 ffect of m-Cresol on Conductivity of Stadis 450 and High Temperature Additive Packages in Dodecane

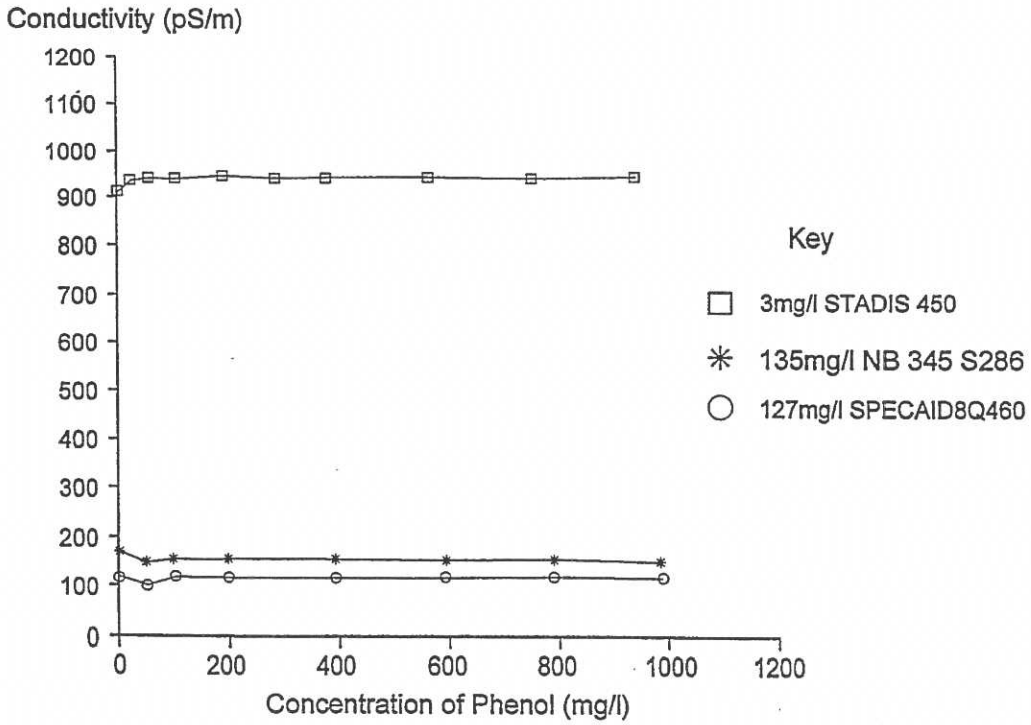

Fig. 4 Effect of 2,6di(tert)butyl-4-methylphenol on Conductivity of Stadis 450 and High Temperature Additive Packages in Dodecane

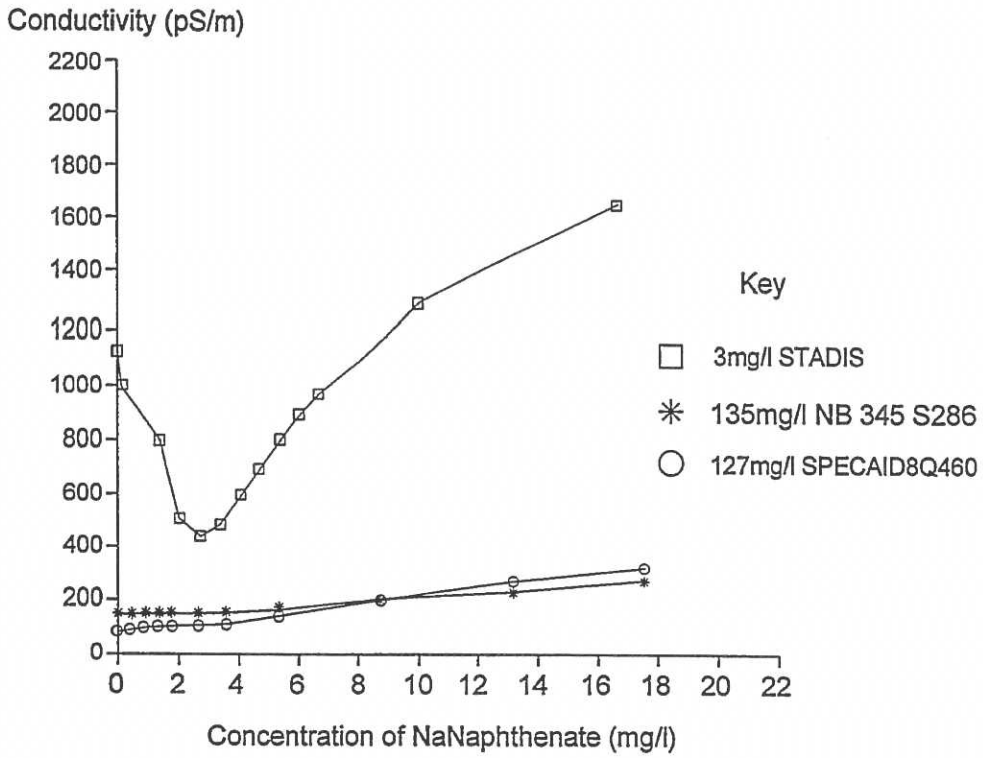

Fig. 5 Effect of Sodium Naphthenate on Conductivity of Stadis 450 and High Temperature Additive Packages in Dodecane

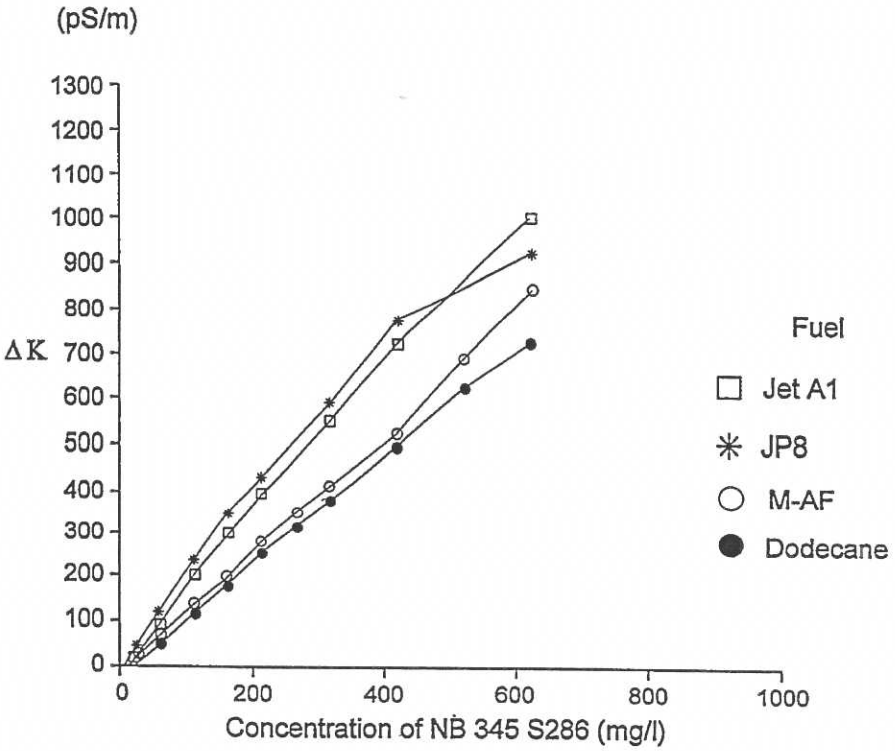

Fig. 6 Effect of NB 345 S286 on the Conductivity of HITTS Fuels

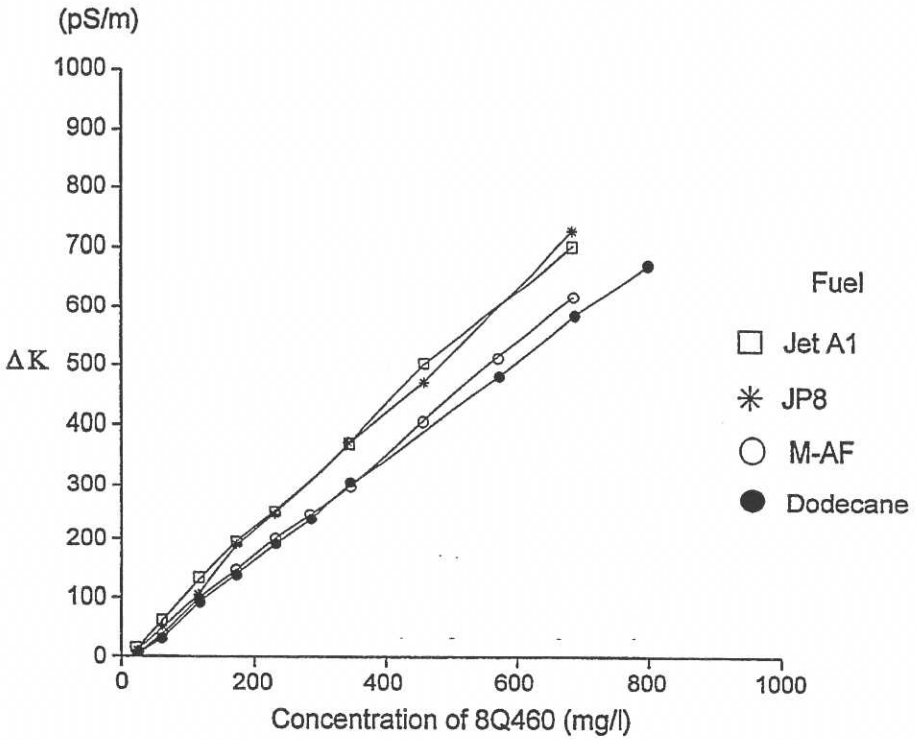

Fig. 7 Effect of 8Q460 on the Conductivity of HITTS Fuels

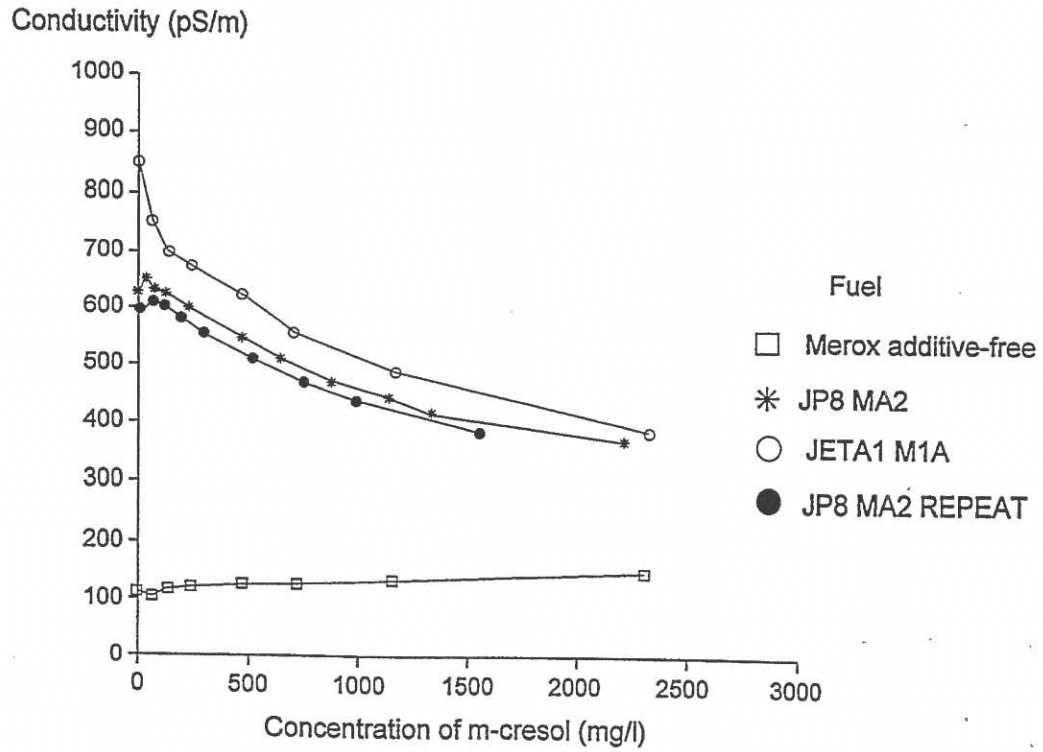

Fig. 8 Effect of m-cresol on Conductivity of 127 mg/l SPECAID 8Q460 in HITTS Fuels

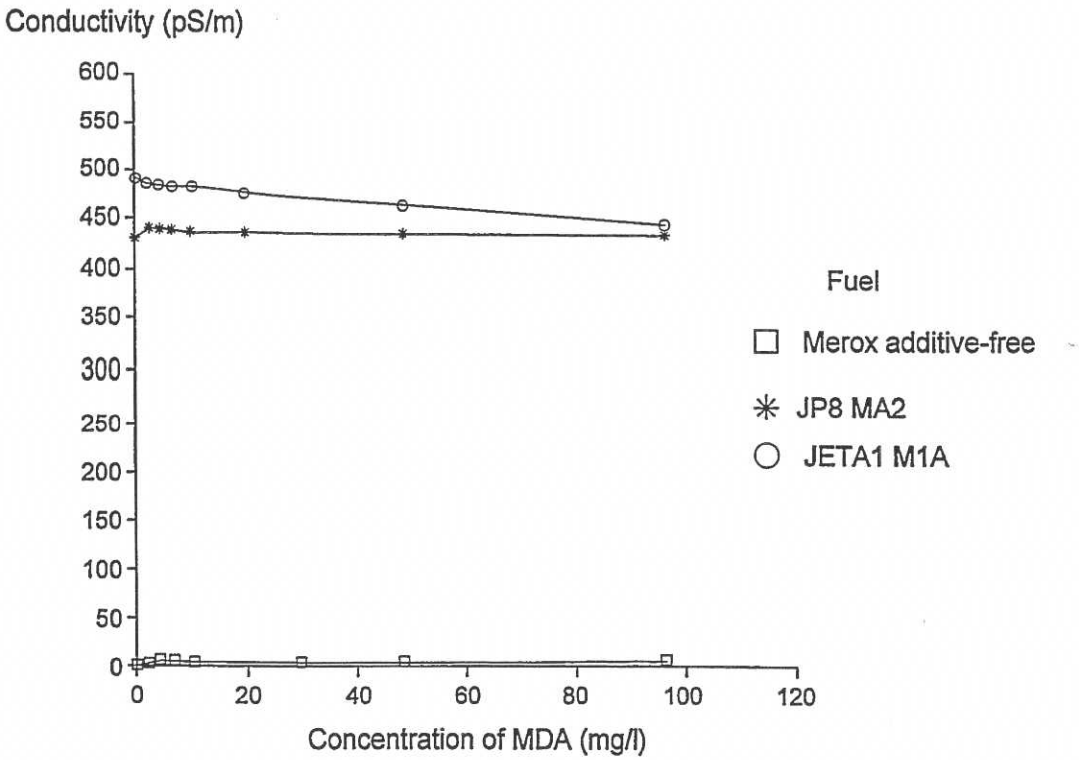

Fig. 9 Effect of MDA (conventional) on Conductivity of HITTS Fuels

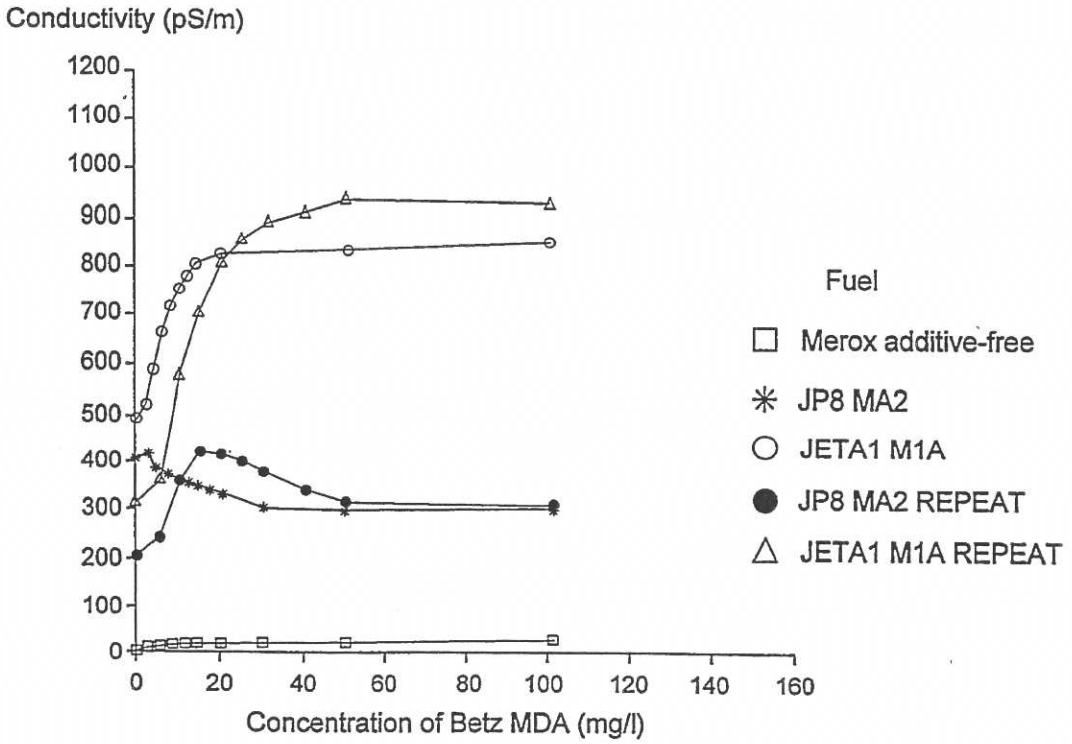

Fig. 10 Effect of Betz MDA on Conductivity of HITTS Fuels

II, 19

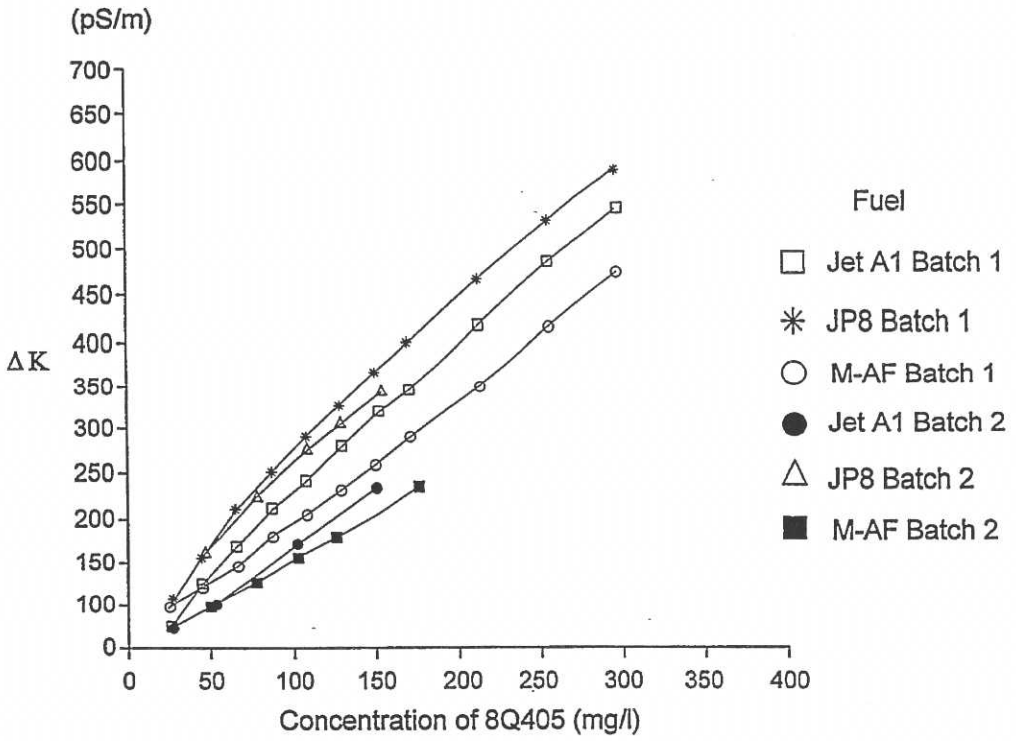

Fig. 11 Effect of 8Q405 and Batch Variation on the Conductivity of HITTS Fuels

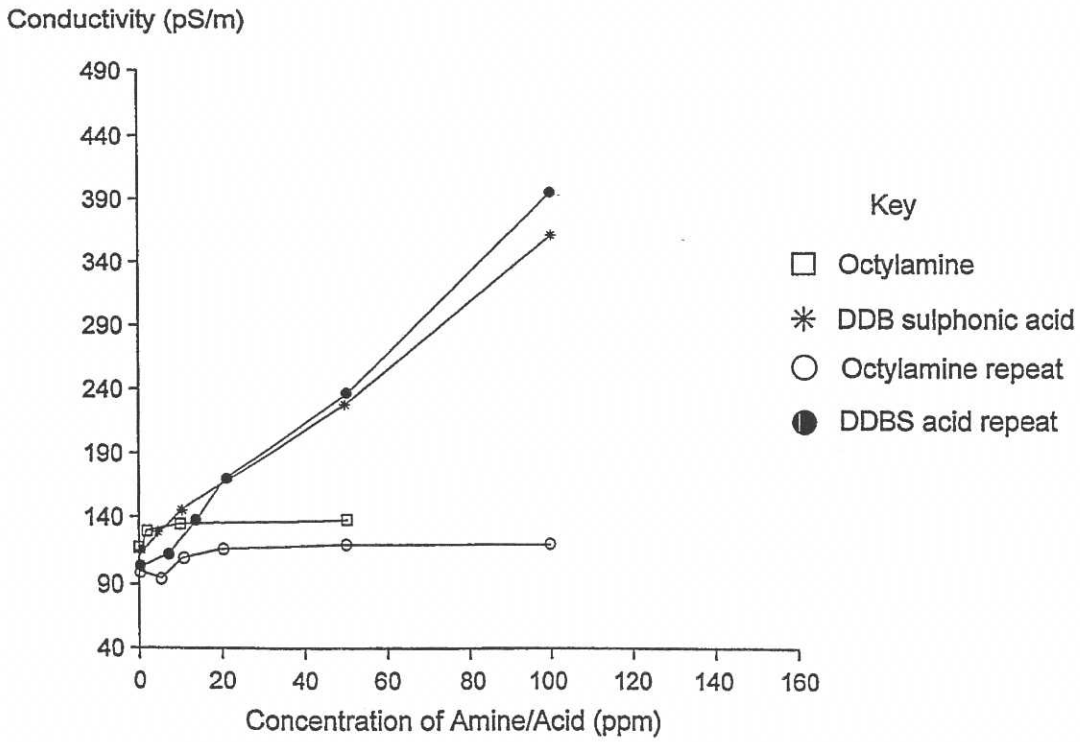

Fig. 12 Betz Dispersant 8Q405(Batch 2) 100mg/l in HITTS Additive-free Merox
Effect of Acid or Amine on Conductivity

II, 20

METRIC

MIL-DTL-83133F
11 April 2008

SUPERSEDING
MIL-DTL-83133E
1 April 1999

DETAIL SPECIFICATION

TURBINE FUEL, AVIATION, KEROSENE TYPE, JP-8 (NATO F-34), NATO F-35, and JP-8+100 (NATO F-37)

This specification is approved for use by all Departments and Agencies of the Department of Defense.

Comments, suggestions, or questions on this document should be addressed to HQ AFPET/AFTT, 2430 C Street, Bldg 70, Area B, Wright-Patterson AFB OH 45433-7632 or e-mailed to AFPET.AFTT@wpafb.af.mil. Since contact information can change, you may want to verify the currency of this address information using the ASSIST Online database at http://assist.daps.dla.mil.

AMSC N/A

FSC 9130

DISTRIBUTION STATEMENT A. Approved for public release; distribution is unlimited.

1. SCOPE

1.1 Scope. This specification covers three grades of kerosene type aviation turbine fuel, JP-8 (NATO F-34), NATO F-35, and JP-8+100 (NATO F-37). This specification was thoroughly reviewed as a part of acquisition reform. While most of the requirements were converted to performance terms, not all requirements could be converted due to the military-unique nature of the product (see 6.1) and the need for compatibility with deployed systems. The issuance of this specification as "detail" is not intended to constrain technology advances in future systems.

1.2 Classification. Aviation turbine fuel will be of the following grades, as specified (see 6.2).

Grade	NATO Code No.	Description
JP-8	F-34	Kerosene type turbine fuel which will contain a static dissipator additive, corrosion inhibitor/lubricity improver, and fuel system icing inhibitor, and may contain antioxidant and metal deactivator.
	F-35	Kerosene type turbine fuel which will contain a static dissipator additive, may contain antioxidant, corrosion inhibitor/lubricity improver, and metal deactivator but will not contain fuel system icing inhibitor.
JP-8+100	F-37	JP-8 type kerosene turbine fuel which contains thermal stability improver additive (NATO S-1749) as described in 3.3.6.

2. APPLICABLE DOCUMENTS

2.1 General. The documents listed in this section are specified in sections 3, 4, or 5 of this specification. This section does not include documents cited in other sections of this specification or recommended for additional information or as examples. While every effort has been made to ensure the completeness of this list, document users are cautioned that they must meet all specified requirements of documents cited in sections 3, 4, or 5 of this specification, whether or not they are listed.

2.2 Government documents.

2.2.1 Specifications, standards, and handbooks. The following specifications, standards, and handbooks form a part of this document to the extent specified herein. Unless otherwise specified, the issues of these documents are those cited in the solicitation or contract.

DEPARTMENT OF DEFENSE SPECIFICATIONS

MIL-DTL-5624	Turbine Fuel, Aviation, Grades JP-4 and JP-5
MIL-PRF-25017	Inhibitor, Corrosion/Lubricity Improver, Fuel Soluble
MIL-DTL-85470	Inhibitor, Icing, Fuel System, High Flash NATO Code Number S-1745

DEPARTMENT OF DEFENSE STANDARDS

MIL-STD-290	Packaging of Petroleum and Related Products

QUALIFIED PRODUCTS LIST

QPL-25017	Inhibitor, Corrosion/Lubricity Improver, Fuel Soluble

(Copies of these documents are available from the Standardization Document Order Desk, 700 Robbins Avenue, Building 4D, Philadelphia PA 19111-5094 or online at http://assist.daps.dla.mil)

2.3 Non-government publications. The following documents form a part of this document to the extent specified herein. Unless otherwise specified, the issues of these documents are those cited in the solicitation or contract.

ASTM International

ASTM D 56	Standard Test Method for Flash Point by Tag Closed Cup Tester (DoD Adopted)
ASTM D 86	Standard Test Method for Distillation of Petroleum Products at Atmospheric Pressure (DoD Adopted)
ASTM D 93	Standard Test Methods for Flash Point by Pensky-Martens Closed Cup Tester (DoD Adopted)
ASTM D 129	Standard Test Method for Sulfur in Petroleum Products (General Bomb Method) (DoD Adopted)
ASTM D 130	Standard Test Method for Corrosiveness to Copper from Petroleum Products by Copper Strip Test (DoD Adopted)
ASTM D 156	Standard Test Method for Saybolt Color of Petroleum Products (Saybolt Chromometer Method) (DoD Adopted)
ASTM D 381	Standard Test Method for Gum Content in Fuels by Jet Evaporation (DoD Adopted)
ASTM D 445	Standard Test Method for Kinematic Viscosity of Transparent and Opaque Liquids (and the Calculation of Dynamic Viscosity) (DoD Adopted)
ASTM D 976	Standard Test Methods for Calculated Cetane Index of Distillate Fuels (DoD Adopted)
ASTM D 1094	Standard Test Method for Water Reaction of Aviation Fuels (DoD Adopted)
ASTM D 1266	Standard Test Method for Sulfur in Petroleum Products (Lamp Method) (DoD Adopted)
ASTM D 1298	Standard Test Method for Density, Relative Density (Specific Gravity), or API Gravity of Crude Petroleum and Liquid Petroleum Products by Hydrometer Method (DoD Adopted)
ASTM D 1319	Standard Test Method for Hydrocarbon Types in Liquid Petroleum Products by Fluorescent Indicator Adsorption (DoD Adopted)
ASTM D 1322	Standard Test Method for Smoke Point of Kerosine and Aviation Turbine Fuels (DoD Adopted)
ASTM D 1840	Standard Test Method for Naphthalene Hydrocarbons in Aviation

	Turbine Fuels by Ultraviolet Spectrophotometry (DoD Adopted)
ASTM D 2276	Standard Test Method for Particulate Contaminant in Aviation Fuel by Line Sampling (DoD Adopted)
ASTM D 2386	Standard Test Method for Freezing Point of Aviation Fuels (DoD Adopted)
ASTM D 2622	Standard Test Method for Sulfur in Petroleum Products by Wavelength Dispersive X-Ray Fluorescence Spectrometry (DoD Adopted)
ASTM D 2624	Standard Test Methods for Electrical Conductivity of Aviation and Distillate Fuels (DoD Adopted)
ASTM D 2887	Standard Test Method for Boiling Range Distribution of Petroleum Fractions by Gas Chromatography (DoD Adopted)
ASTM D 3120	Standard Test Method for Trace Quantities of Sulfur in Light Liquid Petroleum Hydrocarbons by Oxidative Microcoulometry (DoD Adopted)
ASTM D 3227	Standard Test Method for (Thiol Mercaptan) Sulfur in Gasoline, Kerosine, Aviation Turbine, and Distillate Fuels (Potentiometric Method) (DoD Adopted)
ASTM D 3241	Standard Test Method for Thermal Oxidation Stability of Aviation Turbine Fuels (JFTOT Procedure) (DoD Adopted)
ASTM D 3242	Standard Test Method for Acidity in Aviation Turbine Fuel (DoD Adopted)
ASTM D 3338	Standard Test Method for Estimation of Net Heat of Combustion of Aviation Fuels (DoD Adopted)
ASTM D 3343	Standard Test Method for Estimation of Hydrogen Content of Aviation Fuels (DoD Adopted)
ASTM D 3701	Standard Test Method for Hydrogen Content of Aviation Turbine Fuels by Low Resolution Nuclear Magnetic Resonance Spectrometry (DoD Adopted)
ASTM D 3828	Standard Test Methods For Flash Point by Small Scale Closed Cup Tester (DoD Adopted)
ASTM D 3948	Standard Test Method for Determining Water Separation Characteristics of Aviation Turbine Fuels by Portable Separometer (DoD Adopted)
ASTM D 4052	Standard Test Method for Density and Relative Density of Liquids by Digital Density Meter (DoD Adopted)
ASTM D 4057	Standard Practice for Manual Sampling of Petroleum and Petroleum Products (DoD Adopted)
ASTM D 4177	Standard Practice for Automatic Sampling of Petroleum and Petroleum Products (DoD Adopted)
ASTM D 4294	Standard Test Method for Sulfur in Petroleum and Petroleum Products by Energy-Dispersive X-Ray Fluorescence Spectrometry (DoD Adopted)
ASTM D 4306	Standard Practice for Aviation Fuel Sample Containers for Tests Affected by Trace Contamination (DoD Adopted)
ASTM D 4529	Standard Test Method for Estimation of Net Heat of Combustion of Aviation Fuels
ASTM D 4737	Standard Test Method for Calculated Cetane Index by Four Variable Equation

ASTM D 4809	Standard Test Method for Heat of Combustion of Liquid Hydrocarbon Fuels by Bomb Calorimeter (Precision Method) (DoD Adopted)
ASTM D 4952	Standard Test Method for Qualitative Analysis for Active Sulfur Species in Fuels and Solvents (Doctor Test) (DoD Adopted)
ASTM D 5001	Standard Test Method for Measurement of Lubricity of Aviation Turbine Fuels by the Ball-on-Cylinder Lubricity Evaluator (BOCLE)
ASTM D 5006	Standard Test Method for Measurement of Fuel System Icing Inhibitors (Ether Type) in Aviation Fuels (DoD Adopted)
ASTM D 5186	Standard Test Method for Determination of the Aromatic Content and Polynuclear Aromatic Content of Diesel Fuels and Aviation Turbine Fuels by Supercritical Fluid Chromatography
ASTM D 5452	Standard Test Method for Particulate Contamination in Aviation Fuels by Laboratory Filtration (DoD Adopted)
ASTM D 5453	Standard Test Method for Determination of Total Sulfur in Light Hydrocarbons, Spark Ignition Engine Fuel, Diesel Engine Fuel, and Engine Oil by Ultraviolet Fluorescence
ASTM D 5972	Standard Test Method for Freezing Point of Aviation Fuels (Automatic Phase Transition Method)
ASTM D 6045	Standard Test Method for Color of Petroleum Products by the Automatic Tristimulus Method
ASTM D 7153	Standard Test Method for Freezing Point of Aviation Fuels (Automatic Laser Method)
ASTM D 7154	Standard Test Method for Freezing Point of Aviation Fuels (Automatic Fiber Optical Method)
ASTM D 7224	Standard Test Method for Determining Water Separation Characteristics of Kerosine-type Aviation Turbine Fuels Containing Additives by Portable Separometer
ASTM E 29	Standard Practice for Using Significant Digits in Test Data to Determine Conformance with the Specifications (DoD Adopted)
IEEE/ASTM SI 10	American National Standard for Use of the International System of Units (SI): The Modern Metric System (DoD Adopted)

(Copies of these documents are available at ASTM International, 100 Barr Harbor Drive, PO Box C700, West Conshohocken PA 19428-2959. Electronic copies of ASTM standards may be obtained from http://www.astm.org)

2.4 Order of precedence. In the event of a conflict between the text of this document and the references cited herein (except for related specification sheets), the text of this document takes precedence. Nothing in this document, however, supersedes applicable laws and regulations unless a specific exemption has been obtained.

3. REQUIREMENTS

3.1 Materials. Fuel supplied under this specification shall be refined hydrocarbon distillate fuel oils containing additives in accordance with 3.3. The feedstock from which the fuel is refined shall be crude oils derived from petroleum, tar sands, oil shale, or mixtures thereof.

3.1.1 Materials for Blending. With the approval of both the procuring activity and the applicable fuel technical authorities listed below, up to 50 volume % of the finished fuel may consist solely of Synthetic Paraffinic Kerosene (SPK) derived from a Fischer-Tropsch (FT) process meeting requirements of Appendix A. Finished fuel shall contain additives in accordance with 3.3. During the platform certification/approval process, JP-8 containing SPK will be designated JP-8/SPK.

Procuring Activity: Product Technology and Standardization, DESC, 8725 John J. Kingman Road, Fort Belvoir, VA 22060

Cognizant activity for the Navy and Marine Corps: Naval Fuels and Lubricants Cross Functional Team, AIR-4.4.1, Building 2360, 22229 Elmer Road, Patuxent River, MD 20670-1534.

Cognizant activity for the Air Force: Fuels Certification Office, 77th Monohan Street, Area B, Wright-Patterson AFB, OH 45433-7017.

Cognizant activities for the Army:

Army Ground: US Army TARDEC/RDECOM, 6501 E. 11 Mile Road, AMSRD-TAR-D (MS-110), Warren, MI 48397-5000.

Army Aviation: US Army RDECOM, Attn: AMSRD-AMR-AE-P, Building 4488, Room C-211, Redstone Arsenal, AL 35898-5000

3.1.2 Non-FT Materials. The use of synthetic blending materials represents a potential departure from experience and from the key assumptions which form the basis for fuel property requirements. It is the long-term goal of this specification to fully encompass fuels derived from synthetic materials and non-conventional sources once they have been defined but, this is only partially complete. Until this is accomplished, specific fuel formulations from synthetic materials or non-conventional sources may be submitted to AFRL/RZTG, Bldg 490, 1790 Loop Road N, WPAFB, OH 45433 to begin evaluation of compliance with the intent of this specification.

3.2 Chemical and physical requirements. The chemical and physical properties of a finished fuel containing only the materials described in 3.1 shall conform to the requirements listed in Table 1.

3.2.1 Chemical and physical requirements of blended finished fuels. The chemical and physical properties of a finished fuel blend containing any amount of synthetic SPK as described in 3.1.1 shall conform to the requirements listed in Table 2.

3.3 Additives. The type and amount of each additive used shall be made available when requested by the procuring activity or user (6.2.d). The only additives approved for use are those referenced in this specification.

3.3.1 Antioxidants. Immediately after processing and before the fuel is exposed to the atmosphere (such as during rundown into feed/batch tankage), an approved antioxidant (3.3.1.1) shall be blended into the fuel in order to prevent the formation of gums and peroxides after manufacture. The concentration of the antioxidant to be added shall be:

a. Not less than 17.2 milligrams (mg) nor more than 24.0 mg of active ingredient per liter (L) of fuel (6.0 to 8.4 lb/1000 barrels) to all JP-8 fuel that contains blending stocks that have been hydrogen treated or were manufactured from a Fischer-Tropsch process.

b. At the option of the supplier, not more than 24.0 mg of active ingredient per liter of fuel (8.4 lb/1000 barrels) may be added to JP-8 fuels that do not contain hydrogen treated blending stocks nor Fischer-Tropsch products.

3.3.1.1 Antioxidant formulations. The following antioxidant formulations are approved:

a. 2,6-di-tert-butyl-4-methylphenol

b. 6-tert-butyl-2,4-dimethylphenol

c. 2,6-di-tert-butylphenol

d. 75 percent min-2,6-di-tert-butylphenol
25 percent max tert-butylphenols and tri-tert-butylphenols

e. 72 percent min 6-tert-butyl-2,4-dimethylphenol
28 percent max tert-butyl-methylphenols and tert-butyl-dimethylphenols

f. 55 percent min 2,4-dimethyl-6-tert-butylphenol and
15 percent min 2,6-di-tert-butyl-4-methylphenol and
30 percent max mixed methyl and dimethyl tert-butylphenols

3.3.2 Metal deactivator. A metal deactivator, N,N'-disalycylidene-1,2-propanediamine, may be blended into the fuel. The concentration of active material used on initial batching of the fuel at the refinery shall not exceed 2.0 mg/L. Cumulative addition of metal deactivator when redoping the fuel, shall not exceed 5.7 mg/L. Metal deactivator additive shall not be used in JP-8 unless the supplier has obtained written consent from the procuring activity and user.

3.3.3 Static dissipater additive. An additive shall be blended into the fuel in sufficient concentration to increase the conductivity of the fuel at the point of injection to within the range specified in Table 1 for fuel offered in accordance with 3.1 or as specified in Table 2 for finished fuel when allowed per 3.1.1. The point of injection of the additive shall be determined by agreement between the purchasing authority and the supplier. The following electrical conductivity additive is approved: Stadis® 450 marketed by Innospec Fuel Specialties LLC (formerly Octel Starreon LLC), Newark, DE 19702.

3.3.4 Corrosion inhibitor/lubricity improver additive. A corrosion inhibitor/lubricity improver (CI/LI) additive conforming to MIL-PRF-25017 shall be blended into the F-34 (JP-8) grade fuel by the contractor. The CI/LI additive is optional for F-35. The amount added shall be equal to or greater than the minimum effective concentration and shall not exceed the maximum allowable concentration listed in the latest revision of QPL-25017. The contractor or transporting agency, or both, shall maintain and upon request shall make available to the Government evidence that the CI/LI additives used are equal in every respect to the qualification products listed in QPL-25017. The point of injection of the CI/LI additive shall be determined by agreement between the purchasing authority and the supplier.

TABLE 1. Chemical and physical requirements and test methods.

Property	Min	Max	Test Methods ASTM Standards
Color, Saybolt [1]			D 156 [2] or D 6045
Total acid number, mg KOH/gm		0.015	D 3242
Aromatics, vol percent		25.0	D 1319
Sulfur, total, mass percent		0.30	D 129, D 1266, D 2622, D 3120, D 4294 [2], or D 5453
Sulfur mercaptan, mass percent or		0.002	D 3227
Doctor test		negative	D 4952
Distillation temperature, °C [3]			D 86 [2] or D 2887
(D 2887 limits given in parentheses)			
Initial boiling point [1]			
10 percent recovered		205 (186)	
20 percent recovered [1]			
50 percent recovered [1]			
90 percent recovered [1]			
Final boiling point		300 (330)	
Residue, vol percent		1.5	
Loss, vol percent		1.5	
Flash point, °C [4]	38		D 56, D 93 [2], or D 3828
Density			D 1298 or D 4052 [2]
Density, kg/L at 15°C or	0.775	0.840	
Gravity, API at 60°F	37.0	51.0	
Freezing point, °C		-47	D 2386 [2], D 5972, D 7153, or D 7154
Viscosity, at -20°C, mm^2/s		8.0	D 445
Net heat of combustion, MJ/kg	42.8		D 3338, D 4529, or D 4809 [2]
Hydrogen content, mass percent	13.4		D 3343 or D 3701 [2]
Smoke point, mm, or	25.0		D 1322
Smoke point, mm, and	19.0		D 1322
Naphthalenes, vol percent		3.0	D 1840
Calculated cetane index [1]			D 976 [5] or D 4737
Copper strip corrosion, 2 hr at 100°C (212°F)		No. 1	D 130
Thermal stability			D 3241 [6]
change in pressure drop, mm Hg		25	
heater tube deposit, visual rating		<3 [7]	

TABLE 1. Chemical and physical requirements and test methods – Continued

Property	Min	Max	Test Methods ASTM Standards
Existent gum, mg/100 mL		7.0	D 381
Particulate matter, mg/L [8]		1.0	D 2276 or D 5452 [2]
Filtration time, minutes [8]		15	
Water reaction interface rating		1 b	D 1094
Water separation index [9]			D 3948 or D 7224 [2]
Fuel system icing inhibitor, vol percent	0.10	0.15	D 5006 [10]
Fuel electrical conductivity, pS/m [11]			D 2624

NOTES:

1. To be reported – not limited.
2. Referee Test Method.
3. A condenser temperature of 0° to 4°C (32° to 40°F) shall be used for the distillation by ASTM D 86.
4. ASTM D 56 may give results up to 1°C (2°F) below the ASTM D 93 results. ASTM D 3828 may give results up to 1.7°C (3°F) below the ASTM D 93 results. Method IP170 is also permitted.
5. Mid-boiling temperature may be obtained by either ASTM D 86 or ASTM D 2887 to perform the cetane index calculation. ASTM D 86 values should be corrected to standard barometric pressure.
6. See 4.5.3 for ASTM D 3241 test conditions and test limitations.
7. Peacock or Abnormal color deposits result in a failure.
8. A minimum sample size of 3.79 liters (1 gallon) shall be filtered. Filtration time will be determined in accordance with procedure in Appendix B. This procedure may also be used for the determination of particulate matter as an alternate to ASTM D 2276 or ASTM D 5452.
9. The minimum microseparometer rating using a Micro-Separometer (MSEP) shall be as follows:

JP-8 Additives	MSEP Rating, min.
Antioxidant (AO)*, Metal Deactivator (MDA)*	90
AO*, MDA*, and Fuel System Icing Inhibitor (FSII)	85
AO*, MDA*, and Corrosion Inhibitor/Lubricity Improver (CI/LI)	80
AO*, MDA*, FSII and CI/LI)	70

*Even though the presence or absence does not change these limits, samples submitted for specification or conformance testing shall contain the same additives present in the refinery batch. Regardless of which minimum the refiner selects to meet, the refiner shall report the MSEP rating on a laboratory hand blend of the fuel with all additives required by the specification.

10. Test shall be performed in accordance with ASTM D 5006 using the DiEGME scale of the refractometer.
11. The conductivity must be between 150 and 600 pS/m for F-34 (JP-8) and between 50 and 600 pS/m for F-35, at ambient temperature or 29.4°C (85°F), whichever is lower, unless otherwise directed by the procuring activity. In the case of JP-8+100, JP-8 with the thermal stability improver additive (see 3.3.6), the conductivity limit must be between 150 to 700 pS/m at ambient temperature or 29.4°C (85°F), whichever is lower, unless otherwise directed by the procuring activity.

TABLE 2. Chemical and physical requirements and test methods for JP-8 with up to 50 percent SPK blend component

Property	Min	Max	Test Methods ASTM Standards
Color, Saybolt [1]			D 156 [2] or D 6045
Total acid number, mg KOH/gm		0.015	D 3242
Aromatics, vol percent	8.0	25.0	D 1319
Olefins, vol percent		5.0	D 1319
Sulfur, total, mass percent		0.30	D 129, D 1266, D 2622, D 3120, D 4294 [2], or D 5453
Sulfur mercaptan, mass percent or		0.002	D 3227
Doctor test		negative	D 4952
Distillation temperature, °C [3]			D 86
Initial boiling point [1]			
10 percent recovered (T10)	157	205	
20 percent recovered [1]			
50 percent recovered (T50)	168	229	
90 percent recovered (T90)	183	262	
Final boiling point		300	
T50 – T10	15		
T90 – T10	40		
Residue, vol percent		1.5	
Loss, vol percent		1.5	
Flash point, °C [4]	38	68	D 56, D 93 [2], or D 3828
Density			D 1298 or D 4052 [2]
Density, kg/L at 15°C or	0.775	0.840	
Gravity, API at 60°F	37.0	51.0	
Freezing point, °C		-47	D 2386 [2], D 5972, D 7153, or D 7154
Viscosity, at -20°C, mm^2/s		8.0	D 445
Net heat of combustion, MJ/kg	42.8		D 3338, D 4529, or D 4809 [2]
Hydrogen content, mass percent	13.4		D 3343 or D 3701 [2]
Smoke point, mm, or	25.0		D 1322
Smoke point, mm, and	19.0		D 1322
Naphthalenes, vol percent		3.0	D 1840
Calculated cetane index [1]			D 976 [5] or D 4737
Copper strip corrosion, 2 hr at 100°C (212°F)		No. 1	D 130
Thermal stability			D 3241 [6]
change in pressure drop, mm Hg		25	
heater tube deposit, visual rating		<3 [7]	

TABLE 2. Chemical and physical requirements and test methods for JP-8 with up to 50 percent SPK blend component – Continued

Property	Min	Max	Test Methods ASTM Standards
Existent gum, mg/100 mL		7.0	D 381
Particulate matter, mg/L [8]		1.0	D 2276 or D 5452 [2]
Filtration time, minutes [8]		15	
Water reaction interface rating		1 b	D 1094
Water separation index [9]			D 3948 or D 7224 [2]
Fuel system icing inhibitor, vol percent	0.10	0.15	D 5006 [10]
Fuel electrical conductivity, pS/m [11]			D 2624
Lubricity, wear scar diameter, mm		0.85	D 5001

NOTES:

1. To be reported – not limited.
2. Referee Test Method.
3. A condenser temperature of 0° to 4°C (32° to 40°F) shall be used for the distillation by ASTM D 86.
4. ASTM D 56 may give results up to 1°C (2°F) below the ASTM D 93 results. ASTM D 3828 may give results up to 1.7°C (3°F) below the ASTM D 93 results. Method IP170 is also permitted.
5. Mid-boiling temperature may be obtained by ASTM D 86 to perform the cetane index calculation. ASTM D 86 values should be corrected to standard barometric pressure.
6. See 4.5.3 for ASTM D 3241 test conditions and test limitations.
7. Peacock or Abnormal color deposits result in a failure.
8. A minimum sample size of 3.79 liters (1 gallon) shall be filtered. Filtration time will be determined in accordance with procedure in Appendix B. This procedure may also be used for the determination of particulate matter as an alternate to ASTM D 2276 or ASTM D 5452.
9. The minimum microseparometer rating using a Micro-Separometer (MSEP) shall be as follows:

JP-8 Additives	MSEP Rating, min.
Antioxidant (AO)*, Metal Deactivator (MDA)*	90
AO*, MDA*, and Fuel System Icing Inhibitor (FSII)	85
AO*, MDA*, and Corrosion Inhibitor/Lubricity Improver (CI/LI)	80
AO*, MDA*, FSII and CI/LI)	70

*Even though the presence or absence does not change these limits, samples submitted for specification or conformance testing shall contain the same additives present in the refinery batch. Regardless of which minimum the refiner selects to meet, the refiner shall report the MSEP rating on a laboratory hand blend of the fuel with all additives required by the specification.

10. Test shall be performed in accordance with ASTM D 5006 using the DiEGME scale of the refractometer.
11. The conductivity must be between 150 and 600 pS/m for F-34 (JP-8) and between 50 and 600 pS/m for F-35, at ambient temperature or 29.4°C (85°F), whichever is lower, unless otherwise directed by the procuring activity. In the case of JP-8+100, JP-8 with the thermal stability improver additive (see 3.3.6), the conductivity limit must be between 150 to 700 pS/m at ambient temperature or 29.4°C (85°F), whichever is lower, unless otherwise directed by the procuring activity.

3.3.5 Fuel system icing inhibitor. The use of a fuel system icing inhibitor shall be mandatory for JP-8 and shall conform to MIL-DTL-85470. The point of injection of the additive for JP-8 shall be determined by agreement between the purchasing authority and the supplier. The fuel system icing inhibitor is not to be added to NATO F-35 unless so directed by the purchasing authority.

3.3.6 Thermal stability improver additive. Due to logistic concerns, personnel at the operating location shall request written approval from the cognizant activity to add a thermal stability improver additive to the fuel. If approval is given, the concentration of the additive and location of injection shall be specified by the cognizant service activity listed below. For USAF aircraft, this approval does not override the single manager's authority for specifying allowed/disallowed fuels. JP-8 fuel with an approved thermal stability improver additive at the required concentration shall be designated as JP-8+100. Thermal stability improver additive shall not be used in JP-8 without approval, in writing, from:

Cognizant activity for the Navy and Marine Corps: Naval Fuels and Lubricants Cross Functional Team, AIR-4.4.1, Building 2360, 22229 Elmer Road, Patuxent River, MD 20670-1534.

Cognizant activity for the Air Force: HQ Air Force Petroleum Agency, HQ AFPET/AFT, 2430 C Street, Building 70, Area B, Wright-Patterson AFB 45433-7632.

Cognizant activities for the Army:

Army Ground: US Army TARDEC/RDECOM, 6501 E. 11 Mile Road, AMSRD-TAR-D (MS-110), Warren, MI 48397-5000.

Army Aviation: US Army RDECOM, Attn: AMSRD-AMR-AE-P, Building 4488, Room C-211, Redstone Arsenal, AL 35898-5000

3.3.6.1 Qualified additives. Qualified thermal stability improver additives are listed in Table 3.

TABLE 3. Qualified thermal stability improver additives.

Additive Name	Qualification Reference	Manufacturer
SPEC AID 8Q462	AFRL/PRSF Ltr, 9 Dec 97	GE Water & Process Technologies 9669 Grogan Mill Road The Woodlands, TX 77380
AeroShell Performance Additive 101	AFRL/PRSF Ltr, 13 Jan 98	Shell Aviation Limited Shell Centre York Road London, UK SE1 7NA

3.3.7 Premixing of additives. Additives shall not be premixed with other additives before injection into the fuel so as to prevent possible reactions among the concentrated forms of different additives.

3.4 Workmanship. At the time of Government acceptance, the finished fuel or finished fuel blend shall be visually free from undissolved water, sediment or suspended matter, and shall be clear and bright. In case of dispute, the fuel shall be clear and bright at 21°C (70°F) and shall contain no more than 1.0 mg/L of particulate matter as required in Table 1 for any finished fuel containing only the materials described in 3.1 or, Table 2 for finished fuel blends containing any amount of SPK as described in 3.1.1.

3.5 Recycled, recovered, or environmentally preferable materials. Recycled, recovered, or environmentally preferable materials should be used to the maximum extent possible, provided that the material meets or exceeds the operational and maintenance requirements, and promotes economically advantageous life cycle costs.

4. VERIFICATION

4.1 Classification of inspections. The inspection requirements specified herein are classified as quality conformance inspections (see 4.2).

4.2 Qualification inspection conditions. Test for acceptance of individual lots shall consist of tests for all applicable requirements specified in section 3. Quality conformance inspection shall include the test requirements herein.

4.2.1 Inspection lot. For acceptance purposes, individual lots shall be examined as specified herein and subjected to tests for all applicable requirements cited in section 3.

4.3 Inspection.

4.3.1 Inspection conditions. Any finished fuel containing only the materials described in 3.1 shall comply with the limiting values specified in Table 1 using the cited test methods. Any finished fuel blend containing any amount of SPK as described in 3.1.1 shall comply with the limiting values specified in Table 2 using the cited test methods. Any SPK blend component as described in 3.1.1 shall comply with the limiting values specified in Table A-I using the cited test methods. The specified limiting values must not be changed. This precludes any allowance for test method precision and adding or subtracting digits. For the purposes of determining conformance with the specified limiting values, an observed value or a calculated value shall be rounded off "to the nearest unit" in the last right hand place of digits used in expressing the specified limiting value, in accordance with the Rounding-Off Method of ASTM E 29.

4.4 Sampling plans.

4.4.1 Sampling. Each bulk or packaged lot of material shall be sampled for verification of product quality in accordance with ASTM D 4057 or ASTM D 4177, except where individual test procedures contain specific sampling instructions.

4.4.2 Sampling for inspection of filled containers. A random sample of filled containers shall be selected from each lot and shall be subjected to the examination of filled containers as specified in 4.5.1.3.

4.5 Methods of inspection.

4.5.1 Examination of product.

4.5.1.1 Visual inspection. Samples selected in accordance with 4.4.1 shall be visually examined for compliance with 3.4.

4.5.1.2 Examination of empty containers. Before filled, each unit container shall be visually inspected for cleanliness and suitability in accordance with ASTM D 4057.

4.5.1.3 Examination of filled containers. Samples taken as specified in 4.4.2 shall be examined for conformance to MIL-STD-290 with regard to fill, closure, sealing, leakage, packaging, packing, and markings. Any container with one or more defects under the required fill shall be rejected.

4.5.2 Chemical and physical tests. Tests to determine compliance with chemical and physical requirements shall be conducted in accordance with Table 1 or Table 2 and/or Table A-I as follows. Any finished fuel containing only the materials described in 3.1 shall pass all tests listed in Table 1. Any finished fuel containing any amount of SPK as described in 3.1.1 shall pass all tests listed in Table 2. Any SPK blend component as defined in 3.1.1 shall pass all tests listed in Table A-I. No additional testing shall be required. Requirements contained herein are not subject to corrections for test tolerances. If multiple determinations are made, results falling within any specified repeatability and reproducibility tolerances may be averaged. For rounding off of significant figures, ASTM E 29 shall apply to all tests required by this specification.

4.5.3 Thermal stability tests. The thermal stability test shall be conducted using ASTM D 3241. The heated tube shall be rated visually (see Annex A1 of ASTM D 3241).

4.5.3.1 ASTM D 3241 test conditions.

a. Heater tube temperature at maximum point: 260°C (500°F).

b. Fuel system pressure: 3.45 MPa (500 psig).

c. Fuel flow rate: 3.0 mL/min.

d. Test duration: 150 minutes.

4.5.3.2 ASTM D 3241 reported data. The following data shall be reported:

a. Differential pressure in millimeter of mercury at 150 minutes, or time to differential pressure of 25 mm Hg, whichever comes first.

b. Heater tube deposit visual code rating at the end of the test.

5. PACKAGING

5.1 Packaging. For acquisition purposes, the packaging requirements shall be as specified in the contract or order (see 6.2). When actual packaging of materiel is to be performed by DoD or in-house contractor personnel, these personnel need to contact the responsible packaging activity to ascertain packaging requirements. Packaging requirements are maintained by the Inventory Control Point's packaging activities within the Military Service or Defense Agency, or within the military service's system commands. Packaging data retrieval is available from the managing Military Department's or Defense Agency's automated packaging files, CD-ROM products, or by contacting the responsible packaging activity.

6. NOTES

(This section contains information of a general or explanatory nature that may be helpful, but is not mandatory.)

6.1 Intended use. The fuels covered by this specification are intended for use in aircraft turbine engines. JP-8 contains military unique additives that are required by military weapon systems. This requirement is unique to military aircraft and engine designs. When authorized, JP-8 (F-34) may be used in ground - based turbine and diesel engines. NATO F-35 is intended for commercial aviation, but can be converted to JP-8 (F-34) by the addition of the appropriate additives.

6.2 Acquisition requirements. Acquisition documents must specify the following:

a. Title, number, date of this specification, and grade (type) of fuel.
b. Quantity required and size containers desired.
c. Level of packaging and packing required (see 5.1).
d. Location and injection method for addition of electrical conductivity additive, fuel system icing inhibitor and corrosion inhibitor, as required.

6.3 Conversion of metric units. Units of measure have been converted to the International System of Units (SI) (Metric) in accordance with ASTM SI 10. If test results are obtained in units other than metric or there is a requirement to report dual units, ASTM SI 10, should be used to convert the units.

6.4 Definitions.

6.4.1 Bulk lot. A bulk lot consists of an indefinite quantity of a homogeneous mixture of material offered for acceptance in a single isolated container or manufactured in a single plant run through the same processing equipment, with no change in ingredient material.

6.4.2 Packaged lot. A packaged lot consists of an indefinite number of 208-liter (55-gallon) drums, or smaller unit packages of identical size and type, offered for acceptance and filled from an isolated tank containing a homogeneous mixture of material; or filled with a homogeneous mixture of material run through the same processing equipment with no change in ingredient material.

6.4.3 Homogenous product. A homogeneous product is defined as a product where samples taken at various levels of the batch tank are tested for the defining homogeneous characteristics and all values obtained meet the repeatability precision requirements for that test method.

6.4.4 Synthetic Paraffinic Kerosene (SPK) Kerosene consisting solely of n-paraffins, cyclic-paraffins, and iso-paraffins.

6.4.5 Fischer-Tropsch (FT) Process A catalyzed chemical process in which a synthesis gas consisting of carbon monoxide and hydrogen are converted into liquid hydrocarbons of various forms. Typical catalysts used are based on iron and cobalt.

6.5 Subject term (key word) listing.

Antioxidants
Corrosion inhibitor
Fischer-Tropsch
Flash point
Freezing point
Hydrocarbon distillate fuel
Hydrogen content
Icing inhibitor
Synthetic Paraffinic Kerosene (SPK)
Lubricity improver
Static dissipator
Thermal stability improver

6.6 International agreements. Certain provisions of this specification are the subject of international standardization agreement ASIC AIR STD 15/6, ASIC AIR STD 15/9, NATO STANAG 1135, and NATO STANAG 3747. When amendment, revision, or cancellation of this specification is proposed which will modify the international agreement concerned, the preparing activity will take appropriate action through international standardization channels including departmental standardization offices, to change the agreement or make other appropriate accommodations.

6.7 Material safety data sheet. Contracting officers will identify those activities requiring copies of completed Material Safety Data Sheets prepared in accordance with FED-STD-313. The pertinent Government mailing addresses for submission of data are listed in FED-STD-313.

6.8 Test report. Test data required by 4.5 should be available for the procurement activity and user in the same order as listed in Table 1 for materials conforming to 3.2 requirements or as listed in Table 2 for materials conforming to 3.2.1 requirements. The Inspection Data on Aviation Turbine Fuels form published in ASTM D 1655 should be used as a guide. Also, the type and amount of additives used should be reported.

6.9 Changes from previous issue. Marginal notations are not used in this revision to identify changes with respect to the previous issue due to the extent of the changes.

II, 36

MIL-DTL-83133F
APPENDIX A

SYNTHETIC PARAFFINIC KEROSENE (SPK)

A.1 SCOPE

A.1.1 Scope. This Appendix addresses 100 percent SPK derived from manufactured products of a Fischer-Tropsch process (identified in 3.1.1). This Appendix is a mandatory part of the specification. The information contained herein is intended for compliance.

A.2 REQUIREMENTS

A.2.1 Chemical and physical requirements. The chemical and physical requirements of the SPK shall conform to those specified in Table A-I.

A.2.2 Additives.

A.2.2.1 Antioxidants. Addition of antioxidants shall adhere to the criteria specified in 3.3.1.

A.2.2.2 Static dissipater additive (SDA). If SPK is to be transported prior to blending with refined hydrocarbon distillate fuel, static dissipater additive shall be injected in sufficient concentration to increase the conductivity of the fuel to within the range specified in Table A-I. The point of injection of the additive shall be determined by agreement between the purchasing authority and the supplier. The following electrical conductivity additive is approved: Stadis® 450 marketed by Innospec Fuel Specialties LLC (formerly Octel Starreon LLC), Newark, DE 19702.

TABLE A-I. Chemical and physical requirements and test methods for 100 percent SPK.

Property	Min	Max	Test Method
Aromatics, vol percent		1	D 5186
Sulfur, total, mass percent		0.0015	D 2622, D 3120, or D 5453 [1]
Distillation temperature, °C			D 86
Initial boiling point [2]			
10 percent recovered	157	205	
20 percent recovered [2]			
50 percent recovered	168	229	
90 percent recovered	183	262	
Final boiling point		300	
Residue, vol percent		1.5	
Loss, vol percent		1.5	
Flash point, °C	38	68	D 56, D 93 [1], or D 3828
Density			D 1298 or D 4052 [1]
Density, kg/L at 15°C or	0.751	0.840	
Gravity, API at 60°F	37.0	57.0	

MIL-DTL-83133F
APPENDIX A

TABLE A-I. Chemical and physical requirements and test methods for 100 percent SPK - Continued.

Property	Min	Max	Test Method
Freezing point, °C		-47	D 2386 [1] or D 5972
Viscosity at -20°C, mm^2/s		8.0	D 445
Viscosity at 40°C, mm^2/s [2]			D 445
Net heat of combustion, MJ/kg	42.8		D 3338 or D 4809 [1]
Calculated cetane index [2]			D 976 [3] or D 4737
Naphthalenes, vol percent		0.1	D 1840
Thermal stability			D 3241
change in pressure drop, mm Hg		25	
heater tube deposit, visual rating		<3 [4]	
Particulate matter, mg/L [5]		1.0	D 2276 or D 5452 [1]
Filtration time, minutes [5]		15	
Water separation index			D 3948 or D 7224 [1]
With SDA	70		
Without SDA	85		
Electrical conductivity, pS/m [6]	150	450	D 2624

NOTES:
1. Referee Test Method.
2. To be reported – not limited.
3. Mid-boiling temperature may be obtained by ASTM D 86 to perform the cetane index calculation. ASTM D 86 values should be corrected to standard barometric pressure.
4. Peacock or Abnormal color deposits result in a failure.
5. A minimum sample size of 3.79 liters (1 gallon) shall be filtered. Filtration time will be determined in accordance with procedure in Appendix B. This procedure may also be used for the determination of particulate matter as an alternate to ASTM D 2276 or ASTM D 5452.
6. Electrical Conductivity when required per A.2.2.2 shall be determined at ambient temperature or 29.4°C (85°F), whichever is lower, unless otherwise directed by the procuring activity.

MIL-DTL-83133F
APPENDIX B

METHOD FOR DETERMINATION OF FILTRATION TIME AND TOTAL SOLIDS

B.1 SCOPE

B.1.1 Scope. This Appendix describes the method for determining singularly or simultaneously the filterability characteristics and solids contamination of jet fuel. The purpose is to detect and prevent contaminants in jet fuel that can plug and cause rupture of ground filtration equipment, thereby affecting flight reliability of aircraft. This Appendix is a mandatory part of the specification. The information contained herein is intended for compliance.

B.2 METHOD

B.2.1 Summary of method. 3.79 liters (1 gallon) of jet fuel is filtered through a membrane filter in the laboratory. The time required to filter this volume is measured in minutes and solids content is determined gravimetrically.

B.3 APPARATUS

a. Membrane filter: White, plain, 47 mm diameter, nominal pore size 0.8 µm. The membrane filter must be approved by ASTM for use with ASTM D 5452.

b. Filtration apparatus: The apparatus, constructed of stainless steel, consists of a funnel and a funnel base with a filter support such that a membrane filter and a flow reducing washer can be securely held between the sealing surface of the funnel and funnel base (see Figure 2 in ASTM D 5452).

c. Flow reducing washer: A 47-mm diameter flow reducer washer with an effective filtration area of 4.8 cm^2 (Millipore Corporation Part No. XX10 04710).

d. Vacuum flask: A minimum of 4 liters.

e. Vacuum system: That develops in excess of 67.5 kPa (20 inches of mercury) vacuum.

f. Oven: Of the static type (without fan assisted circulation) controlling to 90° ± 5° C (194° ± 9° F).

g. Forceps: Flat-bladed with unserrated nonpointed tips.

h. Dispenser, rinsing solvent (petroleum ether): Containing a 0.45 µm membrane filter in the delivery line. If solvent has been pre-filtered using a 0.45 µm filter then an inline filter is not required.

i. Glass petri dish: Approximately 125 mm in diameter with removable cover.

j. Analytical balance: Single or double pan, the precision standard deviation of which must be 0.07 mg or better.

MIL-DTL-83133F
APPENDIX B

B.4 PREPARATION

B.4.1 Preparation of apparatus and sample containers. All components of the filtration apparatus (except the vacuum flask), sample containers and caps must be cleaned as described in paragraph 9 of ASTM D 5452. All metal parts of the filtration apparatus are to be electrically bonded and grounded, including the fuel sample container. See ASTM D 5452 for other safety precautions.

B.5 SAMPLING

B.5.1 Sampling. Obtain a representative 3.79 L (1 gallon) sample as directed in paragraph 8 of ASTM D 5452. When sampling from a flowing stream is not possible, an all level sample or an average sample, in accordance with ASTM D 4057 and/or ASTM D 4177 shall be permitted. The 3.79 L (1 gallon) sample container shall be an interior epoxy-coated metal can, a brown glass bottle, or a clear glass bottle protected by suitable means from exposure to light.

B.6 PROCEDURE

B.6.1 Test procedure.

a. Using forceps, place a new membrane (test) filter in a clean petri dish. Place the petri dish with the lid slightly ajar in a 90 ± 5°C oven for 30 minutes. Remove the petri dish from the oven and place it near the balance with the lid slightly ajar, but still protecting the filter from airborne contamination, for 30 minutes.

b. Weigh the test filter. A filter weighing in excess of 90 mg will not be used for time filtration testing.

c. Place a flow reducing washer (required only for time filtration testing) on top of funnel base then place a test filter on top of the reducing washer and secure the funnel to the funnel base.

d. Immediately prior to filtering the fuel, shake the sample to obtain a homogeneous mix and assure that fuel temperature does not exceed 30°C (86°F). Clean the exterior or top portion of the sample container to ensure that no contaminants are introduced. Any free water present in the fuel sample will invalidate the filtration time results by giving an excessive filtration time rating.

e. With the vacuum off, pour approximately 200 mL of fuel into the funnel.

f. Turn vacuum on and record starting time. Continue filtration of the 3.79 liters (1 gallon) sample, periodically shaking the sample container to maintain a homogenous mix. Record the vacuum (kPa or inches of mercury) 1 minute after start and again immediately prior to completion of filtration. Throughout filtration, maintain a sufficient quantity of fuel in the funnel so that the membrane filter is always covered.

g. Report the filtration time in minutes expressed to the nearest whole number. If filtration of the 3.79 liters (1 gallon) is not completed within 30 minutes, the test will be stopped and the volume of the fuel filtered will be measured. In these cases, report filtration time as ">30 minutes" and the total volume of fuel filtered.

h. Report the vacuum (kPa or inches of mercury) as determined from the average of the two readings taken in B.6.f.

i. After recording the filtration time, shut off the vacuum and rinse the sample container with approximately 100 mL of filtered petroleum ether and dispense into the filtration funnel. Turn vacuum on and filter the 100 mL rinse. Turn vacuum off and wash the inside of the funnel with approximately 50 mL of filtered petroleum ether. Turn vacuum on and filter. Repeat the funnel rinse with another 50 mL of petroleum ether but allow the rinse to soak the filter for approximately 30 seconds before turning the vacuum on to filter the rinse. With vacuum on, carefully remove the top funnel and rinse the periphery of the filter by directing a gentle stream of petroleum ether from the solvent dispenser from the edge of the filter toward the center, taking care not to wash contaminants off the filter. Maintain vacuum after final rinse for a few seconds to remove the excess petroleum ether from the filter.

j. Using forceps, carefully remove test filter (from the funnel base and flow reducing washer if present) and place in a clean petri dish. Dry in the oven at 90° ± 5°C (194° ± 9°F) for 30 minutes with the cover on the petri dish slightly ajar. Remove the petri dish from the oven and place it near the balance with the lid slightly ajar, but still protecting the filter from airborne contamination, for 30 minutes. Reweigh the filter.

k. Report the total solids content in mg/liter by using the following formula:

$$\frac{\text{Weight gain of filter in mg}}{3.785} = \text{mg/liter}$$

l. Should the sample exceed the 30-minute filtration time and a portion of the fuel is not filtered, the solids content in mg/liter will be figured as follows: Determine the volume of fuel filtered by subtracting the mL of fuel remaining from 3.785.

$$\frac{\text{Weight gain of filter in mg}}{\text{mL of fuel filtered} \times 0.001} = \text{mg/liter}$$

B.7 Test conditions for filtration time

a. The vacuum should exceed 67.5 kPa (20 inches of mercury) throughout the test. The differential pressure across the filter should exceed 67.5 kPa (20 inches of mercury).

b. The fuel temperature shall be between 18° and 30°C (64° and 86°F). If artificial heat (such as a hot water bath) is used to heat the sample, erroneously high filtration times may occur, but this approach is allowed.

B.8 NOTES

B.8.1 Filtration time. If it is desired to determine the filtration time and not the total solids content, perform the test by omitting steps B.6.1i, B.6.1j, B.6.1k, and B.6.1l.

B.8.2 Total solids. If it is desired to determine the total solids content and not the filtration time, use of the flow reducing washer may be omitted. It is also permissible, but not required, to use a control filter for a specific analysis or a series of analyses. When this is accomplished, the procedures specified in ASTM D 5452 apply.

CONCLUDING MATERIAL

Custodians:
Navy – AS
Army – MR
Air Force – 68
DLA – PS

Review activities:
Army – AR, AV, AT
Air Force – 11

Preparing activity:
Air Force – 68
(Project 9130-2007-001)

Note: The activities listed above were interested in this document as of the date of this document. Since organizations and responsibilities can change, you should verify the currency of the information using the ASSIST Online database at http://assist.daps.dla.mil.

III, 1

APPENDIX 3

III, 2

ICAO Aircraft Engine Emissions Databank

Contents

1. Data Sources

This Databank contains information on exhaust emissions of only those aircraft engines that have entered production. The information was provided by engine manufacturers, who are solely responsible for its accuracy. It was collected in the course of the work carried out by the ICAO Committee on Aviation Environmental Protection (CAEP) but has not been independently verified unless indicated. The UK CAA is hosting this Databank on behalf of ICAO and is not responsible for the contents.

2. Background

Standards limiting the emissions of smoke, unburnt hydrocarbons (HC), carbon monoxide (CO) and oxides of nitrogen (NO_x) from turbojet and turbofan aircraft engines are contained in Annex 16 Volume II (Second Edition, July 1993, plus amendments) [Reference 1] to the Convention on International Civil Aviation. The Annex also contains approved test and measurement procedures.

With respect to subsonic applications, the provisions of the Standards for smoke apply to engines whose date of manufacture is on or after 1 January 1983. For the gaseous emissions, the Standards apply only to engines whose rated output is greater than 26.7 kN. For hydrocarbons and carbon monoxide, they apply to engines whose date of manufacture is on or after 1 January 1986. For oxides of nitrogen, the Standards have several levels of stringency depending on the date of manufacture of the engine. These Standards are summarized later in Section 7.

This Databank contains information on exhaust emissions of only those engines that have entered production, irrespective of the numbers actually produced. It has been compiled mainly from information supplied for newly certified engines. However, for some engines, the data has been revised to reflect evidence from subsequent engine tests. It also includes data on older engines which did not have to comply with the emissions standards and some data from a very limited number of in-service engines measured before or after overhaul.

The original version was published as a printed document [Reference 2]. All subsequent updates have been electronic

3. Revision of data

The electronic version of the Databank is updated at periodic intervals. New data are included for:

a) engines certificated since the last issue of the data bank;
b) engines already certificated for which data were not previously available; or
c) engines already certificated and listed in the Databank for which:
    i. emissions data have been recalculated as a result of a better definition of engine performance characteristics with continuing production of an engine type;
    ii. component design changes have been introduced which affect the emissions levels, e.g. new combustor design; or
    iii. improvements in emissions measurement techniques have resulted in changes to the emissions data.

Data will not be removed from the Databank. Where data is superseded the row is marked to indicate that this data should not be used, and the newer data to be used instead is specified. Data is also marked where an engine is no longer in service, and where an engine is no longer in production.

The Record of Changes documents the history of revisions, and the date of latest review.

4. Contacts

New data should be submitted to:

Aircraft Environmental Section
Aircraft Certification Department
Safety Regulation Group
Civil Aviation Authority
Aviation House
Gatwick Airport South
West Sussex
RH6 0YR
United Kingdom

email: Emissions.Databank@srg.caa.co.uk
phone: (+44) 1293 573204

Comments and queries concerning this electronic version of the database should also be sent to the above address.

5. Use of the Databank

The user of the Databank should note the limitations in the emissions data; i.e.:

a) The D_p/F_{oo} values are based on an idealized Landing/Take-Off (LTO) cycle in International Standard Atmosphere (ISA) conditions. In assessing, for example, total aircraft emissions at a specific airport, consideration must be given to the appropriateness of the prescribed thrusts, the times in mode and the reference conditions.

b) The LTO cycle only assesses the emissions below 915 m (3 000 ft) and therefore may not be a good guide for comparing the emissions of different engines in other flight modes, e.g. cruise.

6. Definitions

By-pass ratio: The ratio of the air mass flow through the by-pass ducts of a gas turbine engine to the air mass flow through the engine core, calculated at maximum thrust when the engine is stationary in an international standard atmosphere at sea level.

Characteristic level: The characteristic level of a gaseous pollutant or smoke is the mean D_p/F_{oo} or SN value of a species, for all the engines tested, measured and corrected to the reference standard engine and reference atmospheric conditions, divided by a coefficient corresponding to the number of engines tested. The procedure and coefficients are given in Annex 16, Volume II. This is in recognition that at the certification stage there are usually not many engines to production standard available for testing, so the manufacturer is allowed to select any number of engines, including a single engine if so desired, for testing. Statistically derived coefficients, corresponding to the number of engines tested, are then applied to ensure a high confidence that the mean of the anticipated total engine production will not exceed the regulatory level. The procedure and coefficients are given in Annex 16 Volume II, Appendix 6.

Data Status: This has been grouped into three categories:

1. *Pre-regulation:* Data obtained on engines generally prior to the promulgation of the Standards of Annex 16, Volume II, and for which the manufacturer was not required to apply for emissions certification.

2. *Certification:* Data which have been submitted for certification approval after the applicability dates or which have been obtained at an earlier date, generally after the promulgation of the Standards of Annex 16. Volume II, with the intention of gaining approval.

3. *Revised:* Existing data which have been modified, as noted in paragraph c) under REVISION OF DATA above, and which do not require the engine to be re-certificated.

D_p/F_{oo}: The mass, in grams (D_p), of any pollutant emitted during the reference landing and take-off (LTO) cycle, divided by the rated output (F_{oo}) of the engine.

Emissions index (EI): The mass of pollutant (CO, HC or NO_x), in grams, divided by the mass of fuel used in kilograms.

Fuel: The fuel used is aviation kerosene as specified in Annex 16, Volume II, Appendix 4.

Hydrocarbons (HC): The total of hydrocarbon compounds of all classes and molecular weights contained in a gas sample, calculated as if they were in the form of methane.

International Standard Atmosphere (ISA): The atmosphere defined in the Manual of the ICAO Standard Atmosphere (Doc 7488). These are the atmospheric conditions to which all engine performance data should be corrected.

LTO cycle: The reference emissions LTO cycle defines the thrust settings to be used when making emissions and smoke measurements and the time to be used for each mode in the subsequent calculations of D_p. These thrust settings and times are listed in Annex 16, Volume II, Part III, Chapter 2 (engines for subsonic propulsion).

Oxides of nitrogen (NO_x): The sum of the amounts of the nitric oxide and nitrogen dioxide contained in a gas sample calculated as if the nitric oxide were in the form of nitrogen dioxide.

Pressure ratio (π_{oo}): The ratio of the mean total pressure at the last compressor discharge plane of the compressor to the mean total pressure at the compressor entry plane when the engine is developing take-off thrust rating in ISA sea level static conditions.

Rated output (F_{oo}): The maximum thrust available for take-off under normal operating conditions at ISA sea level static conditions without the use of water injection as approved by the certificating authority. Thrust is expressed in kilonewtons.

Reference Atmospheric Conditions: The atmospheric conditions to which all emissions results should be corrected. The reference atmospheric conditions are ISA at sea level except that the reference absolute humidity shall be 0.00634 kg water/kg dry air.

Regulatory Level: The level below which the characteristic D_p/F_{oo} or Smoke Number value for a pollutant species must fall in order to obtain certification approval. The regulatory levels reproduced from Annex 16, Volume II, Part III, Chapters 2 (subsonic engines) are given below in Section 7.

Smoke Number (SN): The dimensionless term quantifying smoke emissions. Smoke Number is calculated from the reflectance of a filter paper measured before and after the passage of a known volume of a smoke-bearing sample.

7. Regulatory standards

These applicability requirements and regulatory levels are those found in Annex 16, Volume II, Part III, Chapter 2 (subsonic engines) and are included for reference purposes only.

Smoke

Applicability
The regulatory levels are applicable to engines whose date of manufacture is on or after 1 January 1983.

Regulatory smoke number
The characteristic level of the smoke number at any thrust setting, measured in accordance with Annex 16, Volume II, must not exceed 83.6 $(F_{oo})^{-0.274}$ or a value of 50, whichever is lower.

Gaseous emissions

Applicability
The regulatory levels apply to engines whose rated output is greater than 26.7kN and whose date of manufacture is on or after 1 January 1986 and as further specified for oxides of nitrogen.

Regulatory levels
The characteristic levels of the gaseous emissions measured over the LTO cycle in accordance with Annex 16, Volume II, must not exceed the following regulatory levels:

Hydrocarbons (HC): $D_p/F_{oo} = 19.6$

Carbon monoxide (CO): $D_p/F_{oo} = 118$

Oxides of nitrogen (NOx):

a) for engines of a type or model of which the date of manufacture of the first individual production model was on or before 31 December 1995 and for which the date of manufacture of the individual engine was on or before 31 December 1999:

$$D_p/F_{oo} = 40 + 2\pi_{oo}$$

b) for engines of a type or model of which the date of manufacture of the first individual production model was after 31 December 1995 or for which the date of manufacture of the individual engine was after 31 December 1999:

$$D_p/F_{oo} = 32 + 1.6\pi_{oo}$$

c) for engines of a type or model of which the date of manufacture of the first individual production model was after 31 December 2003:

1. for engines with a pressure ratio of 30 or less:

i. for engines with a maximum rated thrust of more than 89.0 kN:

III, 7

$D_p/F_{oo} = 19 + 1.6\pi_{oo}$

ii. for engines with a maximum rated thrust of more than 26.7 kN but not more than 89.0 kN:

$D_p/F_{oo} = 37.572 + 1.6\pi_{oo} - 0.2087F_{oo}$

2. for engines with a pressure ratio of more than 30 but less than 62.5:

i. for engines with a maximum rated thrust of more than 89.0 kN:

$D_p/F_{oo} = 7 + 2.0\pi_{oo}$

ii. for engines with a maximum rated thrust of more than 26.7 kN but not more than 89.0 kN:

$D_p/F_{oo} = 42.71 + 1.4286\pi_{oo} - 0.4013F_{oo} + 0.00642\pi_{oo} \times F_{oo}$

3) for engines with a pressure ratio of 62.5 or more:

$D_p/F_{oo} = 32 + 1.6\pi_{oo}$

d) for engines of a type or model of which the date of manufacture of the first individual production model was after 31 December 2007:

1) for engines with a pressure ratio of 30 or less:

i. for engines with a maximum rated thrust of more than 89.0 kN:

$D_p/F_{oo} = 16.72 + 1.4080\pi_{oo}$

ii. for engines with a maximum rated thrust of more than 26.7 kN but not more than 89.0 kN:

$D_p/F_{oo} = 38.5486 + 1.6823\pi_{oo} - 0.2453F_{oo} - 0.00308\ \pi_{oo} \times F_{oo}$

2) for engines with a pressure ratio of more than 30 but less than 82.6:

i. for engines with a maximum rated thrust of more than 89.0 kN:

$D_p/F_{oo} = -1.04 + 2.0\pi_{oo}$

ii. for engines with a maximum rated thrust of more than 26.7 kN but not more than 89.0 kN:

$D_p/F_{oo} = 46.1600 + 1.4286\pi_{oo} - 0.5303F_{oo} + 0.00642\pi_{oo} \times F_{oo}$

3) for engines with a pressure ratio of 82.6 or more:

$$D_p/F_{oo} = 32 + 1.6\pi_{oo}$$

8. References

1. ICAO Annex 16 "International standards and recommended practices, Environmental protection", Volume II "Aircraft engine emissions", 2nd ed. (1993) plus amendments:

   Amendment 3, 20 March 1997;
   Amendment 4, 4 November 1999;
   Amendment 5, 24 November 2005

2. ICAO Engine Exhaust Emissions Databank, First Edition 1995, ICAO, Doc 9646- AN/943.

ICAO ENGINE EXHAUST EMISSIONS DATA BANK

SUBSONIC ENGINES

III, 9

ENGINE IDENTIFICATION: CFM56-3C-1
UNIQUE ID NUMBER: 1CM007
ENGINE TYPE: TF

BYPASS RATIO: 5.1
PRESSURE RATIO (π_{oo}): 25.5
RATED OUTPUT (F_{oo}) (kN): 104.6

REGULATORY DATA

CHARACTERISTIC VALUE:	HC	CO	NOx	SMOKE NUMBER
D_p/F_{oo} (g/kN) or SN	4.3	65.7	53.1	9.9
AS % OF ORIGINAL LIMIT	21.7 %	55.7 %	58.3 %	42.4 %
AS % OF CAEP/2 LIMIT (NOx)			72.9 %	
AS % OF CAEP/4 LIMIT (NOx)			88.8 %	

DATA STATUS

- \- PRE-REGULATION
- \- CERTIFICATION
- x REVISED (SEE REMARKS)

TEST ENGINE STATUS

- x NEWLY MANUFACTURED ENGINES
- \- DEDICATED ENGINES TO PRODUCTION STANDARD
- \- OTHER (SEE REMARKS)

EMISSIONS STATUS

- x DATA CORRECTED TO REFERENCE (ANNEX 16 VOLUME II)

CURRENT ENGINE STATUS

(IN PRODUCTION, IN SERVICE UNLESS OTHERWISE NOTED)

- x OUT OF PRODUCTION (DATE: -)
- \- OUT OF SERVICE

MEASURED DATA

MODE	POWER SETTING (%F_{oo})	TIME minutes	FUEL FLOW kg/s	EMISSIONS INDICES (g/kg) HC	CO	NOx	SMOKE NUMBER
TAKE-OFF	100	0.7	1.154	0.03	0.9	20.7	7.7
CLIMB OUT	85	2.2	0.954	0.04	0.9	17.8	3.9
APPROACH	30	4.0	0.336	0.07	3.1	9.1	2.5
IDLE	7	26.0	0.124	1.42	26.8	4.3	2.3
LTO TOTAL FUEL (kg) or EMISSIONS (g)			448	287	5591	4810	-
NUMBER OF ENGINES				1	1	1	1
NUMBER OF TESTS				3	3	3	3
AVERAGE D_p/F_{oo} (g/kN) or AVERAGE SN (MAX)				2.76	53.5	45.8	7.7
SIGMA (D_p/F_{oo} in g/kN, or SN)				0.38	2.85	0.82	0.76
RANGE (D_p/F_{oo} in g/kN, or SN)				2.33-3.06	51.2-56.7	45.3-46.8	6.8-8.3

ACCESSORY LOADS

POWER EXTRACTION 0 (kW) AT - POWER SETTINGS
STAGE BLEED 0 % CORE FLOW AT - POWER SETTINGS

ATMOSPHERIC CONDITIONS

BAROMETER (kPa)	95.98-97.49
TEMPERATURE (K)	279 - 286
ABS HUMIDITY (kg/kg)	.002-.009

FUEL

SPEC	Jet A
H/C	1.93
AROM (%)	16

MANUFACTURER: CFMI
TEST ORGANIZATION: CFM56 Evaluation Engineering
TEST LOCATION: Peebles Site IVD
TEST DATES: FROM 11 Nov 83 TO 14 Nov 83

REMARKS

1. Ref GE Report R84AEB579.
2. Engine S/N 692441.
3. Revised based on 3/89 production status cycle.

ICAO ENGINE EXHAUST EMISSIONS DATA BANK

SUBSONIC ENGINES

III, 10

ENGINE IDENTIFICATION:	CF6-50C1, -C2	BYPASS RATIO:	4.3
UNIQUE ID NUMBER:	1GE007	PRESSURE RATIO (π_{oo}):	29.8
ENGINE TYPE:	TF	RATED OUTPUT (F_{oo}) (kN):	230.4

REGULATORY DATA

CHARACTERISTIC VALUE:	HC	CO	NOx	SMOKE NUMBER
D_p/F_{oo} (g/kN) or SN	37.3	99.0	64.3	4.8
AS % OF ORIGINAL LIMIT	190.1 %	83.9 %	64.6 %	25.5 %
AS % OF CAEP/2 LIMIT (NOx)			80.7 %	
AS % OF CAEP/4 LIMIT (NOx)			96.5 %	

DATA STATUS

x PRE-REGULATION
- CERTIFICATION
- REVISED (SEE REMARKS)

TEST ENGINE STATUS

x NEWLY MANUFACTURED ENGINES
- DEDICATED ENGINES TO PRODUCTION STANDARD
- OTHER (SEE REMARKS)

EMISSIONS STATUS

x DATA CORRECTED TO REFERENCE (ANNEX 16 VOLUME II)

CURRENT ENGINE STATUS

(IN PRODUCTION, IN SERVICE UNLESS OTHERWISE NOTED)
x OUT OF PRODUCTION (DATE: -)
- OUT OF SERVICE

MEASURED DATA

MODE	POWER SETTING ($\%F_{oo}$)	TIME minutes	FUEL FLOW kg/s	EMISSIONS INDICES (g/kg) HC	CO	NOx	SMOKE NUMBER
TAKE-OFF	100	0.7	2.487	0.6	0.5	36.3	4.1
CLIMB OUT	85	2.2	1.975	0.7	0.5	29.7	2.7
APPROACH	30	4.0	0.66	1	4.3	9.5	2.7
IDLE	7	26.0	0.215	21.8	61.8	3.6	4.5
LTO TOTAL FUEL (kg) or EMISSIONS (g)			859	7715	21591	14247	-
NUMBER OF ENGINES				6	6	6	6
NUMBER OF TESTS				6	6	6	6
AVERAGE D_p/F_{oo} (g/kN) or AVERAGE SN (MAX)				33.5	93.7	61.8	4.5
SIGMA (D_p/F_{oo} in g/kN, or SN)				3.8	4.6	0.5	1.5
RANGE (D_p/F_{oo} in g/kN, or SN)				-	-	-	-

ACCESSORY LOADS

POWER EXTRACTION	0	(kW)	AT	-	POWER SETTINGS
STAGE BLEED	0	% CORE FLOW	AT	-	POWER SETTINGS

ATMOSPHERIC CONDITIONS

BAROMETER (kPa)	98.3-100.4
TEMPERATURE (K)	270 - 296
ABS HUMIDITY (kg/kg)	.0027-.0103

FUEL

SPEC	Jet A
H/C	1.92
AROM (%)	17.1

MANUFACTURER: GE Aircraft Engines
TEST ORGANIZATION: Production Engine Test
TEST LOCATION: Production Test Cells M34 & M35
TEST DATES: FROM 12 Oct 79 TO 05 Dec 79

REMARKS

Ref Report no FAA-EE-80-27 (GE Report R80AEG420)

ICAO ENGINE EXHAUST EMISSIONS DATA BANK

SUBSONIC ENGINES

**** DATA SUPERSEDED ** SEE SHEET: 8PW089**

ENGINE IDENTIFICATION: PW4084
UNIQUE ID NUMBER: 2PW062
ENGINE TYPE: TF

BYPASS RATIO: 6.4
PRESSURE RATIO (π_{oo}): 36.2
RATED OUTPUT (F_{oo}) (kN): 369.6

REGULATORY DATA

CHARACTERISTIC VALUE:	HC	CO	NOx	SMOKE NUMBER
D_p/F_{oo} (g/kN) or SN	4.5	23.0	72.8	13.5
AS % OF ORIGINAL LIMIT	23.0 %	19.5 %	64.8 %	81.6 %
AS % OF CAEP/2 LIMIT (NOx)			81.0 %	
AS % OF CAEP/4 LIMIT (NOx)			91.7 %	

DATA STATUS

- \- PRE-REGULATION
- x CERTIFICATION
- \- REVISED (SEE REMARKS)

TEST ENGINE STATUS

- \- NEWLY MANUFACTURED ENGINES
- x DEDICATED ENGINES TO PRODUCTION STANDARD
- \- OTHER (SEE REMARKS)

EMISSIONS STATUS

- x DATA CORRECTED TO REFERENCE (ANNEX 16 VOLUME II)

CURRENT ENGINE STATUS

(IN PRODUCTION, IN SERVICE UNLESS OTHERWISE NOTED)

- \- OUT OF PRODUCTION
- \- OUT OF SERVICE

MEASURED DATA

MODE	POWER SETTING ($\%F_{oo}$)	TIME minutes	FUEL FLOW kg/s	EMISSIONS INDICES (g/kg) HC	CO	NOx	SMOKE NUMBER
TAKE-OFF	100	0.7	3.411	0.1	0.1	45	10.5
CLIMB OUT	85	2.2	2.689	0.1	0.1	35.5	-
APPROACH	30	4.0	0.875	0.2	0.4	12	-
IDLE	7	26.0	0.242	2.7	18.73	4.4	-
LTO TOTAL FUEL (kg) or EMISSIONS (g)			1086	1111	7205	23229	-
NUMBER OF ENGINES				1	1	1	1
NUMBER OF TESTS				3	3	3	3
AVERAGE D_p/F_{oo} (g/kN) or AVERAGE SN (MAX)				2.9	19.5	62.8	10.5
SIGMA (D_p/F_{oo} in g/kN, or SN)				-	-	-	-
RANGE (D_p/F_{oo} in g/kN, or SN)				-	-	-	-

ACCESSORY LOADS

POWER EXTRACTION 0 (kW) AT - POWER SETTINGS
STAGE BLEED 0 % CORE FLOW AT - POWER SETTINGS

ATMOSPHERIC CONDITIONS

BAROMETER (kPa)	101.3
TEMPERATURE (K)	288
ABS HUMIDITY (kg/kg)	0.0063

FUEL

SPEC	Jet A
H/C	1.92
AROM (%)	20.3

MANUFACTURER: Pratt and Whitney
TEST ORGANIZATION: Pratt and Whitney
TEST LOCATION: East Hartford, Ct, USA
TEST DATES: FROM 26 Apr 94 TO 02 May 94

REMARKS

Data from X832-4

If REVISED, this data supersedes databank UID 8PW090
Compliance with fuel venting requirements: - ('x' if complies, PR if pre-regulation)

ICAO ENGINE EXHAUST EMISSIONS DATA BANK

SUBSONIC ENGINES

III, 12

ENGINE IDENTIFICATION: JT3D-3B
UNIQUE ID NUMBER: 1PW001
ENGINE TYPE: TF

BYPASS RATIO: 1.4
PRESSURE RATIO (π_{oo}): 13.6
RATED OUTPUT (F_{oo}) (kN): 80.06

REGULATORY DATA

CHARACTERISTIC VALUE:	HC	CO	NOx	SMOKE NUMBER
D_p/F_{oo} (g/kN) or SN	395.4	328.2	37.7	63.9
AS % OF ORIGINAL LIMIT	2,017.6 %	278.2 %	56.1 %	254.1 %
AS % OF CAEP/2 LIMIT (NOx)			70.2 %	
AS % OF CAEP/4 LIMIT (NOx)			88.3 %	

DATA STATUS

x PRE-REGULATION
- CERTIFICATION
- REVISED (SEE REMARKS)

TEST ENGINE STATUS

- NEWLY MANUFACTURED ENGINES
x DEDICATED ENGINES TO PRODUCTION STANDARD
- OTHER (SEE REMARKS)

EMISSIONS STATUS

x DATA CORRECTED TO REFERENCE (ANNEX 16 VOLUME II)

CURRENT ENGINE STATUS

(IN PRODUCTION, IN SERVICE UNLESS OTHERWISE NOTED)
x OUT OF PRODUCTION (DATE: -)
- OUT OF SERVICE

MEASURED DATA

MODE	POWER SETTING (%F_{oo})	TIME minutes	FUEL FLOW kg/s	EMISSIONS INDICES (g/kg) HC	CO	NOx	SMOKE NUMBER
TAKE-OFF	100	0.7	1.174	4	1.5	12.1	-
CLIMB OUT	85	2.2	0.932	2	2.8	9.9	-
APPROACH	30	4.0	0.346	4	24.5	4.8	-
IDLE	7	26.0	0.135	112	98	2.5	-
LTO TOTAL FUEL (kg) or EMISSIONS (g)			466	24363	23092	2740	-
NUMBER OF ENGINES				2	2	2	2
NUMBER OF TESTS				-	-	-	-
AVERAGE D_p/F_{oo} (g/kN) or AVERAGE SN (MAX)				303.9	288.1	34.3	54.5
SIGMA (D_p/F_{oo} in g/kN, or SN)				-	-	-	-
RANGE (D_p/F_{oo} in g/kN, or SN)				-	-	-	-

ACCESSORY LOADS

POWER EXTRACTION 0 (kW) AT - POWER SETTINGS
STAGE BLEED 0 % CORE FLOW AT - POWER SETTINGS

ATMOSPHERIC CONDITIONS

BAROMETER (kPa)	-
TEMPERATURE (K)	-
ABS HUMIDITY (kg/kg)	-

FUEL

SPEC	Jet A
H/C	-
AROM (%)	-

MANUFACTURER: Pratt & Whitney
TEST ORGANIZATION: P&WA
TEST LOCATION: East Hartford, CT, USA.
TEST DATES: FROM 08 Mar 72 TO 12 Sep 74

REMARKS

Emissions data estimated from JT3D-7 engines using JT3D-3B performance data.

IV, 1

APPENDIX 4

IV, 2

WMO Meteorological codes

This document gives details of the Meteorological codes for use at observing stations.

Type / Genus of cloud:

WMO code 0500: **Genus of cloud**

/ - cloud not visible owing to darkness, fog, duststorm, sandstorm or other analogous phenomena
0 - cirrus (CI)
1 - cirricumulus (CC)
2 - cirrostratus (CS)
3 - altocumulus (AC)
4 - altostratus (AS)
5 - nimbostratus (NS)
6 - stratocumulus (SC)
7 - stratus (ST)
8 - cumulus (CU)
9 - cumulonimbus (CB)

High cloud type:

WMO code 0509: **Clouds of genera Cirrus, Cirrocumulus and Cirrostratus.**

/ - cirrus, cirrocumulus & cirrostratus invisible owing to darkness, fog, blowing dust or sand, or other phenomena, or more often because of the presence of a continuous layer of lower clouds
0 - no cirrus, cirrocumulus or cirrostratus clouds
1 - cirrus in the form of filaments, strands or hooks, not progressively invading the sky.
2 - dense cirrus, in patches or entangled sheaves, which usually do not increase & sometimes seem to be the remains of the upper part of a cumulonimbus; or cirrus with sproutings in the form of small turrets; or cirrus having the appearance of cumuliform tufts
3 - dense cirrus, often in the form of an anvil, being the remains of the upper part of cumulonimbus
4 - cirrus in the form of hooks, filaments, or both, progressively invading the sky; they generally become denser as a whole.
5 - cirrus (often in bands converging towards 1 point or 2 opposite points of the horizon) and cirrostratus, or cirrostratus alone;in either case, they are progressively invading the sky, and generally growing denser as a whole, but the continuous veil does not reach 45 degrees above the horizon.
6 - cirrus (often in bands converging towards 1 point or 2 opposite points of the horizon) and cirrostratus, or cirrostratus alone;in either case, they are progressively invading the sky, and generally growing denser as a whole; the continuous veil extends more than 45 degrees above the horizon, without the sky being totally covered.
7 - veil of cirrostratus covering the celestial dome
8 - cirrostratus not progressively invading the sky and not completely covering the celestial dome.
9 - cirrocumulus alone, or cirrocumulus accompanied by cirrus or cirrostratus, or both, but cirrocumulus is predominant

Low cloud type:

WMO code 0513: **Clouds of genera Stratocumulus, Stratus, Cumulus, etc.**

/ - stratocumulus, stratus, cumulus and cumulonimbus invisible owing to darkness, fog, blowing dust or sand, or other phenomena
0 - no stratocumulus, stratus, cumulus or cumulonimbus
1 - cumulus with little vertical extent and seemingly flattened, or ragged cumulus, other than of bad weather, or both
2 - cumulus of moderate or strong vertical extent, generally with protuberances in the form of domes or towers, either accompanied or not by other cumulus or stratocumulus, all having bases at the same level
3 - cumulonimbus, the summits of which, at least partially, lack sharp outlines but are neither clearly fibrous (cirriform) nor in the form of an anvil; cumulus, stratocumulus or stratus may also be present
4 - stratocumulus formed by the spreading out of cumulus; cumulus may also be present
5 - stratocumulus not resulting from the spreading out of cumulus
6 - stratus in a more or less continuous later, or in ragged shreds, or both but no stratus fractus of bad weather
7 - stratus fractus of bad weather or cumulus fractus of bad weather, or both (pannus), usually below altostratus or nimbostratus
8 - cumulus and stratocumulus other than that formed from the spreading out of cumulus; the base of the cumulus is at a different level from that of the stratocumulus
9 - cumulonimbus, the upper part of which is clearly fibrous (cirriform) often in the form of an anvil; either accompanied or not by cumulonimbus without anvil or fibrous upper part, by cumulus, stratocumulus, stratus or pannus

Medium cloud type:

WMO code 0515: **Clouds of the genera Altocumulus, Altostratus, etc.**

/ - altocumulus, altostratus and nimbostratus invisible owing to darkness, fog,

IV, 3

blowing dust, sand, or other phenomena; or because of the presence of a continuous layer of lower clouds
0 - no altocumulus, altostratus or nimbostratus
1 - altostratus, the greater part of which is semi-transparent; through this part the sun or moon may be weakly visible, as through ground glass
2 - altostratus, the greater part of which is sufficiently dense to hide the sun or moon, or nimbostratus
3 - altocumulus, the greater part of which is semi-transparent; the various elements of the cloud change only slowly and are all at a single level
4 - patches (often in the form of almonds or fish) of altocumulus, the greater part of which is semi-transparent; the clouds occur at one or more levels and the elements are continually changing in appearance
5 - semi-transparent altocumulus in bands, or altocumulus, in one or more continuous layer (semi-transparent or opaque), progressively invading the sky; these generally thicken as a whole
6 - altocumulus resulting from the spreading out of cumulus or cumulonimbus
7 - altocumulus in two or more layers, usually opaque in places, and not progressively invading the sky; or opaque layer of altocumulus,not progressively invading the sky; or altocumulus together with altostratus or nimbostratus
8 - altocumulus with sproutings in the form of small towers or battlements, or altocumulus having the appearance of cumuliform tufts
9 - altocumulus of a chaotic sky, generally at several levels

State of ground:

WMO code 0901: **State of ground without snow or measurable ice cover.**

0 - ground dry (no cracks or appreciable amounts of dust/loose sand)
1 - ground moist
2 - ground wet (standing water in small or large pools on surface)
3 - flooded
4 - ground frozen
5 - glaze on ground
6 - loose dry dust or sand not covering ground completely
7 - thin cover of loose dry dust or sand covering ground completely
8 - mod/thick cover of loose dry dust/sand covering ground completely
9 - extremely dry with cracks

WMO code 0975: **State of ground with snow or measurable ice cover.**

0 - ground predominantly covered by ice
1 - compact/wet snow (with or without ice) covering less than 1/2 the ground
2 - compact/wet snow (with or without ice) covering at least 1/2 the ground
3 - even layer of compact or wet snow covering ground completely
4 - uneven layer of compact or wet snow covering ground completely
5 - loose dry snow covering less than 1/2 the ground
6 - loose dry snow covering at least 1/2 the ground (not completely)
7 - even layer of loose dry snow covering ground completely
8 - uneven layer or loose dry snow covering ground completely
9 - snow covering ground completely; deep drifts

Total cloud amount:

WMO code 2700: **Cloud cover / amount**

/ - cloud is indiscernible for reasons other than fog or other meteorological phenomena, or observation is not made.
0 - sky clear
1 - 1 okta : 1/10 - 2/10
2 - 2 oktas : 2/10 - 3/10
3 - 3 oktas : 4/10
4 - 4 oktas : 5/10
5 - 5 oktas : 6/10
6 - 6 oktas : 7/10 - 8/10
7 - 7 oktas or more, but not 8 oktas : 9/10 or more, but not 10/10
8 - 8 oktas : 10/10
9 - sky obscured by fog or other meteorological phenomena

Past weather:

Past weather is defined as weather occurring in the past 6 hours at 00, 06, 12, 18 UTC, and the past 3 hours at 03, 09, 15, 21 UTC.

WMO code 4561: **Past weather**

0 - cloud covering half or less of the sky throughout the period
1 - cloud covering more than half the sky during part of the period & half or less for the rest
2 - cloud covering more than half the sky throughout the period
3 - sandstorm, duststorm or blowing snow
4 - fog or ice fog or thick haze
5 - drizzle
6 - rainl
7 - snow, or rain and snow mixed
8 - shower(s)
9 - thunderstorm(s) with or without precipitation

Present weather:

WMO code 4677: **Present weather reported from a manned station.**

00 - Cloud development not observed or not observable

IV, 4

01 - Cloud generally dissolving or becoming less developed
02 - State of sky on the whole unchanged
03 - Clouds generally forming or developing
04 - Visibility reduced by smoke, e.g. veldt or forest fires, industrial smoke or volcanic ashes
05 - Haze
06 - Widespread dust in suspension in the air, not raised by wind at or near the station at the time of observation
07 - Dust or sand raised by wind at or near the station at the time of observation, but not well-developed dust whirl(s) or sand whirl(s), and no duststorm or sandstorm seen; or, in the case of ships, blowing spray at the station
08 - Well-developed dust or sand whirl(s) seen at or near the station during the preceding hour or at the time of observation, but no dust storm or sandstorm
09 - Duststorm or sandstorm within sight at the time of observation, or at the station during the preceding hour
10 - Mist
11 - Patches of shallow fog or ice fog at the station, whether on land or sea not deeper than about 2 metres on land or 10 metres at sea
12 - More or less continuous shallow fog or ice fog at the station, whether on land or sea, not deeper than about 2m/land or 10m/sea
13 - Lightning visible, or thunder heard
14 - Precipitation within sight, not reaching the ground or the surface of the sea
15 - Precipitation within sight, reaching the ground or the surface of the sea, but distant, i.e. > 5 km from the station
16 - Precipitation within sight, reaching the ground or the surface of the sea, near to, but not at the station
17 - Thunderstorm, but no precipitation at the time of observation
18 - Squalls at or within sight of the station during the preceding hour or at the time of observation
19 - Funnel clouds at or within sight of the station during the preceding hour or at the time of observation
20 - Drizzle (not freezing) or snow grains, not falling as showers, during the preceding hour but not at the time of observation
21 - Rain (not freezing), not falling as showers, during the preceding hour but not at the time of observation
22 - Snow, not falling as showers, during the preceding hour but not at the time of observation
23 - Rain and snow or ice pellets, not falling as showers; during the preceding hour but not at the time of observation
24 - Freezing drizzle or freezing rain; during the preceding hour but not at the time of observation
25 - Shower(s) of rain during the preceding hour but not at the time of observation
26 - Shower(s) of snow, or of rain and snow during the preceding hour but not at the time of observation
27 - Shower(s) of hail, or of rain and hail during the preceding hour but not at the time of observation
28 - Fog or ice fog during the preceding hour but not at the time of observation
29 - Thunderstorm (with or without precipitation) during the preceding hour but not at the time of observation
30 - Slight or moderate duststorm or sandstorm - has decreased during the preceding hour
31 - Slight or moderate duststorm or sandstorm - no appreciable change during the preceding hour
32 - Slight or moderate duststorm or sandstorm - has begun or has increased during the preceding hour
33 - Severe duststorm or sandstorm - has decreased during the preceding hour
34 - Severe duststorm or sandstorm - no appreciable change during the preceding hour
35 - Severe duststorm or sandstorm - has begun or has increased during the preceding hour
36 - Slight/moderate drifting snow - generally low (below eye level)
37 - Heavy drifting snow - generally low (below eye level)
38 - Slight/moderate blowing snow - generally high (above eye level)
39 - Heavy blowing snow - generally high (above eye level)
40 - Fog or ice fog at a a distance at the time of observation, but not at station during the preceding hour, the fog or ice fog extending to a level above that of the observer
41 - Fog or ice fog in patches
42 - Fog/ice fog, sky visible, has become thinner during the preceding hour
43 - Fog/ice fog, sky invisible, has become thinner during the preceding hour
44 - Fog or ice fog, sky visible, no appreciable change during the past hour
45 - Fog or ice fog, sky invisible, no appreciable change during the preceding hour
46 - Fog or ice fog, sky visible, has begun or has become thicker during preceding hour
47 - Fog or ice fog, sky invisible, has begun or has become thicker during the preceding hour
48 - Fog, depositing rime, sky visible
49 - Fog, depositing rime, sky invisible
50 - Drizzle, not freezing, intermittent, slight at time of ob.
51 - Drizzle, not freezing, continuous, slight at time of ob.
52 - Drizzle, not freezing, intermittent, moderate at time of ob.
53 - Drizzle, not freezing, continuous, moderate at time of ob.
54 - Drizzle, not freezing, intermittent, heavy at time of ob.
55 - Drizzle, not freezing, continuous, heavy at time of ob.
56 - Drizzle, freezing, slight
57 - Drizzle, freezing, moderate or heavy (dense)
58 - Rain and drizzle, slight
59 - Rain and drizzle, moderate or heavy
60 - Rain, not freezing, intermittent, slight at time of ob.
61 - Rain, not freezing, continuous, slight at time of ob.
62 - Rain, not freezing, intermittent, moderate at time of ob.
63 - Rain, not freezing, continuous, moderate at time of ob.
64 - Rain, not freezing, intermittent, heavy at time of ob.
65 - Rain, not freezing, continuous, heavy at time of ob.
66 - Rain, freezing, slight
67 - Rain, freezing, moderate or heavy
68 - Rain or drizzle and snow, slight
69 - Rain or drizzle and snow, moderate or heavy
70 - Intermittent fall of snowflakes, slight at time of ob.
71 - Continuous fall of snowflakes, slight at time of ob.
72 - Intermittent fall of snowflakes, moderate at time of ob.
73 - Continuous fall of snowflakes, moderate at time of ob.
74 - Intermittent fall of snowflakes, heavy at time of ob.
75 - Continuous fall of snowflakes, heavy at time of ob.
76 - Diamond dust (with or without fog)
77 - Snow grains (with or without fog)

IV, 5

78 - Isolated star-like snow crystals (with or without fog)
79 - Ice pellets
80 - Rain shower(s), slight
81 - Rain shower(s), moderate or heavy
82 - Rain shower(s), violent
83 - Shower(s) of rain and snow, slight
84 - Shower(s) of rain and snow, moderate or heavy
85 - Snow shower(s), slight
86 - Snow shower(s), moderate or heavy
87 - Shower(s) of snow pellets or small hail, with or without rain or rain and snow mixed - slight
88 - Shower(s) of snow pellets or small hail, with or without rain or rain and snow mixed - moderate or heavy
89 - Shower(s) of hail, with or without rain or rain and snow mixed, not associated with thunder - slight
90 - Shower(s) of hail, with or without rain or rain and snow mixed, not associated with thunder - moderate or heavy
91 - Slight rain at time of observation - Thunderstorm during the preceding hour but not at time of observation
92 - Moderate or heavy rain at time of observation - Thunderstorm during the preceding hour but not at time of observation
93 - Slight snow, or rain and snow mixed or hail at time of observation - Thunderstorm during the preceding hour but not at time of observation
94 - Moderate or heavy snow, or rain and snow mixed or hail at time of observation - Thunderstorm during the preceding hour but not at time of observation
95 - Thunderstorm, slight or moderate, without hail, but with rain and/or snow at time of observation
96 - Thunderstorm, slight or moderate, with hail at time of ob.
97 - Thunderstorm, heavy, without hail, but with rain and/or snow at time of observation
98 - Thunderstorm combined with dust/sandstorm at time of observation
99 - Thunderstorm, heavy with hail at time of observation

Pressure characteristic over last 3 hours:

*WMO code 0200:***Characteristic of pressure tendency.**

0 - Increasing, then decreasing : atmospheric pressure the same as or higher than 3 hrs ago
1 - Increasing, then steady : atmospheric pressure now higher than 3 hrs ago
2 - Increasing (steadily or unsteadily) : atmospheric pressure now higher than 3 hrs ago
3 - Decreasing or steady, then increasing; or increasing, then increasing more rapidly : atmospheric pressure now higher than 3 hrs ago
4 - Steady : atmospheric pressure the same as 3 hrs ago
5 - Decreasing, then increasing : atmospheric pressure the same as or lower than 3 hrs ago
6 - Decreasing, then steady; or decreasing then decreasing more slowly : atmospheric pressure now lower than 3 hrs ago
7 - Decreasing (steadily or unsteadily) : atmospheric pressure now lower than 3 hrs ago
8 - Steady or increasing, then decreasing; or decreasing, then decreasing more rapidly : atmospheric pressure now lower than 3 hrs ago

Day of Thunder:

6000 NCM table 24

0 - no thunderstorm (0000-2400gmt)
1 - thunderstorm with or without precipitation
9 - no thunderstorm (restricted period)

Day of Hail:

6001 NCM table 23

0 - no hail,ice,etc (0000-2400gmt)
1 - diamond dust
2 - snow grains
3 - snow pellets
4 - ice pellets or small hail (less than 5mm diameter)
5 - hail (diameter 5-9 mm)
6 - hail (diameter 10-19 mm)
7 - hail (diameter 20mm or more)
9 - no hail ,ice etc restricted period

Day of snow or sleet:

6002 NCM table 27

0 - no snow or sleet(0000-2400gmt)
1 - sleet
5 - snow
9 - no snow or sleet(restricted period)

Day of fog:

6003 NCM table 25

0 - visibility 1000m or more at 0900 gmt(previous day)
1 - visibility less than 1000m at 0900 gmt

IV, 6

Day of Gale:

```
6004    NCM table 26

0 - no gale(0000-2400 gmt)
1 - day on which wind speed has reached 34 knots (beaufort force 8) for a
    period of at least 10 minutes
9 - no gale (restricted period)
```

State of concrete:

```
6005    NCM table 22

/ - slab covered by snow or not adequately described by codes 0 to 3
0 - slab dry
1 - slab moist
2 - slab wet
3 - slab icy
```

Snow lying at 0900GMT:

```
6006    CDB flag

0 - no snow or less than half cover of snow lying
1 - more than half cover of snow at 0900z today
```

Snow depth:

```
001 - 1cm
002 - 2cm
... - ...
996 - 996cm
997 - Less than 0.5cm
998 - Snow cover, not continuous
999 - Measurement impossible or inaccurate
```

```
020011 CLOUD AMOUNT

0  0
1  1 OKTA OR <1
2  2 OKTAS
3  3 OKTAS
4  4 OKTAS
5  5 OKTAS
6  6 OKTAS
7  7 OKTAS (<8)
8  8 OKTAS
9  SKY OBSCURED METEOROLOGICAL
10 SKY PARTLY  OBSCURED BY FOG AND/OR OTHER METEOROLOGICAL PHENOMENA
11 SCATTERED
12 BROKEN
13 FEW
```

```
020012 CLOUD TYPE

0  CI
1  CC
2  CS
3  AC
4  AS
5  NS
6  SC
7  ST
8  CU
9  CB
10 NO CH CLOUDS
11 CI FIB (UNC)
12 CI SPI SHEAF
13 CI SPI CUGEN
14 CI UNC/FIB
15 CI VEIL <45'
16 CI VEIL >45'
17 CS WHOLE SKY
18 CS NOT COVER
19 CH MOSTLY CC
20 NO CM CLOUDS
21 AS TR
22 AS OP / NS
23 AC TR LEVEL
24 AC TR PATCHY
25 AC TR BANDS
26 AC CU(CB)GEN
27 AC TR LAYERS
28 AC CAS/FLO
29 AC CHAOTIC
30 NO CL CLOUDS
31 CU HUM/FRA
32 CU MED/CON
33 CU CAL
34 SC CUGEN
35 SC NOT CUGEN
36 SC NEB/FRA
37 ST/CU FRA
38 CU/SC LEVELS
```

IV, 7

39 CB CAP
40
41
42
43
44
45
46
47
48
49
50
51
52
53
54
55
56
57
58
59 CLOUD INVIS
60 CH INVISIBLE
61 CM INVISIBLE
62 CL INVISIBLE

V, 1

APPENDIX 5

Updated Aviation Radiative Forcing for 2000

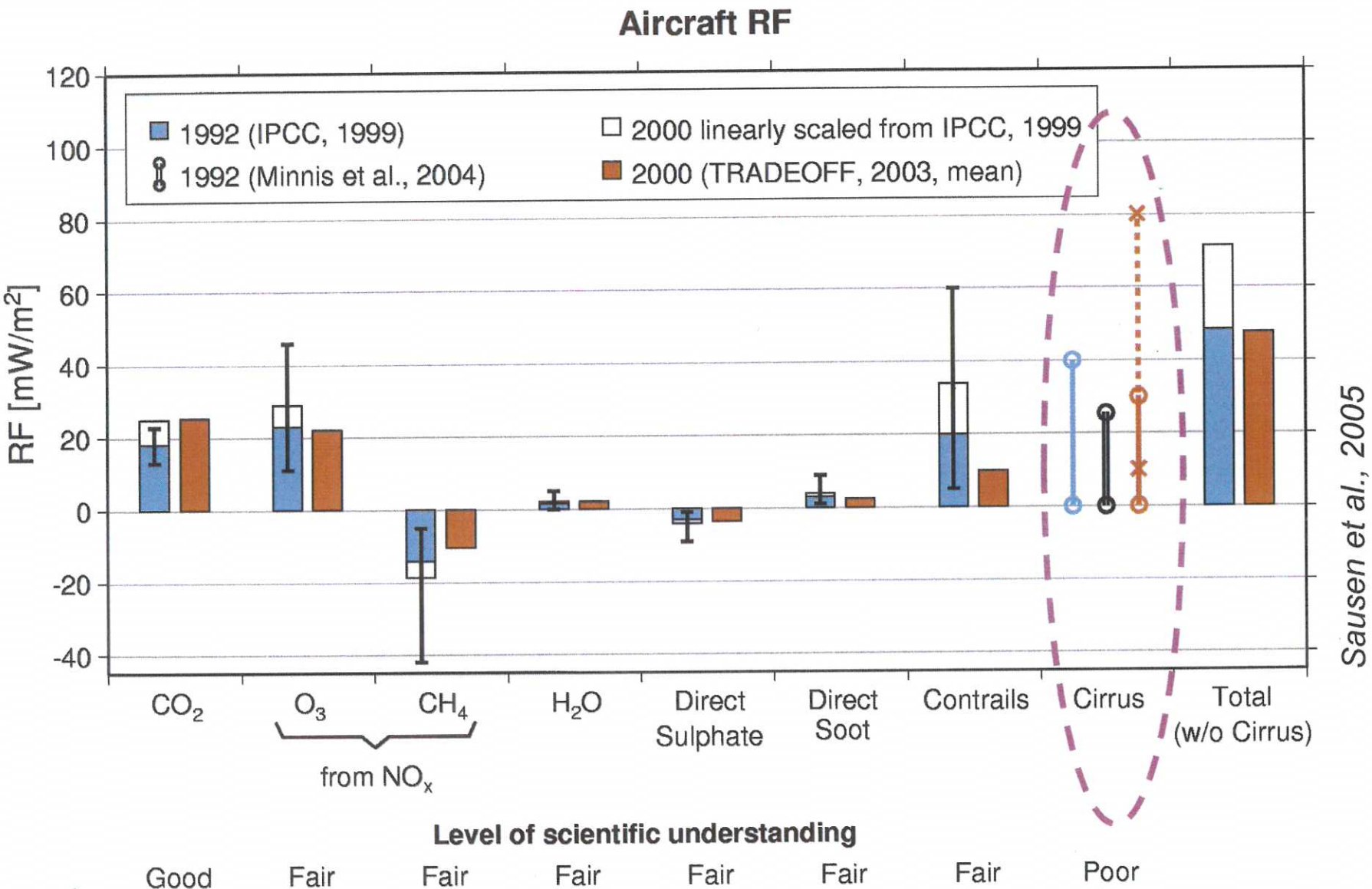

VI, 1

APPENDIX 6

VI, 2

Contrails reduce daily temperature range

A brief interval when the skies were clear of jets unmasked an effect on climate.

The potential of condensation trails (contrails) from jet aircraft to affect regional-scale surface temperatures has been debated for years[1–3], but was difficult to verify until an opportunity arose as a result of the three-day grounding of all commercial aircraft in the United States in the aftermath of the terrorist attacks on 11 September 2001. Here we show that there was an anomalous increase in the average diurnal temperature range (that is, the difference between the daytime maximum and night-time minimum temperatures) for the period 11–14 September 2001. Because persisting contrails can reduce the transfer of both incoming solar and outgoing infrared radiation[4,5] and so reduce the daily temperature range, we attribute at least a portion of this anomaly to the absence of contrails over this period.

We analysed maximum and minimum temperature data[6] from about 4,000 weather stations throughout the conterminous United States (the 48 states not including Alaska and Hawaii) for the period 1971–2000, and compared these to the conditions that prevailed during the three-day aircraft-grounding period. All sites were inspected for data quality and adjusted for the time of observation.

Because the grounding period commenced after the minimum temperatures had been reached on the morning of 11 September and ended before maximum temperatures were attained on 14 September (at noon, Eastern Standard Time), we staggered the calculation of the average diurnal temperature range (DTR) across adjacent days (for example, 11 September maxima minus 12 September minima). We repeated this procedure for the three-day periods immediately before and after the grounding period, and also for the same periods (8–11, 11–14 and 14–17 September) for each year from 1971 to 2000.

DTRs for 11–14 September 2001 measured at stations across the United States show an increase of about 1.1 °C over normal 1971–2000 values (Fig. 1). This is in contrast to the adjacent three-day periods, when DTR values were near or below the mean (Fig. 1). DTR departures for the grounding period are, on average, 1.8 °C greater than DTR departures for the two adjacent three-day periods.

This increase in DTR is larger than any during the 11–14 September period for the previous 30 years, and is the only increase greater than 2 standard deviations away from the mean DTR (s.d., 0.85 °C). Moreover, the 11–14 September increase in DTR was more than twice the national average for regions of the United States where contrail coverage has previously been reported to be most abundant (such as the midwest, northeast and northwest regions)[7].

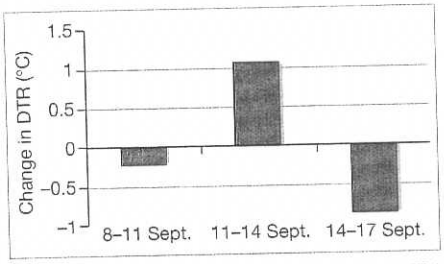

Figure 1 Departure of average diurnal temperature ranges (DTRs) from the normal values derived from 1971–2000 climatology data for the indicated three-day periods in September 2001. These periods included the three days before the terrorist attacks of 11 September; the three days immediately afterwards, when aircraft were grounded and there were therefore no contrails; and the subsequent three days.

Day-to-day changes in synoptic atmospheric conditions can affect regional DTRs[8]. In particular, a lack of cloud cover helps to increase the maximum (and reduce the minimum) temperature. Maps of the daily average outgoing long-wave radiation (OLR)[9,10] — a proxy for optically thick clouds — show reduced cloudiness (that is, larger OLR) over the eastern half of the United States on 11 September, but more cloud (smaller OLR) over parts of the west. Cloud cover subsequently decreased in the west and increased over much of the eastern half of the country during the next two days, producing predominantly negative three-day OLR changes in the east and positive values in parts of the west.

Our findings indicate that the diurnal temperature range averaged across the United States was increased during the aircraft-grounding period, despite large variations in the amount of cloud associated with mobile weather systems (Fig. 2). We argue that the absence of contrails was responsible for the difference between a period of above-normal but unremarkable DTR and the anomalous conditions that were recorded.

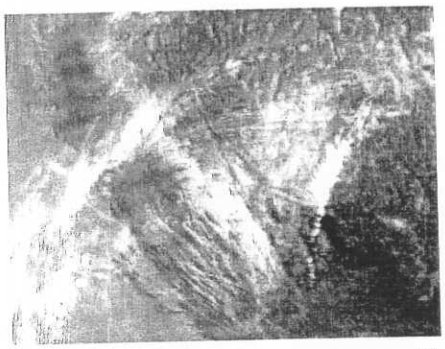

NOAA SATELLITE ACTIVE ARCHIVE

Figure 2 Flight lines: jet contrails can clearly be seen as thin streaks in this satellite image of the southwestern United States.

David J. Travis*, Andrew M. Carleton†, Ryan G. Lauritsen*

**Department of Geography and Geology, University of Wisconsin–Whitewater, Whitewater, Wisconsin 53190, USA*
e-mail: travisd@.uww.edu
†Department of Geography, Pennsylvania State University, University Park, Pennsylvania 16801, USA

1. Changnon, S. A. *J. Appl. Meteorol.* **20**, 496–508 (1981).
2. Travis, D. J. & Changnon, S. A. *J. Weather Modification* **29**, 74–83 (1997).
3. Sassen, K. *Bull. Am. Meteorol. Soc.* **78**, 1885–1903 (1997).
4. Duda, D. P., Minnis, P. & Nguyen, L. *J. Geophys. Res.* **106**, 4927–4937 (2001).
5. Meerkotter, R. *et al. Ann. Geophys.* **17**, 1080–1094 (1999).
6. National Oceanic and Atmospheric Administration. *TD3200/3210 Data Set for 1971–2001* (Natl Climate Data Center, Asheville, North Carolina, 2001).
7. DeGrand, J. Q., Carleton, A. M., Travis, D. J. & Lamb, P. J. *Appl. Meteorol.* **39**, 1434–1459 (2000).
8. Karl, T. R. *et al. Bull Am. Meteorol. Soc.* **74**, 1007–1023 (1993).
9. Liebmann, B. & Smith, C. A. *Bull Am. Meteorol. Soc.* **77**, 1275–1277 (1996).
10. http://www.cdc.noaa.gov (NOAA-CIRES Climate Diagnostics Center, Boulder, Colorado, USA).

Competing financial interests: declared none.

Animal behaviour

Male parenting of New Guinea froglets

Male parental care is exceptionally rare in nature, although one of the most fascinating aspects of New Guinea's biodiversity is the evolution of male care in the frog family Microhylidae[1]. Here I report a new mode of parental care: transport of froglets by the male parent, which was recently discovered in two species of microhylid frogs from the mountains of Papua New Guinea. As the offspring jump off at different points, they may benefit from reduced competition for food, lower predation pressure and fewer opportunities for inbreeding between froglets, which may explain why this unusual form of parental care evolved.

I quantified the parental care behaviour of several species of microhylid frog at the Crater Mountain Biological Research Station, Chimbu Province, Papua New Guinea (6° 43′ S, 145° 05′ E), which is located on the largest tropical island in

VI, 3

Regional Variations in U.S. Diurnal Temperature Range for the 11–14 September 2001 Aircraft Groundings: Evidence of Jet Contrail Influence on Climate

DAVID J. TRAVIS

Department of Geography and Geology, University of Wisconsin—Whitewater, Whitewater, Wisconsin

ANDREW M. CARLETON

Department of Geography and Environment Institute, The Pennsylvania State University, University Park, Pennsylvania

RYAN G. LAURITSEN

Department of Geography, Northern Illinois University, Dekalb, Illinois

(Manuscript received 26 November 2002, in final form 3 September 2003)

ABSTRACT

The grounding of all commercial aircraft within U.S. airspace for the 3-day period following the 11 September 2001 terrorist attacks provides a unique opportunity to study the potential role of jet aircraft contrails in climate. Contrails are most similar to natural cirrus clouds due to their high altitude and strong ability to efficiently reduce outgoing infrared radiation. However, they typically have a higher albedo than cirrus; thus, they are better at reducing the surface receipt of incoming solar radiation. These contrail characteristics potentially suppress the diurnal temperature range (DTR) when contrail coverage is both widespread and relatively long lasting over a specific region. During the 11–14 September 2001 grounding period natural clouds and contrails were noticeably absent on high-resolution satellite imagery across the regions that typically receive abundant contrail coverage. A previous analysis of temperature data for the grounding period reported an anomalous increase in the U.S.-averaged, 3-day DTR value. Here, the spatial variation of the DTR anomalies as well as the separate contributions from the maximum and minimum temperature departures are analyzed. These analyses are undertaken to better evaluate the role of jet contrail absence and synoptic weather patterns during the grounding period on the DTR anomalies.

It is shown that the largest DTR increases occurred in regions where contrail coverage is typically most prevalent during the fall season (from satellite-based contrail observations for the 1977–79 and 2000–01 periods). These DTR increases occurred even in those areas reporting positive departures of tropospheric humidity, which may reduce DTR, during the grounding period. Also, there was an asymmetric departure from the normal maximum and minimum temperatures suggesting that daytime temperatures responded more to contrail absence than did nighttime temperatures, which responded more to synoptic conditions. The application of a statistical model that "retro-predicts" contrail-favored areas (CFAs) on the basis of upper-tropospheric meteorological conditions existing during the grounding period, supports the role of contrail absence in the surface temperature anomalies; especially for the western United States. Along with previous studies comparing surface climate data at stations beneath major flight paths with those farther away, the regionalization of the DTR anomalies during the September 2001 "control" period implies that contrails have been helping to decrease DTR in areas where they are most abundant, at least during the early fall season.

1. Introduction

An important consideration in identifying the climate impacts of changes in cloud radiative forcing are the role of high clouds, including the "false cirrus" condensation trails (contrails) generated by jet aircraft. Contrails may persist as "outbreaks" on multihour (3–6 h) time scales and over space scales of more than 1000 km^2 (Travis et al. 1997; Penner et al. 1999; Minnis et al. 2002). These contrail outbreaks may obscure a substantial portion of the sky or mix with "natural" cirrus to enhance the total cloud amount (Bakan et al. 1994; Travis et al. 1997; Duda et al. 2001; Fig. 1). Hence, the radiative forcing produced by contrails may be significant for those regions of the United States characterized by many such outbreaks (e.g., the Midwest, parts of the West Coast, the Northeast and Southeast; Minnis et al. 1997; Sassen 1997; DeGrand et al. 2000).

Some researchers have speculated that persisting contrails exacerbate "global warming" in areas where they

Corresponding author address: Dr. David J. Travis, Department of Geography and Geology, University of Wisconsin—Whitewater, Whitewater, WI 53190.
E-mail: travisd@uww.edu

FIG. 1. AVHRR thermal IR (band 4) image (at 1.1-km resolution) of a contrail "outbreak" over the Midwest taken at 1000 UTC 11 Sep 1995. The southern tip of Lake Michigan can be seen at the top of the image.

most frequently occur, due to their ability to reduce outgoing infrared radiation while transmitting some solar radiation to the surface; similar to natural cirrus (e.g., Meerkotter et al. 1999). However, there is probably a diurnal dependence to the role of contrails in radiative forcing that is missing in the case of natural cirrus, and that is enhanced by the strong diurnal variability of aircraft flight frequencies. Because contrails contain a higher density of relatively small ice crystals compared with natural cirrus clouds (Murcray 1970; Gothe and Grassl 1993), the contrail radiative forcing during daylight hours may be dominated by the higher albedo of contrails versus natural cirrus, leading to a potential surface "cooling" (Mims and Travis 1997). At night, the infrared forcing of contrails dominates relative to clear-sky conditions, producing a surface "warming" effect similar to natural clouds. Thus, when considered across a 24-h period it is possible that the net contrail radiative forcing is relatively small. However, the combination of both the daytime cooling and nighttime warming effects should result in a decrease in the diurnal temperature range (DTR), as shown in previous case studies (e.g., Travis and Changnon 1997; Travis et al. 2002). Thus, a need exists to investigate the net effect of contrails on surface temperature across a range of geographic regions and synoptic conditions, especially because significant decreases in DTR have been reported for some areas of the United States during the second half of the twentieth century, including those where contrails are most abundant (e.g., Karl et al. 1993; Travis and Changnon 1997).

Previous attempts to identify a contrail effect in the

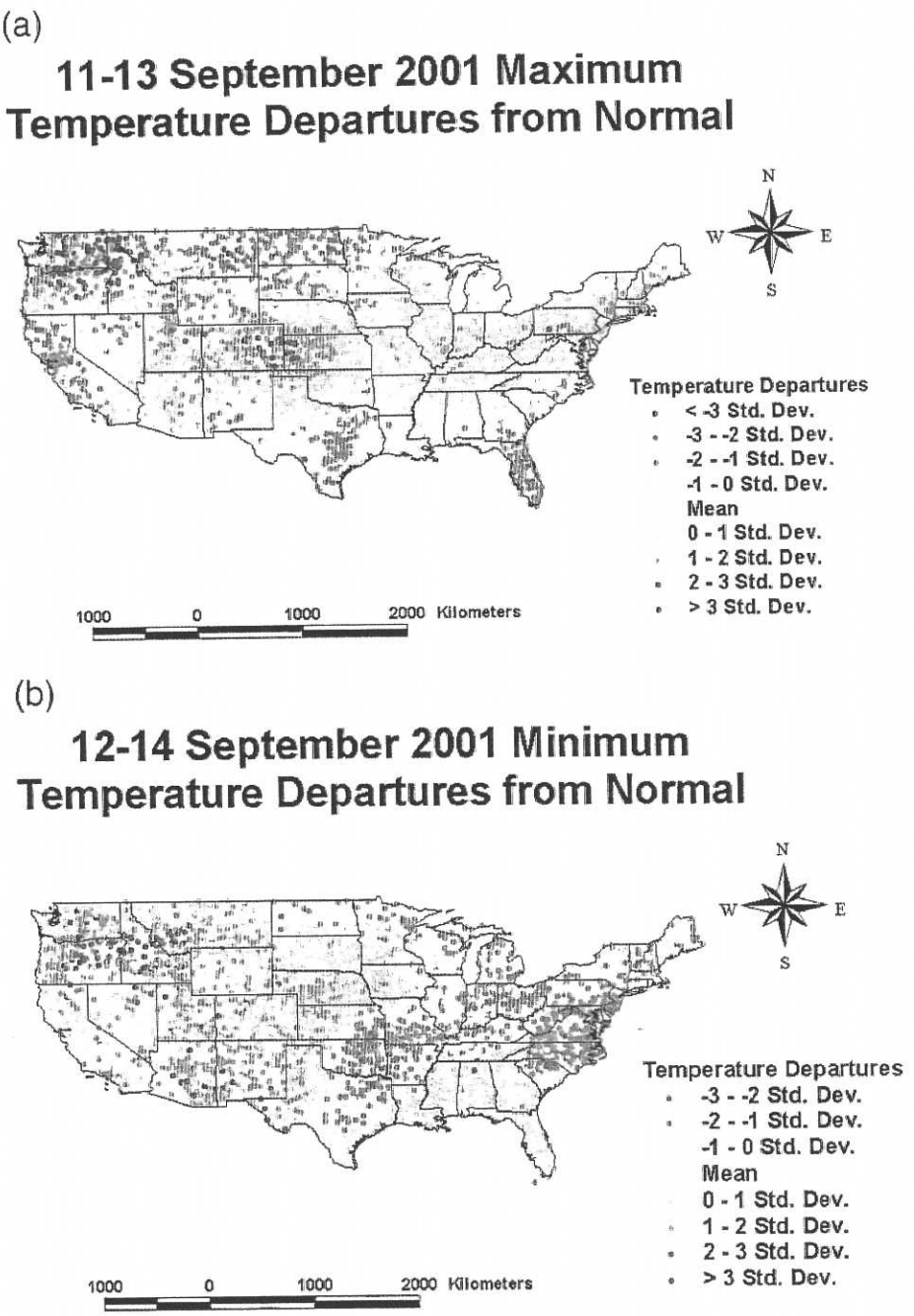

FIG. 2. Map of weather station std dev departures from normal of (a) 11–13 Sep 2001 max temperature (T_{max}), and (b) 12–14 Sep 2001 min temperature (T_{min}).

climate record have been based mostly on circumstantial evidence; from comparisons of locations with high frequencies of jet aircraft flights or contrails to adjacent locations having fewer (Changnon 1981; Travis and Changnon 1997; Allard 1997). Accordingly, it has been difficult to quantify a contrail effect because of the lack of a comparison "control" period during which persisting contrails were absent significantly longer than their typical life span. The grounding of all commercial aviation in U.S. airspace for approximately 72 h between 11 and 14 September 2001 that followed the terrorist hijackings of four jetliners in U.S. airspace pro-

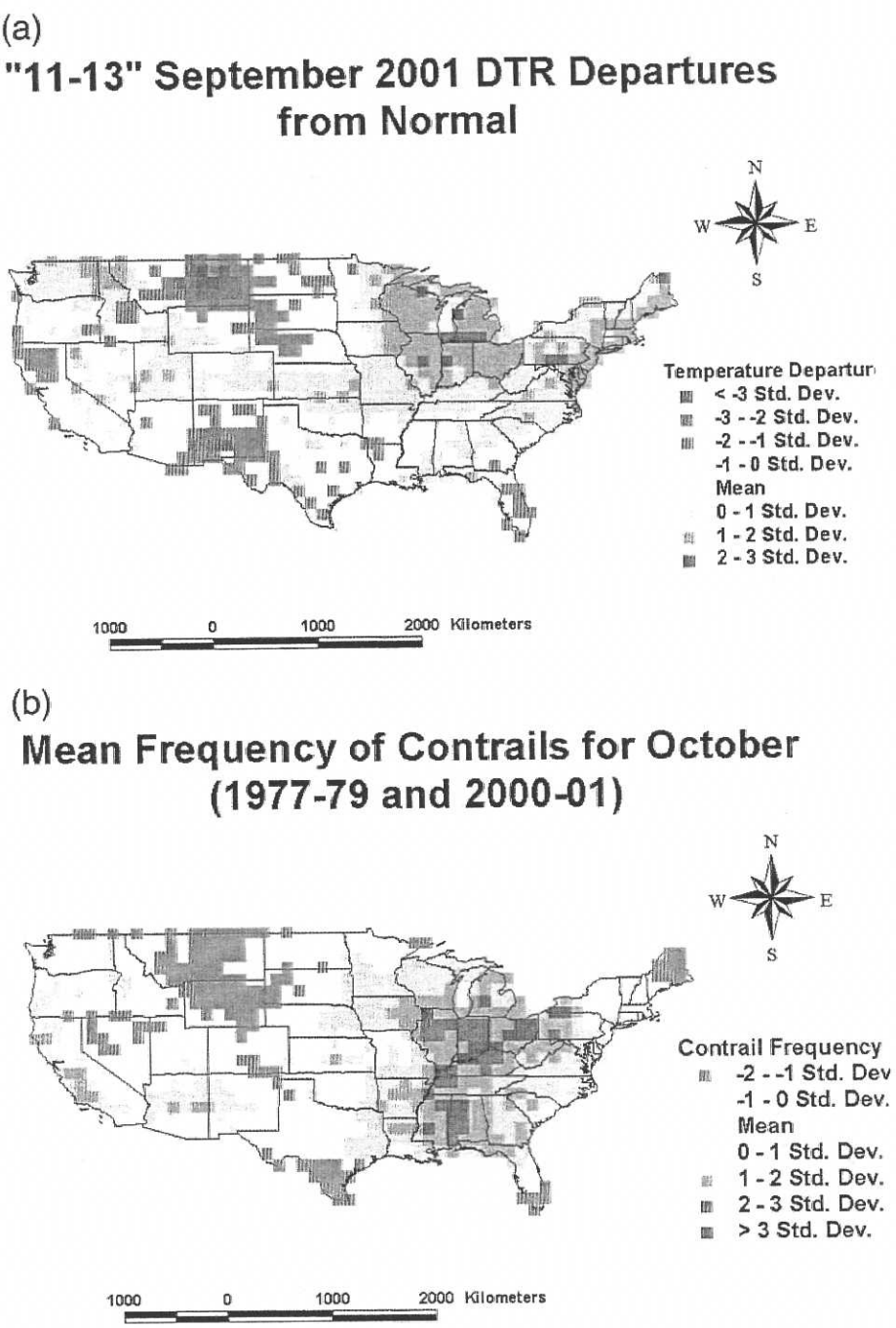

FIG. 3. Map of 1° × 1° resolution (a) grid cell–averaged DTR std dev departure values from long-term (1971–2000) normals for 11–13 Sep 2001, and (b) the combined 1977–79 and 2000–01 mean contrail frequency for Oct.

vides an unexpected opportunity to investigate the regional-scale as well as U.S.-wide effects of contrails on DTR. Our previous study (Travis et al. 2002) has shown that the U.S.-averaged DTR departure for the grounding period increased by approximately 1°C compared to the long-term normals (1971–2000), and 1.8°C compared to the average departure of the adjacent 3-day periods.

To evaluate the presence and magnitude of U.S. re-

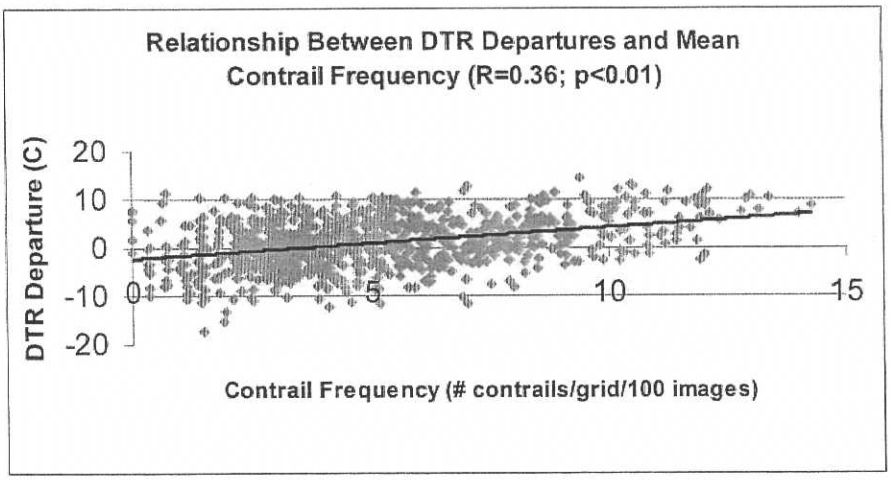

FIG. 4. Scatterplot of the relationship between 11–13 Sep 2001 DTR departures and mean combined 1977–79 and 2000–01 contrail frequency for Oct ($R = 0.36$; $p < 0.01$).

gional-scale DTR anomalies during the grounding period, and determine any associations with the frequency of contrail coverage typically experienced during the fall season, we utilize combinations of surface temperature observations, high-resolution satellite data, and synoptic-scale meteorological reanalyses. Moreover, we provide evidence linking the lack of jet contrails during the grounding period to most observed increases in regional DTR, and also to the asymmetric changes in maximum and minimum temperatures from which DTR is derived.

2. Data and methods

a. Station temperature data

Station data on the daily maximum temperature (T_{max}) and minimum temperature (T_{min}) for all first-order, automated, and cooperative stations in the United States, were obtained from the National Climate Data Center (NCDC 2003) for the most recent 30-yr "normals" period (1971–2000), plus 2001 for the grounding period. Although daily normals were available for a total of 5556 stations, data for only 5404 of those stations were available for the 2001 study period. In addition, many of the stations were cooperative observing sites that record maximum and minimum temperatures from only one observation per 24-h period, unlike the remaining first- and second-order stations that compute daily maxima and minima from continuous observations starting after midnight each day. Thus, it was necessary to standardize the cooperative data by observing time. To ensure that the daily maxima and minima for 11–14 September 2001 were assigned to the correct day, we only included those stations that recorded observations between 0700–0900 or after 1600 local time (LT). When observations were recorded between 0700 and 0900 LT the T_{max} value was assumed to represent the value for the previous day, and when observed after 1600 LT, for the current day. Because only observations from 0700 LT and later were included, each daily T_{min} was assumed to represent the current day's value. These standardization efforts still allowed 4233 stations to be utilized in the temperature analyses, with a reasonably even distribution across the United States (Fig. 2).

Because the aircraft-grounding period began during midmorning (eastern standard time) on 11 September and ended around noon on 14 September,[1] it was necessary to stagger the calculations of average T_{max}, T_{min}, and DTR across adjacent days. Thus, the afternoon of 11 September and the morning of 14 September represent the beginning and end periods, respectively, of the analysis. The average T_{max} was calculated as the mean of all such observations for 11–13 September (Fig. 2a) and the mean T_{min} was calculated as the average of all such observations for 12–14 September (Fig. 2b). The DTR values for "11 September" were calculated by subtracting each station's minimum temperature on 12 September from its maximum on 11 September, and similarly for the rest of the grounding period. The DTR values so calculated were then averaged for the "11–13" September 2001 period. To evaluate DTR values for the 3-day grounding period in context of the contemporary climatology, we calculated DTR in a similar way for each 11–13 September period for 1971–2000; thus, providing long-term station DTR normals (NCDC 2003). DTR departures for 11–13 September 2001 were then calculated by subtracting station values for 2001 from the corresponding 1971–2000 normals.

[1] A relatively small number of short flights (approximately 4000) took place during the evening of 13 September to reposition aircraft that were redirected during the shutdown on the morning of 11 September. These should not affect the conclusions of this study.

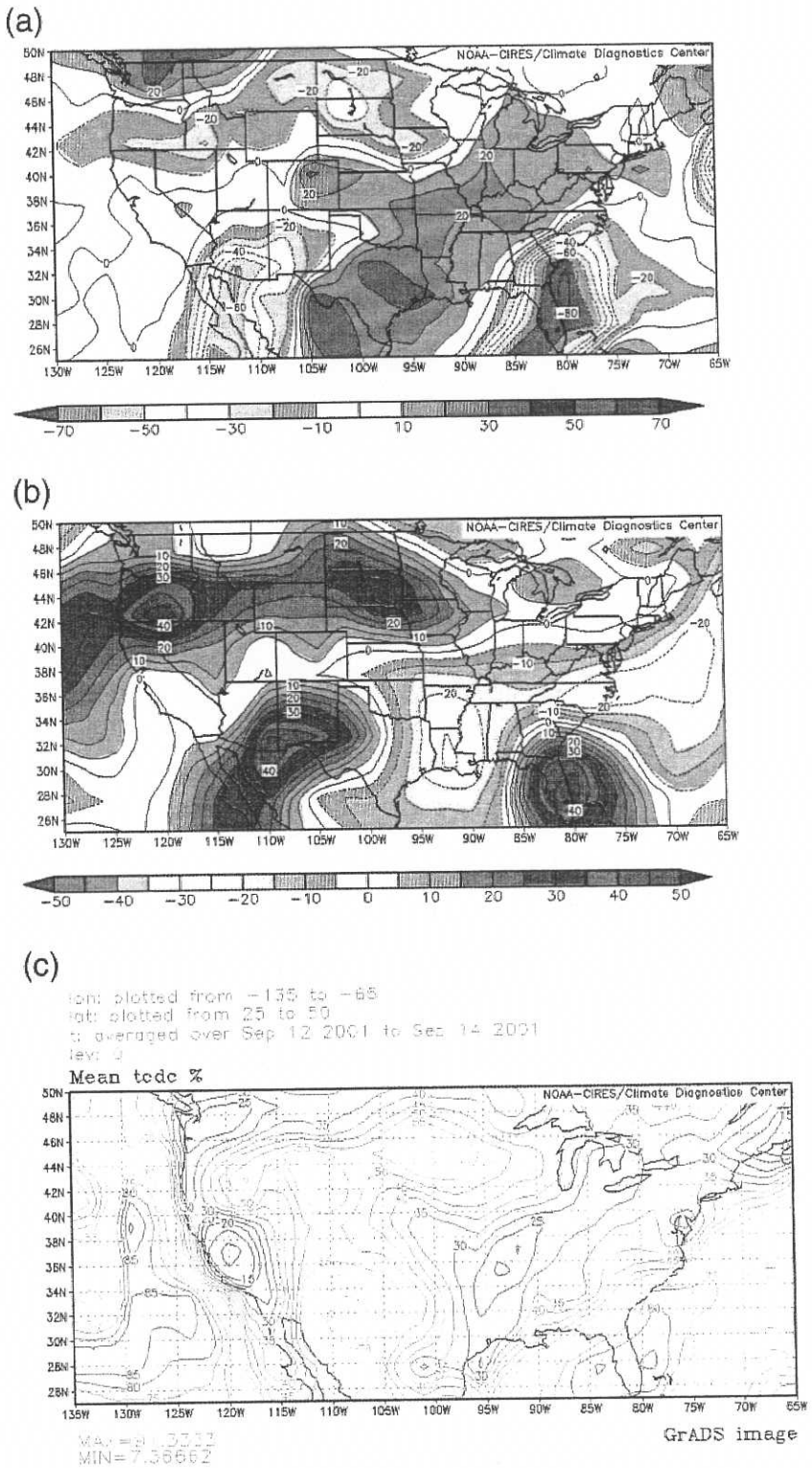

FIG. 5. Mapped 3-day average (12–14 Sep 2001) of (a) anomalies of OLR in W m^{-2}, (b) anomalies of relative humidity at 500 hPa; RH(500) in percent; and (c) mean percentage of total cloud sky coverage, derived using the NCEP–NCAR reanalyses.

b. Satellite data on contrail outbreaks

To best represent the variations in frequency and density of "typical" contrail coverage across the United States during the fall season for both the recent historical and contemporary periods, we combined two satellite-based data sources of contrail frequency: one previously published and the other original. The first was an analysis of contrail frequency over the conterminous United States for the 1977–79 period based on manual interpretation of high-resolution (0.6 km) Defense Meteorological Satellite Program (DMSP) satellite imagery (DeGrand et al. 2000). This study determined the frequency of contrail occurrence per $1° \times 1°$ grid cells for each of the four midseason months. October was the closest month to our study period and provides an approximation of contrail frequency for the fall season (DeGrand et al. 2000). The procedures used in the recent historical contrail study were duplicated here for the months of October 2000 and 2001, to estimate contrail frequency for the contemporary fall season period. The only exception to this was the satellite data source. For 2000–01, the nonavailability of a dataset having identical temporal and spatial resolutions to the DMSP imagery necessitated that we use data from the Advanced Very High Resolution Radiometer (AVHRR). The AVHRR has a slightly coarser nadir resolution (1.1 km) yet comparable temporal and spatial coverage to that of the DSMP for the 1977–79 period. The slight decrease in resolution of the AVHRR compared with the DMSP should have only a small impact on the ability to recognize *single* contrails (Detwiler and Pratt 1984). More importantly, from the climatic perspective, our use of AVHRR should not substantially impact the relative frequency of regional contrail coverage (i.e., that due to multiple contrails occurring simultaneously). An average of four images per day were analyzed across the two study periods to approximate the regional variations in mean contrail frequency during the climate normals and 2001 periods. The locations of each contrail were stored in a geographic information system (GIS) database [Environmental Systems Research Inc., (ESRI) 1999] for subsequent manipulation and statistical analyses.

Contrails are best distinguished from natural clouds using the infrared band 4 of the AVHRR that is present on all of the National Oceanic and Atmospheric Administration (NOAA) polar-orbiting satellites. We followed the manual pattern recognition method described in Carleton and Lamb (1986) and DeGrand et al. (2000). This method identifies contrails as linear cloud features that are oriented in random directions, unlike natural high clouds, which typically follow the prevailing synoptic flow of the upper troposphere (e.g., Fig. 1). We obtained the contrail dataset for the recent historical period and combined it with our contemporary data to produce mean $1° \times 1°$ resolution contrail frequencies for the conterminous United States.

To permit statistical analyses comparing DTR departures with these satellite-based contrail data it was also necessary to convert all of the point-location weather station observations into grid-averaged ($1° \times 1°$) values. This was accomplished using the same contrail grid GIS database, and spatially associating the location of each grid cell with the underlying weather stations. We then calculated the average temperature values for all weather stations within each cell. The U.S.-averaged number of stations per grid cell was 3.2. When no weather stations existed in a particular grid cell (for 26 of 900 total grids) the grid value was interpolated from the four adjacent grid values. If four adjacent grid values were not available (e.g., along international border and coastal regions) the grid was not included in any further analysis. This procedure resulted in a total of 882 grid cells (98%), containing both fall season contrail frequencies and 11–13 September DTR anomalies, to test the hypothesis that an association existed between the two.

c. Analysis of synoptic weather conditions

To more definitively link the regional DTR anomalies with the absence of jet contrails during the grounding period, it is necessary to evaluate the synoptic weather conditions occurring over the conterminous United States. For example, a stagnant weather pattern with anomalously dry air (i.e., low humidity, lack of optically thick clouds) over a large region of the United States for the greater part of the 3-day period, could provide an alternative explanation for the observed anomalous increases in U.S.-averaged DTR (Travis et al. 2002). We used the National Centers for Environmental Prediction–National Center for Atmospheric Research (NCEP–NCAR) reanalysis daily-averaged data on top-of-the-atmosphere outgoing longwave radiation (OLR) as a surrogate for cloud cover, and 500-hPa relative humidity to depict tropospheric moisture for the grounding period [NOAA–CIRES (Cooperative Institute for Research in Environmental Sciences) 2002]. We computed the 3-day-averaged departure of each parameter for the grounding period (12–14 September) from its corresponding climatological normal. These were compared to the maps of DTR and T_{max} and T_{min} for the same period for visual associations.

d. Application of a contrail outbreak "retro-prediction" method

It is instructive to estimate where contrails likely would have occurred if commercial aircraft flights had continued as normal for the 11–13 September period. For this purpose we developed a "retro-prediction" (retrodiction) statistical method for contrail outbreaks occurring in otherwise clear air. The retrodiction method uses statistical composites (i.e., ensemble averages and variances) of the upper-tropospheric (300, 250, 200 hPa)

meteorological conditions associated with 48 outbreaks that occurred over the conterminous United States during the 8–16 September periods of 1995–97 and 1999–2001 (the calibration period). Data on meteorological parameters (temperature, humidity, vertical wind shear, vertical motion) previously shown (e.g., Appleman 1953; Schrader 1997; Travis 1996; Travis et al. 1997; Chlond 1998; Kästner et al. 1999) to influence the formation likelihood and persistence time of contrails, were acquired for each outbreak using the 6-hourly NCEP–NCAR reanalyses (Kistler et al. 2001). The outbreak data were then expressed as anomalies from the long-term means for each variable, pressure level, and location, and averaged to yield the composites. For the calibration period, the following outbreak meteorological variables/tropospheric levels were statistically different from climatology: increased values of humidity at 300 hPa (RH range = +7.5%–+58.0%), lower temperature and reduced Z_{300}–Z_{200} thickness (−6.5 m), light easterly u-wind anomalies at 250 hPa (range = −2.2 to −2.9 m s^{-1}), and slightly negative (i.e., upward) vertical motion (mean = -0.54×10^{-3} Pa s^{-1} at 250 hPa). Using GIS, we applied the outbreak composite statistical ranges to two independent sets of reanalyses "test" periods: 8–16 September 1998, and the day immediately preceding, and also immediately following the grounding period. The AVHRR imagery for these periods was also inspected for contrail outbreaks. Using a test criterion of a minimum of 50% spatial overlap between the retrodicted and observed contrail outbreaks, we found good agreement (25 out of the 30 cases). This allowed us confidently to apply the method to the upper-tropospheric reanalyses for the grounding period. The resulting contrail-favored areas (CFAs) mapped locations, and their associations with DTR departures, are discussed in section 3d.

3. Results and discussion

a. T_{max} and T_{min} spatial trends

Although both the 3-day U.S.-averaged T_{max} and T_{min} were warmer than normal for the grounding period, the T_{min} increase (0.3°C) was about one-fourth that of T_{max} (1.2°C). This asymmetric variation from the long-term means may indicate that the lack of contrails impacted the daytime temperatures more than those at night. Such a possibility accords with the observed greater frequencies of contrails during daytime versus nighttime hours, in association with diurnal differences in the frequencies of jet aircraft flights (Bakan et al. 1994; Minnis et al. 1997).

The spatial patterns of T_{max} for 11–13 September 2001 (Fig. 2a) show strongest increases in the Intermountain West and Pacific Northwest, extending through the Midwest and into the northeast United States. Strongest decreases of T_{max} occurred in California, the northern Great Plains, the Southwest, and Florida. For T_{min} (Fig. 2b) the largest increases were in the West (except California) and the Gulf Coast states. The largest combined increase of T_{max} and T_{min} occurred in portions of the Northwest. This can be partially attributed to a persistent southerly flow that was produced from synoptic-scale circulations associated with a storm system centered off the northern California coast for much of the grounding period. This storm also likely contributed to the large decrease in T_{max} seen in northern California due to extensive daytime cloud coverage. Strong decreases in T_{min} occurred through the southern Great Plains, Midwest and Great Lakes, the Mid-Atlantic region, and the northeast United States. Possible associations between these spatial variations of T_{max} and T_{min} departures, and the lack of contrails during the grounding period, are discussed in section 3c.

b. DTR spatial trends and associations with contrail frequency

The spatial variation of the grid-averaged DTR anomalies for the grounding period (Fig. 3a) shows that the largest positive departures extended across portions of the central and northeast United States as well as the Pacific Northwest. Because these regions have previously been reported (Minnis et al. 1997; DeGrand et al. 2000) as being climatologically favorable for outbreaks of persisting contrails, we argue that this anomalous increase was associated with the absence of contrails during the aircraft groundings (Travis et al. 2002), in combination with synoptic conditions.

To identify the relationship between the regional DTR increases of the grounding period and spatial variations in the typical fall-season contrail coverage, Fig. 3b summarizes the mean contrail frequency (combined 1977–79, 2000–01) averaged for the same 1° × 1° grids as the DTR data. The frequency pattern of contrails for this period appears broadly similar to that shown in previous studies for other times of the year (Minnis et al. 1997; DeGrand et al. 2000), with the contrail frequency maxima occurring in the Midwest, Southeast, and parts of the West.

Visual comparison of Figs. 3a and 3b suggests some agreement between those regions having the largest increases in DTR during the grounding period and those typically experiencing the greatest contrail coverage during the fall season. To quantify the presence and strength of this relationship a Pearson correlation coefficient was calculated between DTR departure and contrail frequency for the 882 grids available for analysis (Fig. 4). The statistically significant positive relationship ($R = 0.36$; $p < 0.01$) supports our contention that a contrail-induced suppression of DTR was present in the 1971–2000 normals throughout much of the United States, and especially in areas where contrails are typically most prevalent. Moreover, the gradual reduction in statistical scatter about the trend line as contrail frequency increases may indicate that the contrail "sig-

nal" in DTR departure was more distinguishable from synoptic-scale "background" influences for those grids having the highest mean contrail frequency.

c. Synoptic variations in cloud and humidity during the grounding period

The 3-day average (12–14 September 2001) OLR anomaly map (Fig. 5a) shows positive departures (i.e., fewer clouds or lower mean cloud-top altitude) in a swath extending from the south-central United States through the Midwest and into the mid-Atlantic regions. A smaller area of OLR positive departures also occurred in the Pacific Northwest. In contrast, OLR negative departures (i.e., more clouds or higher mean cloud-top altitude) occurred over the Southwest, Florida, and the extreme southeast United States, and parts of the Intermountain West extending through the northern Great Plains. The remainder of the country had close to normal departures of OLR for the grounding period. A comparison of the OLR anomaly field with that of the midtropospheric (500 hPa) relative humidity [RH(500); Fig. 5b], shows general consistency: areas of positive (negative) relative humidity departure accompany increased moisture and ascent of air (decreased moisture and subsidence), and tend to be associated with negative (positive) anomalies of OLR (Fig. 5a). Thus, about one-half of the United States experienced fewer or lower-altitude clouds than normal during the grounding period; the other half had either near-normal or more than normal/deeper clouds. This statement is supported by the analysis of the mean percentage of total cloud coverage (TCDC; departures not available) for the grounding period (Fig. 5c), which shows good agreement with the OLR departures in most areas of the United States. Stratifying the 3-day averaged RH(500) into daytime and nighttime components (Fig. 6) also shows strong spatial consistency and reduces the possibility that the asymmetrical departures of T_{max} and T_{min} reported in section 3a are a result of large diurnal variations in relative humidity.

It is particularly interesting that some of the largest DTR and T_{max} anomalies in the Intermountain West occurred near the outer edges of the areas having the most positive anomalies of humidity and deepest cloud cover (i.e., Colorado, Utah; Fig. 5). The lack of clouds in the adjacent areas suggests that although moisture levels were above normal (Fig. 5b), they were not sufficient for substantial cloud coverage to form through natural processes. However, because such environments are often conducive to contrail formation [i.e., high humidity but few clouds; Travis et al. (1997); section 3d], it is reasonable to assume that contrails likely would have formed in these areas had airplanes been flying. This implies that the lack of contrails in those areas helped offset the tendency for DTR to decrease when averaged over the 3-day grounding period. Such a possibility is now evaluated using the CFA retrodictions for the same period.

d. Retrodicted contrail outbreaks and associations with DTR anomalies

Figure 7 depicts the grounding-period CFAs derived from the contrail-outbreak retrodiction method (section 2d). To facilitate visual comparisons with the DTR departure map (Fig. 3a), the CFAs were converted to $1° \times 1°$ grids for locations where contrail occurrence was favorable for a minimum of at least 12 h during the grounding period ("moderate susceptibility"). Grid cells over which CFAs existed for more than 50% of the grounding period (i.e., 36 h) were deemed to have "high susceptibility." All remaining grid cells were designated as having "low susceptibility" (Fig. 7). The Pacific Northwest, Intermountain West, and Southwest U.S. regions were highly susceptible to contrails during the grounding period (Fig. 7). Smaller regions of contrail high susceptibility included the Midwest, Great Lakes, and Florida. These high susceptibility CFAs coincide with the edges of the positive moisture anomaly areas (Fig. 5b). Such a result concurs well with previous research on contrail–synoptic weather associations, which has reported that contrails occur most commonly along the leading edge of cirrus shields associated with frontal cyclones and convective storms (Detwiler and Pratt 1984; Travis et al. 1997; DeGrand et al. 2000).

A visual comparison of the departure maps for T_{max} and T_{min} (Figs. 2a,b) with Figs. 5 and 7 suggests that T_{max} shows a closer association with the CFA high susceptibility retrodiction (except for Florida), whereas T_{min} shows a closer association with the synoptics; specifically, OLR and total cloud cover. This may imply that the lack of contrails affected T_{max} more than T_{min} during the grounding period, especially in the West. There, the combination of a warm, moist southerly flow and the lack of airplanes led to increasing humidity and temperature but less cloud coverage than otherwise would have occurred from contrail formation; especially during the daytime when air traffic would normally have been greatest (with less impact on T_{max}). In the eastern half of the United States, the increased DTR seems to have resulted from a combination of dry air and lack of clouds (lowers T_{min}, raises T_{max} and DTR) and the lack of contrails. This is consistent with the observation (section 3a) that the U.S.-averaged T_{max} increased more than T_{min} during the grounding period.

Comparing Fig. 7 with the DTR departure map (Fig. 3a) shows strong agreement for much of the west, especially in the Intermountain and Northwest regions. For the entire conterminous United States the average DTR departure for the high susceptibility grid cells (+1.3°C) is statistically greater ($p < 0.01$) than that for the moderate susceptibility (+0.9°C) and the low susceptibility grid cells (+0.8°C). The slightly higher av-

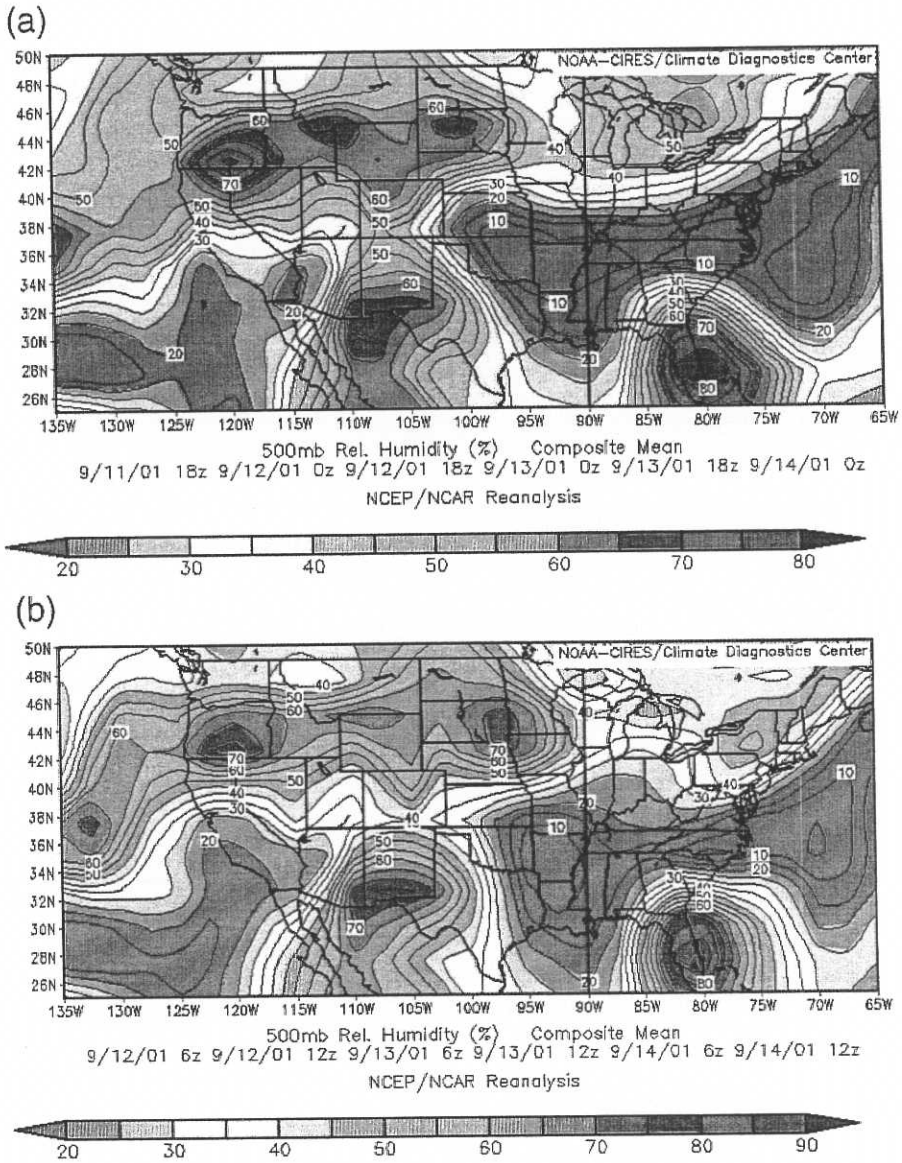

FIG. 6. Mapped 3-day average (1800 UTC 11 Sep 2001–1800 UTC 14 Sep 2001) anomalies of relative humidity at 500 hPa: RH(500) in percent for (a) daytime periods (0000 and 1800 UTC) and (b) nighttime periods (0600 and 1200 UTC), derived using the NCEP–NCAR reanalysis.

erage DTR departures in the moderate susceptibility grid cells compared with the low susceptibility cells are not statistically different. These results further support our contention that the lack of commercial aircraft flying, especially in the areas of contrail high susceptibility, contributed to the 11–13 September DTR anomaly. In combination with the statistical relationship shown earlier between DTR departure and the fall-season contrail frequency (section 3b), this finding implies that the 11–13 September DTR anomaly was caused by a combination of regional-scale, contrail-induced suppression of DTR in the long-term climatological normals and the presence of extensive areas of contrail high susceptibility, which remained unexploited owing to the lack of commercial aircraft flights.

4. Summary and conclusions

These results support the hypothesis that the grounding of all commercial aircraft in U.S. airspace, and the consequent elimination of substantial jet contrail coverage during the 11–14 September 2001 grounding pe-

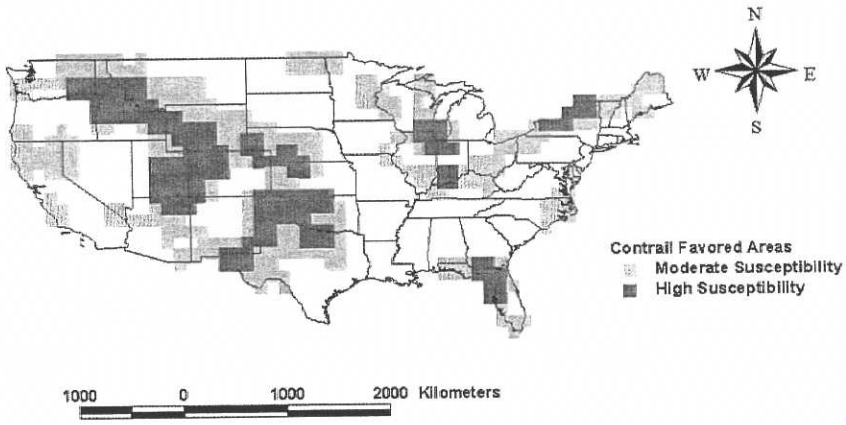

FIG. 7. Grid cell-averaged (1° × 1° resolution) map of CFAs determined for the grounding period (1800 UTC 11 Sep 2001–1800 UTC 14 Sep 2001) using the contrail-outbreak retrodiction method applied to the six-hourly NCEP–NCAR reanalyses of the upper troposphere (refer to text). The lighter (darker) shading refers to moderate (highest) susceptibility of contrail outbreaks. Those regions that were not susceptible to outbreaks are not shaded.

riod, helped produce an enhanced surface DTR in those areas that typically experience the greatest numbers of jet contrails during the fall season (e.g. the Midwest). The DTR anomaly occurred primarily due to large increases in T_{max} that were not matched by similar magnitude increases in T_{min}. In the West, synoptic weather patterns (mostly cyclonic) during the grounding period appear to have played an important role in enhancing (e.g., the Intermountain region) or negating (e.g., coastal California) the effect of contrail absence on surface temperature. For the country as a whole, the synoptic weather conditions during the grounding period suggest a better association of these with T_{min} than T_{max} thus providing a possible partial explanation for the asymmetric response of these two components of DTR.

Our analyses of the AVHRR imagery available for the grounding period indicated several occurrences of single contrails (no outbreaks) produced by military aircraft, including some in the Northeast that demonstrated extensive persistence and spreading characteristics (Minnis et al. 2002). Moreover, the analysis of other imagery showed many contrails occurring just over the border in Canada. When combined with the statistical model retrodictions, these observations suggest that if commercial airplanes had not been grounded, substantial contrail coverage would have been present over large parts of the United States, especially the Pacific Northwest, Intermountain West, upper Midwest, and Great Lakes and the Northeast.

Predicted future increases in aircraft flight frequencies, and subsequent increased occurrences of contrails in the climatologically susceptible extratropics (e.g., Gierens et al. 1999; Minnis et al. 1999), could lead to an even greater influence on DTR. However, potential changes in upper-tropospheric conditions related to global-scale climate change, which can influence both the formation likelihood and persistence time of contrails, need to be considered when projecting future impacts of contrails onto regional-scale climate.

Acknowledgments. This research was sponsored by grants from the National Science Foundation (BCS-0099011 and BCS 0099014). We are grateful to the following for their contributions to this research: Mr. Jeff Johnson (University of Wisconsin—Whitewater) for assisting with the 2000–01 contrail satellite analysis; Mr. James Q. DeGrand (The Ohio State University) for providing the 1977–79 satellite contrail frequency dataset; and the two anonymous reviewers, for their many helpful and insightful comments.

REFERENCES

Allard, J., 1997: The climatic impacts of jet airplane condensation trails (contrails) in the Northeast U.S. M.S. thesis, Dept. of Geography, The Pennsylvania State University, 152 pp. [Available from Dept. of Geography, The Pennsylvania State University, University Park, PA 16802.]

Appleman, H., 1953: The formation of exhaust condensation trails by jet aircraft. *Bull. Amer. Meteor. Soc.*, **34**, 14–20.

Bakan, S., M. Betancor, V. Gayler, and H. Grassl, 1994: Contrail frequency over Europe from NOAA-satellite images. *Ann. Geophys.*, **12**, 962–968.

Carleton, A. M., and P. J. Lamb, 1986: Jet contrails and cirrus cloud: A feasibility study employing high-resolution satellite imagery. *Bull. Amer. Meteor. Soc.*, **67**, 301–309.

Changnon, S. A., 1981: Midwestern cloud, sunshine and temperature records since 1901: Possible evidence of jet contrail effects. *J. Appl. Meteor.*, **20,** 496–508.

Chlond, A., 1998: Large-eddy simulations of contrails. *J. Atmos. Sci.*, **55,** 796–819.

DeGrand, J. Q., A. M. Carleton, D. J. Travis, and P. Lamb, 2000: A satellite-based climatic description of jet aircraft contrails and associations with atmospheric conditions, 1977–79. *J. Appl. Meteor.*, **39,** 1434–1459.

Detwiler, A., and R. Pratt, 1984: Clear-air seeding: Opportunities and strategies. *J. Wea. Modif.*, **16,** 46–60.

Duda, D. P., P. Minnis, and L. Nguyen, 2001: Estimates of cloud radiative forcing in contrail clusters using GOES imagery. *J. Geophys. Res.*, **106,** 4927–4937.

ESRI, 1999: ArcView 3.2. Environmental Systems Research Inc.

Gierens, K., R. Sausen, and U. Schumann, 1999: A diagnostic study of the global distribution of contrails. Part II: Future air traffic scenarios. *Theor. Appl. Climatol.*, **63,** 1–9.

Gothe, M. B., and H. Grassl, 1993: Satellite remote sensing of the optical depth and mean crystal size of thin cirrus and contrails. *Theor. Appl. Climatol.*, **48,** 101–113.

Karl, T. R., and Coauthors, 1993: Asymmetric trends of daily maximum and minimum temperature. *Bull. Amer. Meteor. Soc.*, **74,** 1007–1023.

Kästner, M., R. Meyer, and P. Wendling, 1999: Influence of weather conditions on the distribution of persistent contrails. *Meteor. Appl.*, **6,** 261–271.

Kistler, R., and Coauthors, 2001: The NCEP–NCAR 50-Year Reanalysis: Monthly means CD-Rom and documentation. *Bull. Amer. Meteor. Soc.*, **82,** 247–267.

Meerkotter, R., U. Schumann, D. R. Doelling, P. Minnis, T. Nakajima, and Y. Tsushima, 1999: Radiative forcing by contrails. *Ann. Geophys.*, **17,** 1080–1094.

Mims, F. M., III, and D. J. Travis, 1997: Reduced solar irradiance caused by aircraft contrails. *Eos, Trans. Amer. Geophys. Union*, **78,** 448.

Minnis, P., J. K. Ayers, and S. P. Weaver, 1997: Surface-based observations of contrail occurrence frequency over the U.S., April 1993–April 1994. NASA Ref. Publ. 1404, May 1997, 12 pp. and tables and figs.

——, U. Schumann, D. R. Doelling, K. M. Gierens, and D. W. Fahey, 1999: Global distribution of contrail radiative forcing. *Geophys. Res. Lett.*, **26,** 1853–1856.

——, L. Nguyen, D. P. Duda, and R. Palikonda, 2002: Spreading of isolated contrails during the 2001 air traffic shutdown. Preprints, *10th Conf. on Aviation, Range, and Aerospace Meteorology*, Portland, OR, Amer. Meteor. Soc., 33–36.

Murcray, W. B., 1970: On the possibility of weather modification by aircraft contrails. *Mon. Wea. Rev.*, **98,** 745–748.

NCDC, 2003: Data documentation for Data Set 3200 (DSI-3200). National Climatic Data Center Tech. Doc. 3200, Asheville, NC, 18 pp. [Available online at ftp://ftp.ncdc.noaa.gov/pub/data/documentlibrary/tddoc/td3200.doc.]

NOAA–CIRES, cited 2002: Online Reanalysis Data. NOAA–CIRES Climate Diagnostics Center, Boulder, CO. [Available online at www.cd.noaa.gov.]

Penner, J. E., D. H. Lister, D. J. Griggs, D. J. Dokken, and M. McFarland, Eds., 1999: Aviation and the Global Atmosphere. Intergovernmental Panel on Climate Change, 12 pp.

Sassen, K., 1997: Contrail-cirrus and their potential for regional climate change. *Bull. Amer. Meteor. Soc.*, **78,** 1885–1903.

Schrader, M. L., 1997: Calculations of aircraft contrail formation critical temperatures. *J. Appl. Meteor.*, **36,** 1725–1728.

Travis, D. J., 1996: Variations in contrail morphology and relationships to atmospheric conditions. *J. Wea. Modif.*, **28,** 50–58.

——, and S. A. Changnon, 1997: Evidence of jet contrail influences on regional-scale diurnal temperature range. *J. Wea. Modif.*, **29,** 74–83.

——, ——, and S. A. Changnon, 1997: An empirical model to predict widespread occurrences of contrails. *J. Appl. Meteor.*, **36,** 1211–1220.

——, ——, and R. Lauritsen, 2002: Contrails reduce daily temperature range. *Nature*, **418,** 601.

VI, 15

About
Search news archive
Public Relations
Add an event

News highlights

Print version

Proof that airports are air polluters

22 Apr 2010, PR 89/10

Scientists in the Environmental Research Group (ERG) at King's have undertaken research into the effects of the closure of UK airspace on air quality surrounding major airports after the Icelandic volcano eruption, following a number of enquiries from the public.

In response the ERG analysed the concentrations of NOX (the generic term for oxides of nitrogen combined) and NO2 (nitrogen dioxide) surrounding Gatwick and Heathrow airports during the first three days of closure, Thursday 15 to Saturday 17 April 2010. This period was chosen due to the stable weather conditions with light north easterly winds, allowing a cross-sectional analysis upwind and downwind of the airports.

This period of unprecedented closure during good weather conditions allowed the scientists to demonstrate that the airports have a clear measurable effect on nitrogen concentrations and that this effect disappeared entirely during the period of closure.

Pollution impact

Such nitrogen pollutants can increase breathing difficulties in people with existing sensibilities, cardiac conditions or in older people. Under the impact of sunlight they can transform into the even more damaging pollutant ozone. NOx and NO2 are particularly associated with jet aircraft, as they are produced by the high-temperature mix of aviation with fuel.

The analysis was undertaken by Dr Ben Barratt and Dr Gary Fuller of the Environmental Research Group, School of Biomedical and Health Sciences. *'We have always been fairly confident that there was this 'airport effect' but we have never been able to show it,'* said Dr Barratt. *'The closure gave us the opportunity to look at it, and there is a very strong indication that it is the case.*

'This exceptional closure has allowed us to demonstrate the impacts of airport emissions on their immediate neighbourhood. We did not consider the impact of decreased traffic flows on airport feeder roads in this preliminary study. Decreased traffic flows are likely to have a significant effect on concentrations of vehicle-related pollutants close to such roads, but unfortunately

News by year
News highlights
News archive 2009
News archive 2008
News archive 2007
News archive 2006
News archive 2005
News archive 2004
News archive 2003
News archive 2002
News archive 2001
News feed

VI, 16

we did not have sufficient traffic data to carry out this analysis at that time,' he continued.

A full version of the report is available for download from the ERG's *London Air Quality Network* website.

Notes to editors

King's College London
King's College London is one of the top 25 universities in the world (*Times Higher Education* 2009) and the fourth oldest in England. A research-led university based in the heart of London, King's has nearly 23,000 students (of whom more than 8,600 are graduate students) from nearly 140 countries, and some 5,500 employees. King's is in the second phase of a £1 billion redevelopment programme which is transforming its estate.

King's has an outstanding reputation for providing world-class teaching and cutting-edge research. In the 2008 Research Assessment Exercise for British universities, 23 departments were ranked in the top quartile of British universities; over half of our academic staff work in departments that are in the top 10 per cent in the UK in their field and can thus be classed as world leading. The College is in the top seven UK universities for research earnings and has an overall annual income of nearly £450 million.

King's has a particularly distinguished reputation in the humanities, law, the sciences (including a wide range of health areas such as psychiatry, medicine and dentistry) and social sciences including international affairs. It has played a major role in many of the advances that have shaped modern life, such as the discovery of the structure of DNA and research that led to the development of radio, television, mobile phones and radar. It is the largest centre for the education of healthcare professionals in Europe; no university has more Medical Research Council Centres.

King's College London and Guy's and St Thomas', King's College Hospital and South London and Maudsley NHS Foundation Trusts are part of King's Health Partners. King's Health Partners Academic Health Sciences Centre (AHSC) is a pioneering global collaboration between one of the world's leading research-led universities and three of London's most successful NHS Foundation Trusts, including leading teaching hospitals and comprehensive mental health services. For more information, visit: www.kingshealthpartners.org.

Further information
Kate Moore
Public Relations Officer (Health Schools)
Email: kate.moore@kcl.ac.uk
Tel: 020 7848 4334

Next:
Who is watching you?
More Swedes than Brits survive lung cancer
Edmund-Davies Professor of Criminal Law appointed
Santander's chairman visits King's
Leading academic warns of 'care squeeze' in NHS

VII, C

APPENDIX 7

VII, 2

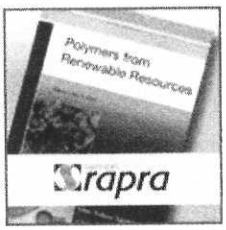

Email / Share Back One

Does Air Pollution Increase Rainfall

Posted in | Energy | Climate Change | Global Warming | Pollution | Water

An international team of scientists, headed by Prof. Daniel Rosenfeld of the Institute of Earth Sciences at the Hebrew University of Jerusalem, has come up with a surprising finding to the disputed issue of whether air pollution increases or decreases rainfall. The conclusion: both can be true, depending on local environmental conditions.

The determination of this issue is one with significant consequences in an era of

VII, 3

- Popular
- Latest
- Random

Morgan Solar Raises $8.2 Million for Concentrated Photovoltaic Solar Panel Development

Evergreen Solar's String Ribbon Panels to power Patriot Place

SunRun Announces Low-Cost Solar Power for Homes in New Jersey

Four Winds Renewable Energy Offers Grid-Tie Solar Electric Systems

Puget Sound Energy Customers Connect Solar Systems to Utility Grid

UD5 and UJ6 PV Modules from Mitsubishi Electric Ready for Installation Near Salt Water

Energy Conversion Devices and Enfinity Corporation to Develop Rooftop Solar Installations in Ontario, Canada

Umwelt-Sonne-Energie Completes Largest Solyndra Rooftop PV System Project in Belgium

A-Power Energy Generation Systems Delivers Wind Turbines in China

Canadian Solar Enters into PV Modules Sales Contract with Fire Energy Group

Northside Lofts Geothermal Project by Middleton Geothermal Services

Energy Conversion Devices and Enfinity Corporation to

climate change and specifically in areas suffering from manmade pollution and water shortages, including Israel.

In an article appearing in the Sept 5 issue of the journal Science, the scientific team, which included researchers from Germany, has published the results of its research untangling the contradictions surrounding the conundrum. They do this by following the energy flow through the atmosphere and the ways it is influenced by aerosol (airborne) particles. This allows the development of more exact predictions of how air pollution affects weather, water resources and future climates.

Mankind releases huge amounts of particles into the air that are so tiny that they float. Before being influenced by man, air above land contained up to twice as many of these so called aerosol particles as air above oceans.

VII, 4

and Enfinity Corporation to Develop Rooftop Solar Installations in Ontario, Canada

Research Aims to Reduce Energy Usage in the Home

eSolar and Penglai Electric Announce Licensing Agreement to Build Solar Thermal Power Plants in China

Northern Power Systems Selects Analog Devices' SHARC Processors for its Northwind 100 Community-Scale Wind Turbines

Nowadays, this ratio has increased to as much as a hundredfold.

Natural and manmade aerosols influence our climate – that much is agreed. But which way do they push it? They produce more clouds and more rain, some say. They produce fewer clouds and less rain, say others. This disputed role of aerosols has been the greatest source of uncertainties in our understanding of the climate system, including the question of global warming.

Smoke from agricultural fires suppresses rainfall from a cloud over the Amazon (right). A similar size cloud (left) rains heavily on the same day some distance away in the pristine air. (Hebrew University photo)

"Both camps are right", says Prof. Meinrat O. Andreae, director of the Max Planck Institute for Chemistry in Germany, a coauthor of the publication. "But you have to consider how many aerosol particles there are." The lead author, Prof. Rosenfeld of the Hebrew University, adds: "The amount of aerosols is the critical factor controlling how the energy is distributed in the atmosphere." Clouds, and therefore precipitation, come about when moist, warm air rises from ground level and water condenses or freezes on the aerosols aloft. The energy responsible for evaporating the water from the earth's surface and lifting the air is provided by the sun.

Aerosols act twofold: On the one hand, they act like a sunscreen reducing the amount of sun energy reaching the ground. Accordingly, less water evaporates and the air at ground level stays cooler and drier, with less of a tendency to rise and form clouds.

On the other hand, there would be no cloud droplets without aerosols. Some of them act as gathering points for air humidity, so called condensation nuclei. On these tiny particles with diameters of less than a thousandth of a millimeter the water condenses – similar to dew on cold ground – releasing energy in the process. This is the same energy that was earlier used to evaporate the water from the earth's surface. The

VII, 5

released heat warms the air parcel so that it can rise further, taking the cloud droplets with it. But if there is a surplus of these gathering points, the droplets never reach the critical mass needed to fall to earth as rain – there just is not enough water to share between all the aerosol particles. Also, with a rising number of droplets their overall surface increases, which increases the amount of sunlight reflected back to space and thus cooling and drying the earth.

In a nutshell, then, the study results show the following: With rising pollution, the amount of precipitation at first rises, than maxes out and finally falls off sharply at very high aerosol concentrations. The practical result is that in relatively clean air, adding aerosols up to the amount that releases the maximum of available energy increases precipitation. Beyond that point, increasing the aerosol load even further lessens precipitation. Therefore, in areas with high atmospheric aerosol content, due to natural or manmade conditions, the continuation or even aggravation of those conditions can lead to lower than normal rainfall or even drought.

Prof. Rosenfeld states: "These results have great significance for countries like Israel where rainfall is scarce and can be easily affected by over-production of aerosols. Our study should act as a red light to all of those responsible for controlling the amounts of pollution we release into the atmosphere."

"With these results we can finally improve our understanding of aerosol effects on precipitation and climate," summarizes Andreae, "since the direct contradiction of the different aerosol effects has seriously hindered us from giving more accurate predictions for the future of our climate, and especially for the availability of water."

Published Date: 8/9/2008

Click here for Cleantech news archive

Δ Top

VIII

APPENDIX 8

VIII, 2

Rain Men: Scientists Here Tried to Change the Weather

By Chrissie Reilly
Staff Historian

(Note: This article appeared in the 20 Feb 2009 issue of the *Monmouth Message*)

Everybody talks about the weather, but nobody does anything about it.

Except here at Fort Monmouth, where researchers changed the course of nature, and of history, in 1947.

This installation was home to Project Cirrus, a five-year foray into the science, and sometimes the art, of weather modification.

The discoveries and experiments in our very own Signal Corps Laboratories as part of Project Cirrus are still relevant, and the technology is still used worldwide.

The project was led by Nobel laureate Dr. Irving Langmuir and his protégé Dr. Vincent Schaefer, both from General Electric (GE).

Langmuir defined serendipity as "the art of profiting from unexpected occurrences." Their discovery of cloud seeding certainly qualified as one such serendipitous event.

The cloud seeding project originated with experiments in de-icing aircraft that took them to Mount Washington, New Hampshire— home of extremely harsh winter weather.

To recreate these conditions in a lab, Schaefer invented a "cold box" to test his theories. This was a GE home freezer with a black velvet lining and a viewing light.

Employees from Fort Monmouth work on the Project Cirrus equipment.

Breathing into the cold box produced a tiny cloud of supercooled water droplets, just like in the upper parts of a cloud.

Schaefer later discovered that the addition of any substance that was -40 degrees Celsius would cause millions of ice crystals to form in the cloud. They extrapolated that this would work in atmospheric clouds, too.

So the men attempted to 'seed' clouds with dry ice by flying over them and releasing the particles.

On Nov 13, 1946, Shaefer dropped 1.4 kg of dry ice pellets from an airplane into a supercooled stratus cloud near Schenectady, New York. And snow fell!

In February 1947, the US Army Signal Corps became involved in these cloud seeding missions, and it earned the name Project Cirrus.

The project was a joint effort of the Army, Navy, Air Force, and GE.

William R. Cotton and Roger A. Pielke wrote about Langmuir's and Schaefer's exploration into cloud seeding with cirrus clouds, supercooled stratus clouds, cumulus clouds, and even hurricanes in their book *Human Impacts on Weather and Climate*.

The supercooled stratus clouds were the most responsive to seeding, and patterns (including L-shapes, race tracks, and Greek gammas) could be seeded into the clouds.

Retired Fort Monmouth physicist Sam Stine worked at the Evans Signal Laboratory designing experiments. He then had the job of getting into the airplanes and actually testing them.

According to Stine, "We flew about 37 experimental flights in the first year and a half. Flying into thunderstorms, line squalls, the tops of tornadoes, you have it."

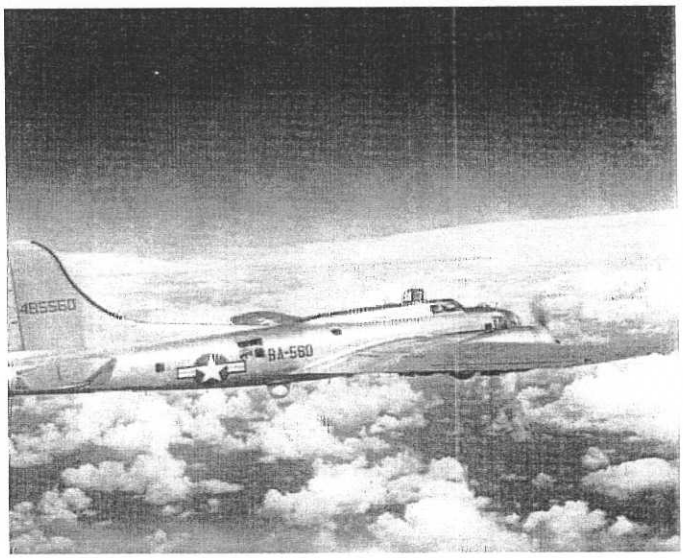

Project Cirrus plane in flight.

Because of the inherent variability in weather patterns, attempts to modify weather did not always yield perfect or consistent results; there was also the problem of reliably attributing results to specific scientific actions.

Dr. Harold Zahl recalled in his book, *Electrons Away, or Tales of a Government Scientist*, "There were conditions when rain or snow could be precipitated, but the moisture had to be there in the first place. Nature had to be a cooperating partner and, when needed most, it seemed that she was not always ready to help."

Cloud seeding did not always produce the expected results.

The first attempt at modifying a tropical cyclone or hurricane occurred in 1947. It was October and a hurricane was head eastward off the coast of Florida and into the Atlantic.

After 80 lbs of dry ice were dispersed into the hurricane, it briefly paused, and then headed for the shore. Winds of 85 mph were clocked in Savannah, GA, a resident there was killed, coastal areas flooded, and the damage totaled over $20 million.

Jay Barnes and Steve Lyons reported in *Florida's Hurricane History*, that many believed that the seeding was responsible for the turn, including Langmuir. Hurricanes had however behaved like this in the past without seeding – only 40 years prior a hurricane did the same thing and headed due west into the coast.

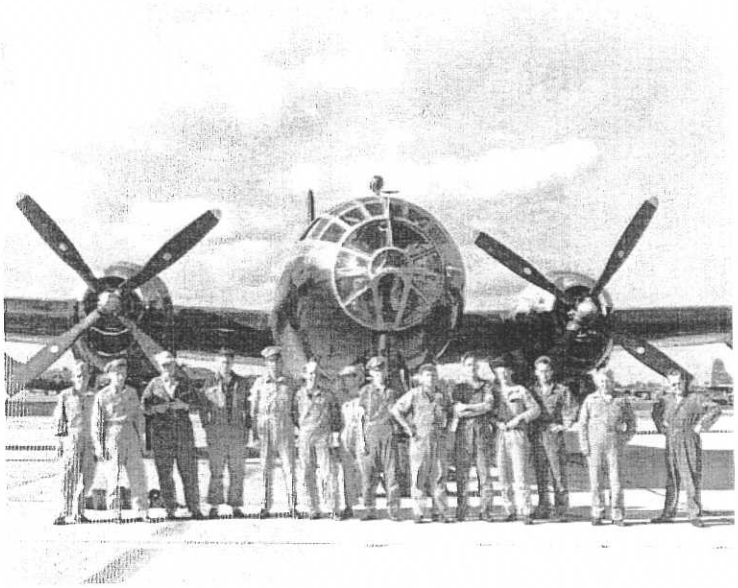

Project Cirrus was a joint effort of the Army, Navy, Air Force, and General Electric. This photo was taken before one of the many flights in 1948.

Zahl reported that "we concluded it was 'an act of God.' If it could happen once, it could happen twice."

Either way, GE's lawyers told Langmuir not to discuss the hurricane until the statute of limitations had run out for prosecution.

The technology involved in Cirrus was put to good use also in October 1947, when clouds were seeded above a Maine forest fire to help extinguish the blaze.

Despite the often mixed results of Project Cirrus, Langmuir was a noted workaholic. *The New York Times* reported that upon his retirement from GE in 1950, he did not even take a vacation, but went straight to devoting more time to Cirrus.

Langmuir told reporters for a March 2, 1950 *New York Times* article that "within the past year, Project Cirrus has grown very greatly in importance, and now I believe that the best service that I can render to the national welfare is to increase my activities in this field."

He also expected the same rigorous work ethic from his lab personnel. On Thanksgiving 1951, he complained that his employees wanted days off for the holiday!

Cloud seeding and weather modification in general declined over the years, due to a number of reasons.

Weather modification was largely oversold to the public and legislative members; an abnormal wet period in the United States reduced demand; and changes in government and public attitudes towards other weather and climate concerns all contributed to less seeding projects over the years.

Despite this controversy, it has not stopped people continuing to try to control the weather.

VIII, 5

The 2008 Olympic Games held in Beijing were scheduled during northern China's rainy season.

In order to prevent rain from ruining the opening ceremonies in the open-air birds nest stadium, the Chinese government seeded clouds with silver iodide to make it rain elsewhere. And there was no rain in Beijing for the opening events.

The Signal Corps Laboratories at Fort Monmouth were at the forefront of scientific exploration. What rain dances had been attempting to do for centuries, Fort Monmouth accomplished.

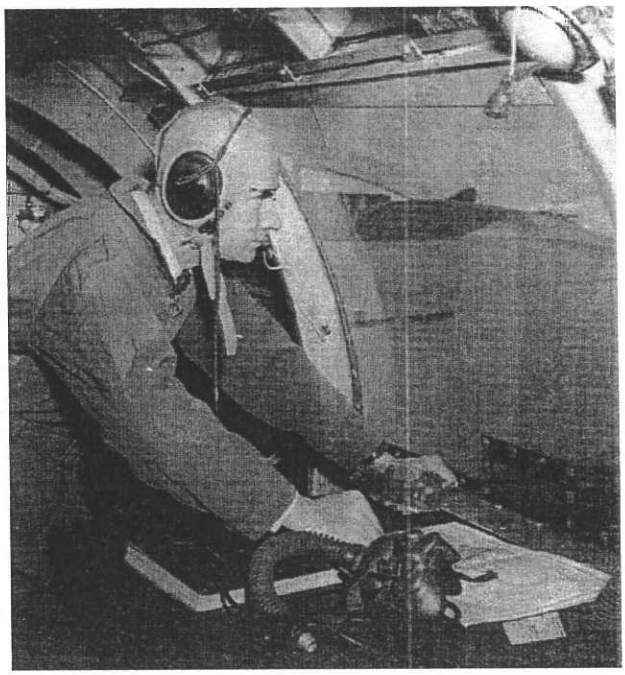

Dr. Vincent Schaefer prepares for a Project Cirrus flight in 1948.